BROWN TIDE CONSULTING SERVICES

FINAL REPORT

Contract between Research Foundation of CUNY on behalf of the Hunter College of CUNY and the Suffolk County Department of Health

ADMINISTRATIVE INFORMATION

Research Foundation (CUNY) Project Number…..70694
Project Start…… September 1, 2006
Principal Investigator..…….Karl H. Szekielda
Co-Investigator…….Frank Buonaiuto
Research Assistant……Hyojin Ahn
CUNY, Hunter College, Department of Geography
695 Park Avenue
New York, NY 10021
e-mail: szekielda@aol.com

TABLE OF CONTENTS

PART B

ESTIMATION OF LAND COVER CHANGE IN SUFFOLK COUNTY, NY, USING LANDSAT AND ALI DATA

PART A: 1 INTRODUCTION

The project had the objectives of detecting with remote sensing data the locations and extent of high concentrations of algal blooms as well as in using remote sensing for the mapping of coastal processes and vegetation. The application of different satellite systems and different spectral channels allows for the identification of water masses and its related dynamics of coastal waters carrying varying load of total suspended sediments, chromophoric dissolved organic matter (CDOM) and chlorophyll. Problems in identification arise however in regions where high nutrient transport leads to eutrophication and consequently, it is difficult to quantify radiance or reflectance data in terms of biomass or its equivalence in chlorophyll. Studying in a synoptic way large areas within a short time frame has the advantage of obtaining information that can hardly be retrieved from ship measurements alone. As several satellite systems are in operational mode, the following study of Peconic Bay also addresses the issue of selecting the most suitable data that can be used for coastal zone management and for integration into survey work and to do so in a most cost-effective way.

Advantage was taken of several data sources that were available to project personnel through data user agreements, at no cost to the project and allowing a wider temporal coverage. The project also required satellite imaging for detailed land-use classification in an attempt to supplement possible future research and management efforts for preservation and where necessary, for restoration of environmental conditions.

Bloom occurrence is frequently observed in highly populated regions where there is discharge from waste water treatment facilities, runoff from agricultural fields and discharge of ground water input of phosphate and nitrogenous compounds into the coastal ecosystem. Data of temporal and spatial distribution of HABs are limited however due to short spans of hydrographic conditions that are not easily recognized with conventional methods. Plankton blooms in general occur in high concentrations and can be recognized to be present close to the surface. As plankton species can be identified through their composition and concentration of photosynthetic pigments, efforts have been undertaken to use high resolution multi-spectral data either obtained from aircraft or satellite altitudes.

The major controlling factors in biogeochemical provinces include vertical mixing rates, stratification of the euphotic zone, nutrient supply and irradiance at the sea surface. Modifications of these forcing factors result from changes in surface circulation that defines the location and boundaries of provinces with varying primary productivity.

The Peconic estuary is subject to fast fluctuations due to physical processes (wind stress) and tides that prevent long-term column stability. The largest vertical temperature difference in the area is not greater than $1.^0$C between the surface and the bottom water indicating that no significant stratification is present throughout the whole year although temporary stratification between 0.5 and 2.5 m over several hours have been reported by Bruno et al. (1983). This vertical mixing of water in the bay is a result of the influx of coastal water through either side of the channels of Shelter Island. Furthermore, eutrophication takes place in the vicinity of the Peconic River outflow and the discharge from the waste water treatment facility into Flanders Bay. As a result, high chlorophyll concentrations and occasional plankton blooming are observed. This is demonstrated with sampling from ship for which chlorophyll data from station 170 have been analyzed over a time frame of 19 years. In order to operate with a homogeneous set of data set, the data were transformed into a uniform X-spacing (time) for which Julian days had to be used and spline estimation was applied to create an interpolated data set. The data that had the highest frequency of ship observations were normalized against the zero mean and analyzed for the time frame 1985 to 2004, of which the results are shown in Figure 1. This procedure to normalize the data set shows basically the deviations from the average and enhances the times during which blooming events can be recognized. It is evident that blooming conditions halted a few years before the year 2005.

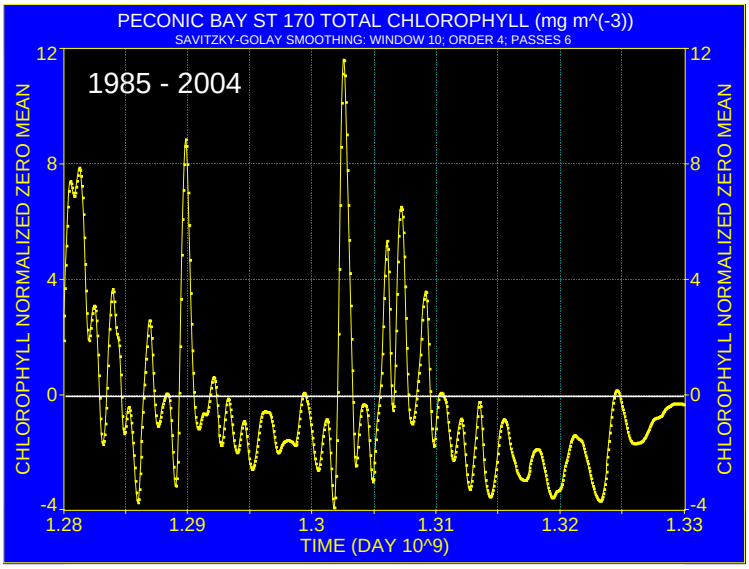

Figure 1: Historical chlorophyll changes based on normalized zero mean ship data in Peconic Bay for station 170 (which corresponds to station 6 in Figure 2) for the period 1985 to 2004.

2 MONITORING OF ALGAL BLOOMS

In the open ocean (Case I water), color can be converted to total pigment concentrations (see for instance Morel and Maritorena, 2001). A shortcoming, however, with satellite derived data of chlorophyll is that with the common algorithm, based on the absorption properties of phytoplankton at 443 nm with respect to 550 nm, the final signal is not vertically resolved and is heavily weighted towards the surface. Furthermore, the water leaving radiance in Case II water varies in connection with the changing composition of the main contributor to the water-leaving radiance. McClain et al. (1993) showed that in the interpretation of recognized patterns, it has to take into account that chlorophyll concentrations derived from water-leaving radiance $L_{w(}\lambda)$s represent not only a composite of various pigments, but is also an optically weighted concentration of a portion of the upper water column from which the light is reflected. In Case II water, chromophoric dissolved organic matter (CDOM), inorganic particulate matter, organic debris and phytoplankton vary in their relative compositions, and consequently, do not necessarily co-vary with the water-leaving radiance and pigment concentrations and are decoupled.

2. a. SPECTRAL PROPERTIES OF ALGAL BLOOMS

Absorption of chlorophyll occurs at two different spectral regions, in the blue and red regions, where high correlation between chlorophyll concentration and the water-leaving radiance exists. Sun-induced fluorescence of chlorophyll is at 685 nm and is also used as an indicator for phytoplankton, (Gower and Borstad, 1981, Bricaud et al., 1995, Garcia and Maske, 1996, Gower et al., 1999, Roesler and Perry, 1995). Solar-induced chlorophyll fluorescence was used by Hoge and Swift (1987) to study the ocean color spectral variability, whereas Gitelson (1992) analyzed the peak near 700 nm on radiance spectra, and found a good correlation with chlorophyll concentrations. A ratio technique using the defined envelope showed that a good relationship exists between the ratio of the reflectance R680/R670 and chlorophyll concentrations (Szekielda et al., 2003). Han et al. (1994) pointed out that there is evidence that suspended matter seemed to have little or no effect on the position of the red part of the chlorophyll absorption band.

During several cruises, in cooperation with the former Long Island University, spectral observations were carried out in the Peconic Bay. Selected individual spectral data that were collected in the Peconic Bay for various salinity domains are shown in Figure 2. They demonstrate that in addition to the well pronounced *in vivo* chlorophyll absorption, other accessory pigments that are associated with plankton influence the shape and intensity of the spectra.

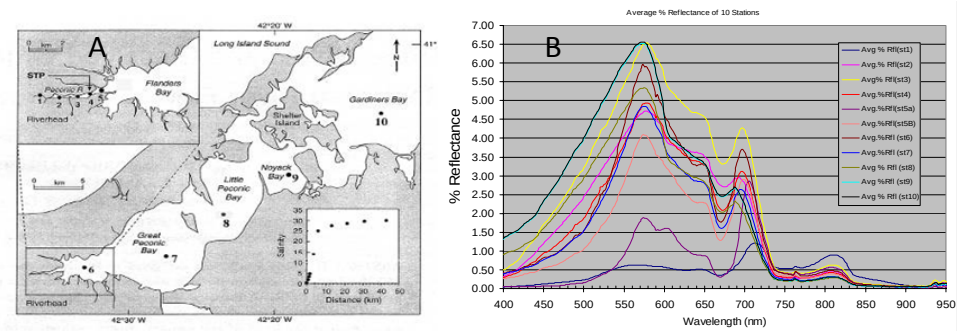

Figure 2: A: station locations in the different bays and salinity distribution as a function of distance from Riverhead based on data collected on a cruise in 2002. (after Szekielda et al.,2003). B: Averaged reflectance spectra through salinity gradients. Stations 6 and 7 correspond to stations 170 and 130, respectively that were monitored by Suffolk County Department of Health Services.

The interpretation of the spectra for coastal eutrophic water shows the major absorption band of chlorophylls at around 420 nm and accessory pigments at 470 nm and 530 nm to 570 nm can be recognized. The spectral region between 400 nm and 500 nm is characterized by strong absorptions of CDOM, carotenoids and the various chlorophylls. The different constituents are responsible for the low sensitivity of reflectance at shorter wavelengths to phytoplankton pigments. Consequently, this wavelength region is not ideal for identifying plankton blooms or related pigments at high chlorophyll concentrations. Minimum absorption of all phytoplankton pigments was observed in the range of 550 nm to 570 nm and results in a peak of reflectance mainly due to scattering by organic and inorganic particles including phytoplankton cells.

Lower salinity regions are characterized by strong absorption at shorter wavelengths that can be attributed to the absorption of high concentrations of CDOM, expressed as dissolved organic carbon concentrations around 550 µM/L. Towards the meso-haline region, carbon concentrations decrease to 180 to 230 µM/L and at the area of Peconic Bay, where mixing completes, the concentrations eventually reach 170 to 180 µM/L with corresponding salinities of about 29. Eutrophication is evident at salinities around 15 and is characterized by the strong absorption over the second absorption band of pigments between 600nm and 700 nm. The distinctive second chlorophyll absorption band is located at 670 nm but its absorption intensity at concentrations > 20 mg m^{-3} is offset by scattering of cell walls. Sun-induced

* Personal communication Prof. C. Gobler

fluorescence is diagnostic at 685 nm but can be significantly altered by re-absorption at chlorophyll concentrations > 15-20 mg m^{-3} (Gitelson, 1992). Chlorophyll still has a significant absorption at wavelengths 690nm to 715 nm although it is partially offset by scattering that result in a shift of the peak position towards longer wavelengths.

2. b. SATELLITE REMOTE SENSING SYSTEMS USED FOR THE PECONIC BAY

The project analyzed data sets from several satellite systems and a description of each is given with emphasis on ground and spectral resolutions, taking into account the spectral properties of phytoplankton organisms.

Sea-viewing Wide Field-of View Sensor (SeaWiFS)

SeaWiFS is designed for ocean color and estimates of chlorophyll in open ocean water. Although the project used the final chlorophyll product as obtained through NASA Goddard Space Flight Center (GSFC), the spectral bands as shown in Table 1 have the potential to derive regional algorithms when applied with supporting ship operations.

Table 1: Band number, center wavelength and bandwidth of SeaWiFS

Band	Center Wavelength (nm)	Bandwidth (nm)
1	412	20
2	443	20
3	490	20
4	510	20
5	555	20
6	670	20
7	765	40
8	865	40

The first band of SeaWiFS is located around the wavelength where most photosynthetic pigments and their degraded products absorb. The second band located at around 443 nm is in the spectral region in which phytoplankton strongly absorbs and has minimum reflectance. At the wavelength around 555 nm, at the “hinge-point”, reflectance is almost independent of chlorophyll concentrations. The second chlorophyll absorption band is covered by SeaWiFS at 670 nm. The channels covering the spectral range at 760 nm and 860 nm were used for atmospheric corrections. From SeaWiFS channels, the

calculated chlorophyll concentrations are based on an algorithm that uses the ratio of 490 nm and 555 nm:

Chl = -0.040 + 10^[0.341 - 3.001 * X + 2.811 * X^2 - 2.041 * X^3]
X = log10 [Rrs(490)/ Rrs(555)]

The SeaWiFS bio-optical algorithm applied for chlorophyll has the objective of performing at 35% accuracy over a range of 0.05-50 mg m^{-3} although this algorithm was established for open ocean water.

Moderate Resolution Spectrometer (MODIS)

MODIS is a passive imaging spectroradiometer which views the Earth and space by means of a continuously rotating scan mirror and collects data over the spectral region 412 nm to 14,235 nm of which only a few are suitable for water color determination. The instrument has a ground nadir resolution of 1000 m and the scan mirror has coverage of ±55˚ from nadir that results in a cross track swath of 2330 km and an along track swath of 10 km at nadir. For more details refer to Hatten et al., (1999). MODIS channels selected for this study are shown in Table 2.

Table 2: Band characteristics of the Moderate Resolution Spectroradiometer (MODIS) as applied in the present study

Band	Center Wavelength (nm)	Bandwidth (nm)	MODIS Spectral Region	Ground Resolution (m)
8	412	15	VIS	1000
9	443	10	VIS	1000
10	488	10	VIS	1000
11	531	10	VIS	1000
12	551	10	VIS	1000
13	667	10	NIR	1000
14	678	10	NIR	1000

The chlorophyll-*a* data derived from the MODIS sensor are experimental and show significant deviation from actual chlorophyll concentrations based on ship measurements. However, “chlorophyll” derived from MODIS observations can be used for feature identification and tracking. The actual value of the chlorophyll-*a* is somewhat controversial due to differences when compared to data derived from the SeaWiFS sensor. Based on this

discrepancy, the project focused on the analysis of SeaWiFS after statistical comparison between MODIS and SeaWiFS was undertaken. The disadvantage of both sensors, SeaWiFS and MODIS, is the low ground resolution of about 1000 m.

Landsat and Advanced Land Imager (ALI)

Landsat 7 carries the Enhanced Thematic Mapper Plus (ETM+) which is an improved Thematic Mapper (TM). The ETM+ design provides for a nadir-viewing, eight-band multi-spectral scanning radiometer capable of providing high-resolution image information of the Earth's surface The ETM+ is designed to collect, filter and detect radiation from the Earth in a swath 185 km wide as it passes overhead and provides the necessary cross-track scanning motion while the spacecraft orbital motion provides an along-track scan.

ALI, in connection with Hyperion, is flown on the Earth Observatory and flies in tandem with Landsat-7 in the same orbit one minute apart. The overall configuration is given in Figure 3 with the corresponding ground tracks for both satellite systems and swath coverage. The spectral bands for ALI are listed in Table 3.

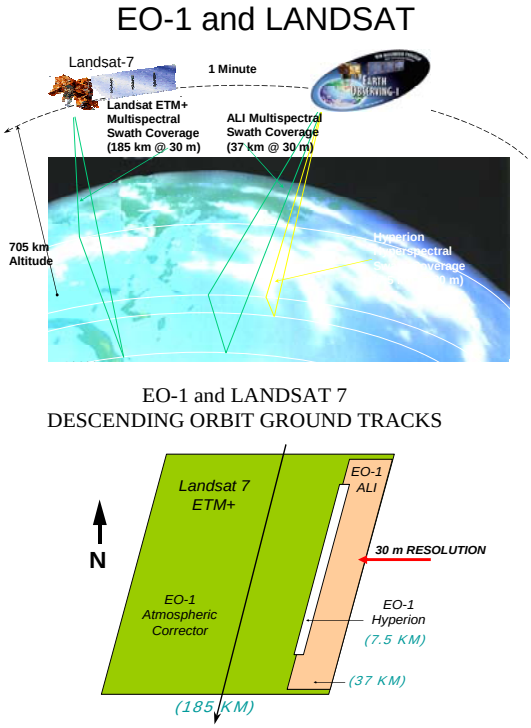

Figure 3: Satellite configuration for Landsat 7 and EO-1 with the corresponding ground tracks.

Table 3

ADVANCED LAND IMAGER

BAND	WAVELENGTH (µm)	GROUND SAMPLE DISTANCE (m)
PANCHROMATIC	0.48 - 0.69	10
MS - 1'	0.433 - 0.453	30
MS - 1	0.45 - 0.515	30
MS - 2	0.525 - 0.605	30
MS - 3	0.63 - 0.69	30
MS - 4	0.775 - 0.805	30
MS - 4'	0.845 - 0.89	30
MS - 5'	1.2 - 1.3	30
MS - 5	1.55 - 1.75	30
MS - 7	2.08 - 2.35	30

The advantage of ALI is the ground resolution of 30 meters for the spectral bands and 10 meters for the panchromatic band that covers the spectral region between 480 nm to 690 nm which is also the spectral region where plankton has the major absorption and reflectance properties. Furthermore, the panchromatic band can be used for image fusion that results in a higher ground sample distance for the other channels with 30 meter ground resolution.

3 INVENTORIES AND PROCESSING OF DATA

Under the project, acquisition of satellite data for the Peconic Bay were accessed under user agreements with NASA Goddard Space Flight Center and the United States Geological Survey (USGS) while processing of the received data was conducted with available software and hardware at City University of New York, Hunter College. Only TableCurve software for additional processing and statistics was procured under the project. The available data base that was established is in digital form and includes Landsat MSS, Landsat TM and Landsat TM+ and MODIS. Except for ALI data, images have been acquired through user agreements with NASA and the United States Geological Service at no cost to the project.

3. a. Satellite data acquired for Peconic Bay

The use and evaluation of satellite coverage concentrated on the application of SeaWiFS, MODIS, Landsat TM 5, Landsat 7 ETM+ and ALI. In addition,

land cover data were acquired from the USGS for the spring of 2001. The acquired data for this project are summarized in Annex 1.

Advanced Land Imager (ALI)

A data acquisition Request (DAR) for the Peconic Bay was placed in July 2007. The first opportunity for coverage by the USGS was announced on October 31, 2007 for which arrangements were also made to have ship coverage. However, at that time, no satellite coverage was provided as another test site had priority. The USGS made alternative arrangements on November 8, 2007 and November 28, 2007 but the data collected were contaminated with greater than 20% clouds. Information that coverage with cloud contamination was completed was related several days after. An additional collection under cloud-free conditions was fulfilled on December 1, 2007. The corresponding screen image as JPEG was transmitted for consideration. Careful examination of the image, however, showed also slight cloud contamination and, subsequently, no order was placed. However, two images that existed in the USGS data bank were procured under commercial terms.

Sea-Viewing-wide Field-of-View Sensor (SeaWiFS)

The project personnel registered with NASA and were granted access to the data bank as an authorized user for scientific research. All data for 2001 were screened for scene quality, coverage and contamination by clouds for the area under investigation, and data were processed and subjected to geometric correction. The selected images over the Peconic Bay were subsets for a region that covered the area from the New Jersey coast to the Gulf of Maine. Further sub-setting was done in order to narrow the coverage for the Peconic Bay. The processed images that were acquired in digital form and preprocessed with ENVI are given in Annex 2.

Moderate Resolution Imaging Spectroradiometer (MODIS)

The Moderate Resolution Imaging Spectroradiometer (MODIS) has an improved signal to noise ratio (SNR) and spectral and radiometric performance compared to SeaWiFS. As MODIS has more bands than SeaWiFS, it has the capability to provide additional spectral information. All acquired MODIS images were reprocessed for chlorophyll concentrations and geo-referenced. In addition, ratioing techniques were applied to retrieve further information aside from chlorophyll.

3. b. Data Processing

ENVI, a product of Research Systems, Inc.in Boulder, CO., was used as a software package for the visualization, analysis, and presentation of all digital imagery. Its processing package includes spectral tools, geometric correction, terrain analysis, and raster and vector GIS capabilities. ENVI includes all of the remote sensing basics required for the research, such as registration, calibration, band math, classification, contrast enhancement, filtering, principal components transforms, band ratios, vegetation indices, edge detection, image sharpening, batch processing and map composition. In addition to traditional classifications (isodata, k-means, parallelepiped, minimum distance, maximum likelihood, and Mahalanobis distance), ENVI was used for spectral analyses and pixel classification.

The software TableCurve 2D allows for fitting approximating functions, fitting parametric functions, non-parametric interpolation, noise reduction and derivative estimation. The primary automation uses MS Excel or text files. These multiple sets are then processed with the ease of a single set. The automation output can be written to an MS Word (or generic RTF) file for all graphs and numeric summaries and to MS Excel for numeric data.

Many of the acquired Landsat data were found to be noise contaminated and had to be processed with a filter. Among various filters available in the ENVI main filter menu is one adaptive filter, the Enhanced Lee filter that reduces speckle while simultaneously preserving edge sharpness or texture information. It was applied with local statistics (coefficient of variation) within individual filter windows. Basically, each pixel is put into one of three classes, namely, homogeneous, heterogeneous or point target. For the homogeneous class, the pixel value is replaced by the average of the filter window. For the heterogeneous class, the pixel value is replaced by a weighted average. For the point target class, the pixel value is not changed.

Atmospheric corrections and Lee filtering demonstrated that a better image could be generated and it became evident that the overall quality of the image was an improvement over the original data set.

For a quantitative analysis of surface reflectance, atmospheric corrections were applied for the visible and near-infrared data of Landsat 7 ETM+. To correct for atmospheric effects in the Landsat images, ENVI's atmospheric correction module, FLAASH (Fast Line-of-sight Atmospheric Analysis of Spectral Hypercubes) was used. This module incorporates the MODTRAN 4 radiation transfer code and produces an estimate of the true surface reflectance.

4 RESULTS OF SATELLITE OBSERVATIONS

4.a. Sea-Viewing-wide Field-of-View Sensor SeaWiFS

All available SeaWiFS chlorophyll data for the year 2001 were geometrically corrected and the corresponding values for the stations 170 and 130 are shown in Figure 4.

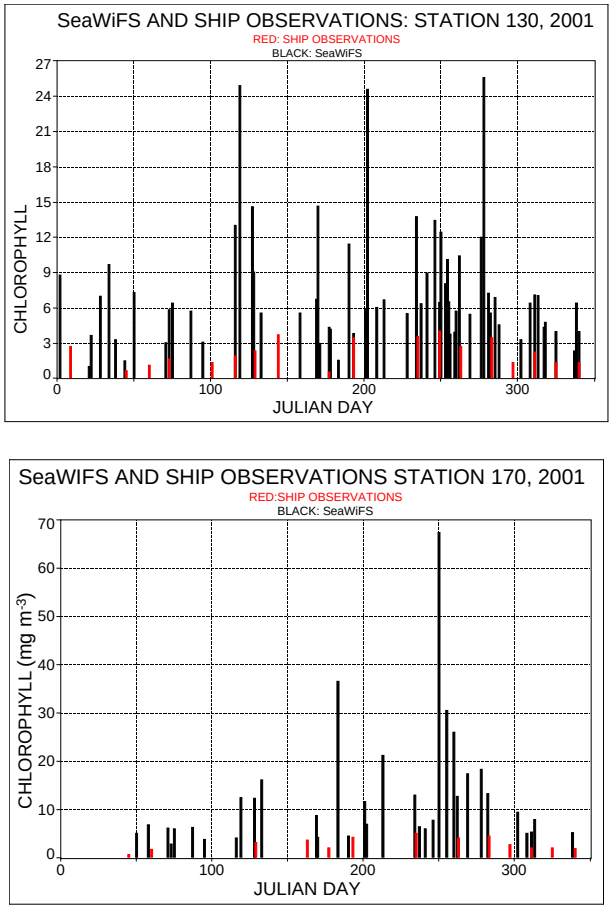

Figure 4: Chlorophyll observations in the Peconic Bay with conventional ship observations (red) and SeaWiFS (black) for station 130 (upper graph) and station 170 (lower graph). For location of the station, refer to Figure 2.

In that time frame, aside from the higher frequency of observations with SeaWiFS, it is evident that the ship observations had no indication of significant bloom events while the satellite observations showed at several occasions elevated chlorophyll concentrations. In particular, station 170,

which is located in Flanders Bay, reached maximum concentrations close to 70 mg m^{-3}.

As only two ship measurements throughout coincided with the satellite observations, the two data sets were processed with spline interpolation and the Savitzy-Golay smoothing technique. Figure 5 presents the results for station 130 and shows the expected general yearly trend. However, only thirteen ship measurements for 2001 were obtained for comparison with the satellite observations and, therefore, the trend of ground measurements is not very reliable compared to the higher density of satellite observations, although the time of spring maxima and early summer minima for both data sets were observed.

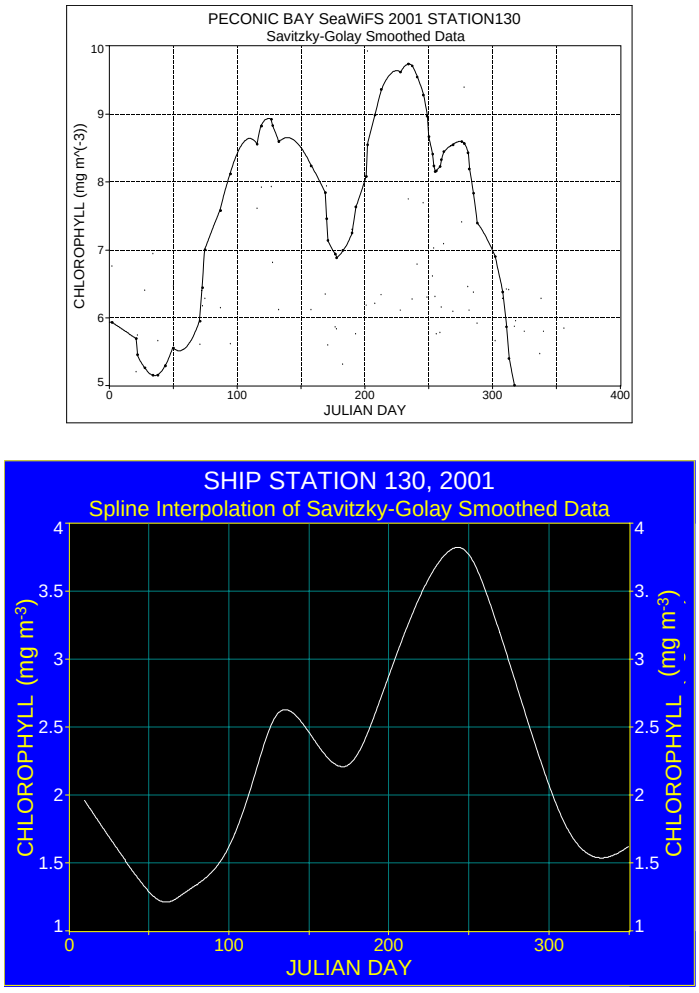

Figure 5: Processed chlorophyll data for station 130 derived from SeaWiFS (upper graph) and ship observations (lower graph).

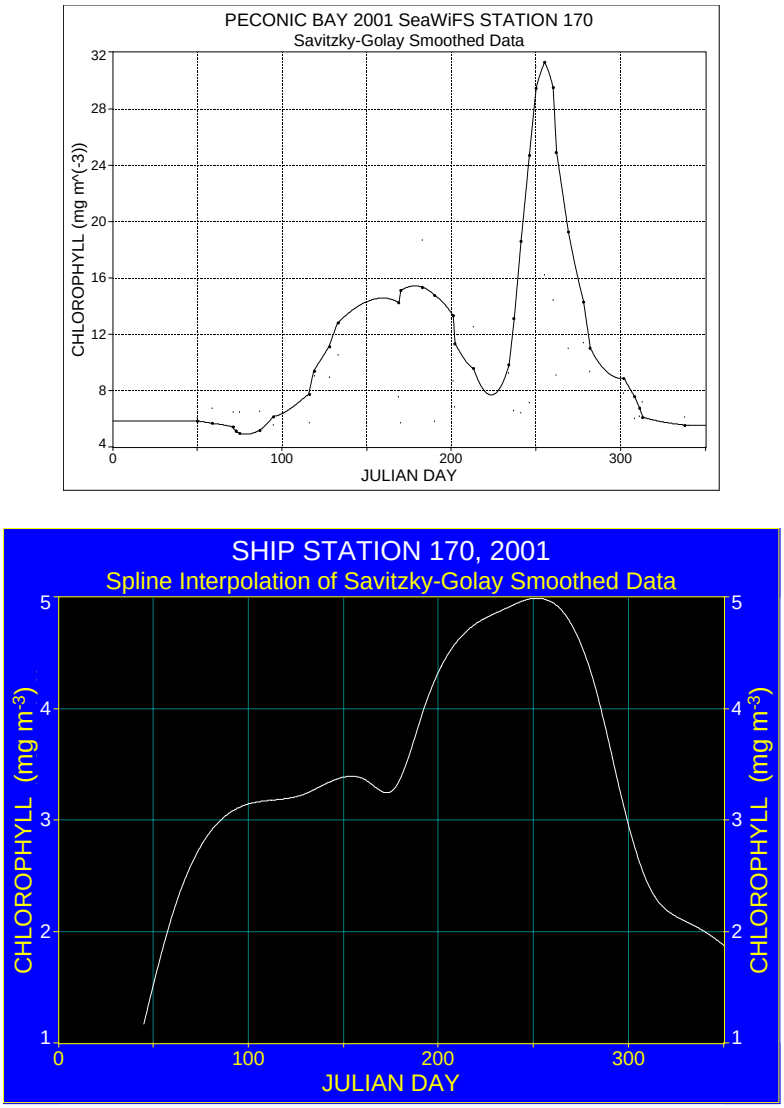

Figure 6: Processed chlorophyll data for station 170 derived from SeaWiFS (upper graph) and ship observations (lower graph).

SeaWiFS and ship data for station 170 are displayed in Figure 6. The satellite observation revealed intense blooming during the late summer when maximum chlorophyll reached close to 32 mg m^{-3}. Although general trends can be established with a statistical method, one has to take into account that spline interpolation and the application of Savitzky-Golay smoothing result in a general description of the annual changes but to a certain degree suppress short-lived blooms that are recognized in the original data (compare with Figure 4). Moreover, the ground resolution of one kilometer integrates the concentration over a large area and, consequently, it is difficult to appraise

against a single measurement on the ground. Furthermore, the tidal range and patchiness dispersion may change the horizontal and vertical distributions of plankton within a time frame of minutes to hours which make it problematic to use the "data of opportunity". For the year 2001, several ship operations were executed with regular sampling and continuous recording of chlorophyll by fluorescence allowing an approximation for the validation of SeaWiFS data. Figure 7 shows continuous recordings of chlorophyll estimated by fluorescence from Shinnecock Canal through Peconic Bay to Riverhead 18 September 2001. In the vicinity of station 130, chlorophyll concentrations of about 7 mg m^{-3}were observed. SeaWiFS on September 17, indicated concentrations of chlorophyll at 5.8 m^{-3} and two days later on September 19, SeaWiFS measured 10.5 mg m^{-3}.

For station 170, ship measurements indicated concentrations of chlorophyll of around 12 mg m^{-3} for September 18. The closest SeaWiFS measurements on September 17 showed concentrations of 26.2 $m^{-}3$ and the corresponding SeaWiFS measurements for September 19 were 12.9 m^{-3}.

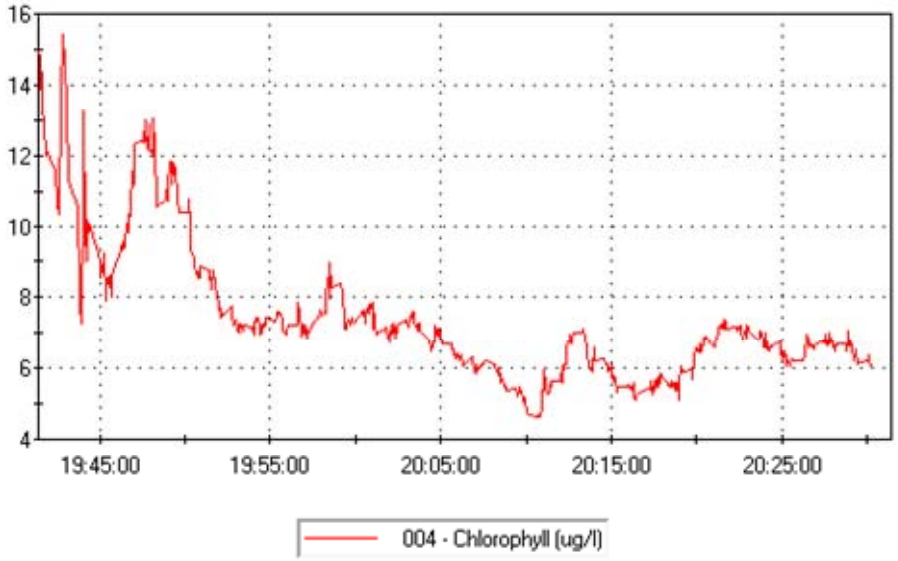

Figure 7: Continuous chlorophyll recordings by fluorescence from Shinnecock Canal through Peconic Bay to Riverhead September 18, 2001.

Another record of chlorophyll that was obtained through continuous fluorescence measurements on October 16, 2001 (Figure 8) showed lower concentrations of chlorophyll compared to the concentrations found on September 18. For station 130, the concentrations were around 5 mg m^{-3}. The closest match of ground observations with SeaWiFS was for October 15 and the corresponding chlorophyll concentrations were found to be 4.6 mg m^{-3}.

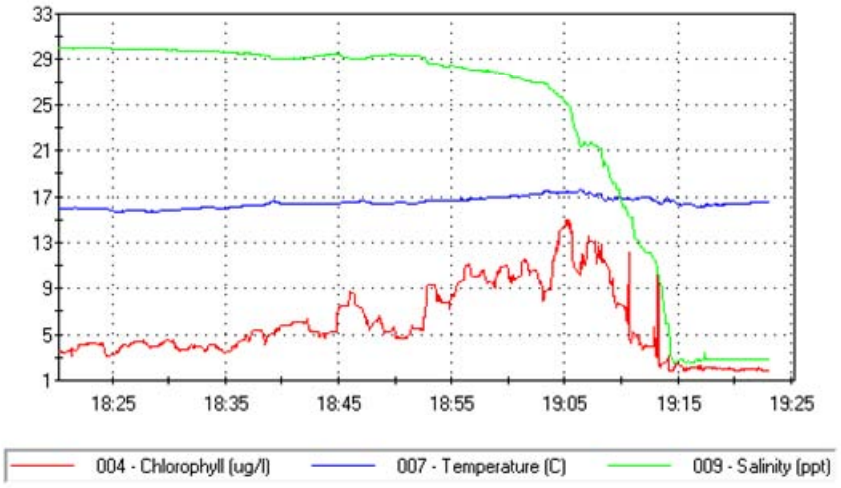

Figure 8: Continuous chlorophyll recordings by fluorescence, temperature and salinity from the middle of the Peconic Bay to Riverhead on October 16, 2001.

4. b. Moderate Resolution Imaging Spectroradiometer (MODIS)

As MODIS radiometric specifications have the appropriate spectral bands that are close to the absorption bands of chlorophyll, it is useful to apply the data in the spectral region of the second absorption band of chlorophyll near 667 nm. This spectral region is not only chlorophyll specific but is also less influenced by the presence of other optically relevant substances such as suspended inorganic matter and chromophoric dissolved organic matter. The concept of using a ratio has been evaluated in coastal water with high concentrations of chlorophyll (Szekielda et al. 2003). In this study, an approach was introduced to apply the ratio technique using MODIS bands that have their full width at half maximum (FWHM) at 667 nm and 678 nm, respectively, and to relate them to the ratio 443 nm/551 nm. Normalized water-leaving radiance from MODIS, as described in detail by Gordon and Voss (1999), was used.

As the components in suspended matter of the coastal environment respond spectrally differently from each other and due to the fact that the photon penetration depth is a function of wavelength, the ratio 443 nm/550 nm is not necessarily correlated with ratios at longer wavelengths. This is shown in Figure 9 in which identified clusters are displayed as referenced regions of interest. In order to interpret the clusters as well as the mapped regions of interest, it is meaningful to compare the region that characterizes open ocean water. According to the low photon penetration depth, the ratio 678 nm/ 667 nm is close to constant because the low concentrations of chlorophyll and the water-leaving reflectance are received from a short water column. The ratio 443

nm/551 nm, in contrast, shows the reflectance over a deeper water column and absorption of incident light by chlorophyll at the spectral region where the Soret band is located. Figure 10 shows the clusters displayed with the corresponding color annotation shown in Figure 9. Purple identifies the open ocean water (Case 2 water) that is characterized by low chlorophyll concentrations. While the ratio 443 nm/551 nm decreases with increasing chlorophyll concentration, the ratio 678 nm/667 nm increases with increasing chlorophyll concentration and as a result, an inverse relationship exists.

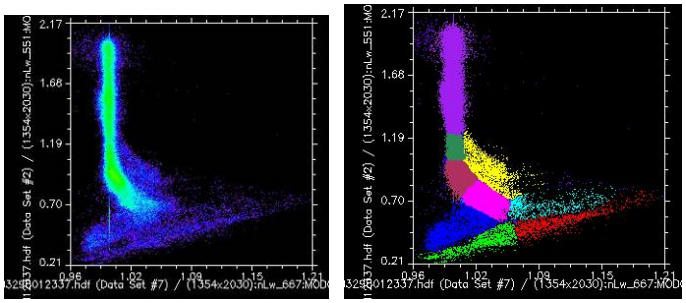

Figure 9: Scatter diagram for the region for the ratio 443 nm/551 nm versus the ratio 678 nm/667 nm. Right side shows the corresponding identified cluster used to identify regions of interest presented in Figure 10.

Figure 10 shows the chlorophyll concentration patterns as derived with the standard algorithm that is applied to MODIS data. The major problem associated with this algorithm is that it breaks down in coastal Case 2 water and no additional information is obtained to differentiate the various water constituents and their origin through river discharge, sediment erosion and eutrophication.

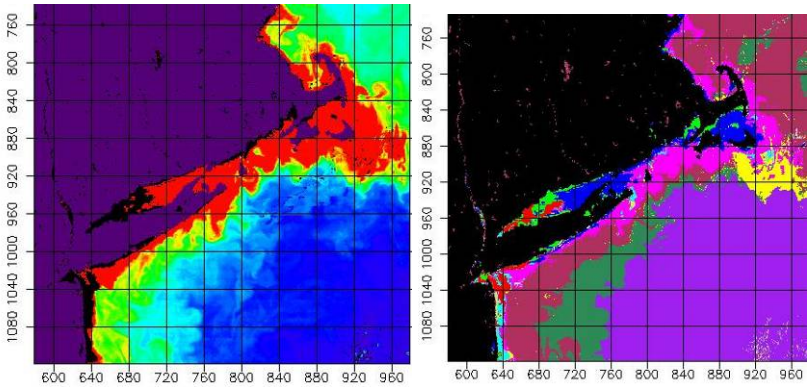

Figure 10: Left graph: Chlorophyll distribution along the East coast of the United States based on MODIS observations on September 8, 2002. Right graph: Identification of different bio-geochemical provinces based on regions of interest as shown in Figure 9.

Variability in the biogeneous compartment of Case 2 water and the decoupling between chlorophyll, chromophoric dissolved organic matter, inorganic suspended matter, organic detritus and bacteria may be the cause for recognition of biogeochemical provinces in cluster diagrams. Therefore, distinctive clustering appears in spectral space allowing the use of two dimensional scatter plots to design pattern classifiers. It can be concluded that this approach can be used as separating biogeochemical provinces in connection with chlorophyll measurements based on the use of the first and second absorption bands of chlorophyll. However, similar to SeaWiFS, the coarse resolution of MODIS is not very useful in covering small areas like the Peconic Bay, and small scale features in the distribution of particulate and dissolved matter may not be recognized. Therefore, higher spatial and spectral resolution data that can be obtained by HYPERION will provide more detailed information on the pattern distribution of different water masses. Due to budget constraints, however, and problems of timely acquisition through the USGS, only one HYPERION that unfortunately did not cover Peconic Bay, but was obtained free of charge, could be analyzed. The results of this study are presented in Annex 3 and document that higher spatial resolution of 30 meters and high spectral resolution, have far better information compared to the other satellite systems from which data were analyzed.

4.c. Advanced Land Imager (ALI)

Multi-spectral imagery that were recorded by the Advanced Land Imager (ALI) and procured from the USGS proved to be a valuable and promising tool for plankton detection in the Peconic Bay. As ALI has so far the best optical characteristics and spatial resolutions of 10 and 30 meters, it was decided to pursue coverage and define the conditions under which planning needed to be made with the USGS to provide data for the Peconic Bay.

Unfortunately, USGS could not provide an overflight when a timely planned ship operation was scheduled for ground truthing, and alternative times of coverage was given only days after ground sampling was accomplished. There was coverage over the Peconic Bay of which only one was under quasi cloud-free conditions. A careful examination of the JPEG image, however, showed slight contamination by low clouds. All three acquisition approaches are documented in Figure 11 of which none was procured.

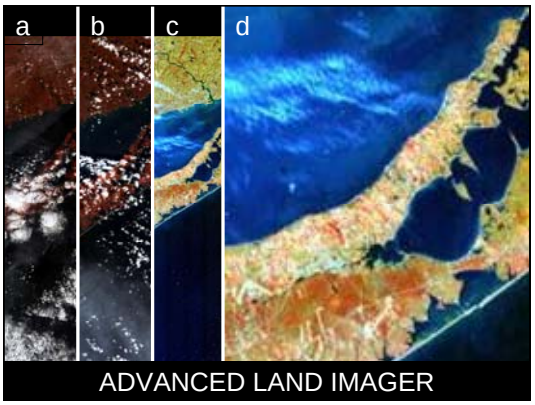

Figure 11: Peconic Bay coverage with ALI. a: First attempt, November 8, 2007 (Julian day 312). b: second, November 28, 2007 (Julian day 332) c: third, December 1, 2007 (Julian day 335). d: Enlarged JPEG browse image December 1, 2007 (Julian day 335). Cloud coverage that was recognized over Long Island Sound extended partly into the Peconic Bay.

ALI products obtained with sets of multi-spectral images were procured under commercial terms from the USGS. A few image samples are documented that resulted in the use of various image processing techniques.

Single channel display

Figure 12 shows a display of ALI data for the spectral region between 525-605 nm where plankton has its maximum reflectance, but bathymetry may have an impact on the recognized patterns in this spectral region. The high absorption on the northern part of the Peconic Bay indicates that blooming occurred mainly in the central part of the bay.

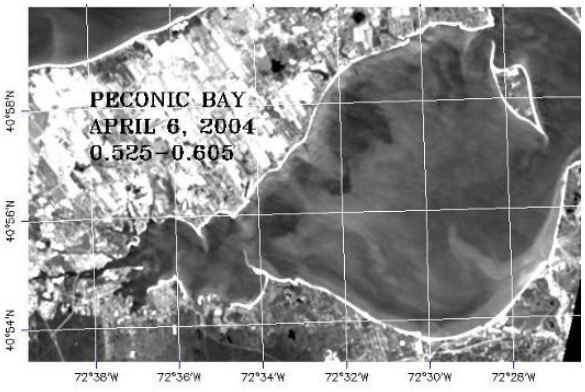

Figure 12: Patch recognition in Peconic Bay on April 6, 2004 for the spectral band 0.525-0.605 µm.

Extraction of spectral information

Spectral sampling from ALI data were carried out in connection with the image analysis. Although ALI has very broad spectral bands, the response as shown in Figure 13 for spectral sampling of area 1 compared to area 2, shows the high absorption at shorter wavelengths with a slight shift in the absorption maxima where a higher concentration of plankton is apparent. The spectral response for the near-shore station 1 shows an absorption minimum at 492 nm and a maximum at 572 nm, whereas station 2 has higher reflectance properties with an absorption minimum at 477 nm and a reflection maximum at 565 nm. Although small in spectral shift, in combination with the large difference in radiance, the data show that variation in the composition of suspended material in the water column is present.

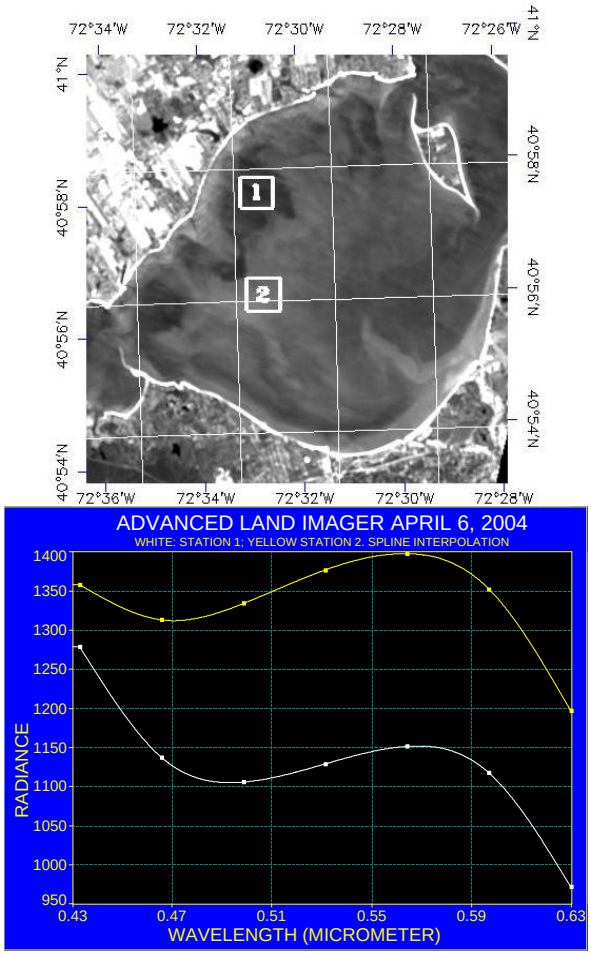

Figure 13: ALI image on April 6, 2004 from which spectra were extracted as shown in the lower graph.

Cluster analysis, ratioing techniques and establishing regions of interest (ROI)

Ratioing techniques partly eliminate the atmospheric impact and sun angle changes. Therefore, ratios were applied to ALI data using the spectral bands that are closest to the absorptions band of chlorophyll in the blue and red regions, respectively, and as a reference point the spectral region at around 525 nm where phytoplankton has its highest reflectance. Two selected ratios are displayed in Figure 14 and were combined with the band that is spectrally located at around 0.630 µm. The result from this multi-spectral composite is shown in Figure 15.

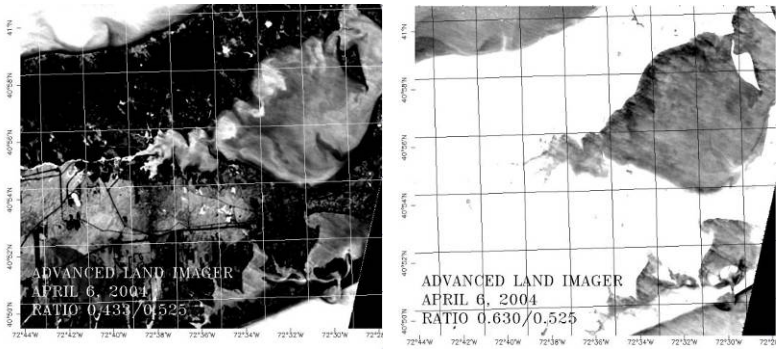

Figure 14: Ratio building of wavelengths 0.433 µm/0.525 µm (left figure) and 0.630 µm /0.525 µm (right figure).

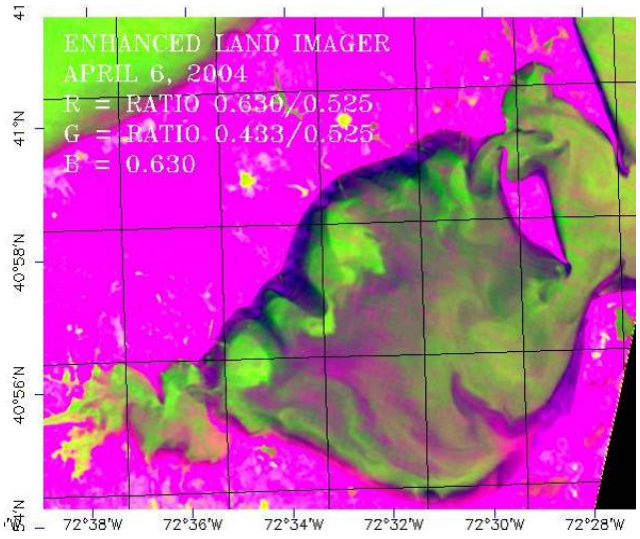

Figure 15: Color composite of ratio bands 0.630/0.525 and 0.433/0.525 with incorporation of the spectral band at 0.630 µm.

The application of MODIS data (see section 4b) showed that biogeochemical provinces can be detected through the use of clustering techniques. The same approach of using cluster identification was used with ALI data by isolating "regions of interest" (ROI) with subsequent color annotations as shown in Figure 16. The resulting Figure 17 incorporates the regions of interest and demonstrates that biochemical provinces can be separated to a detail.

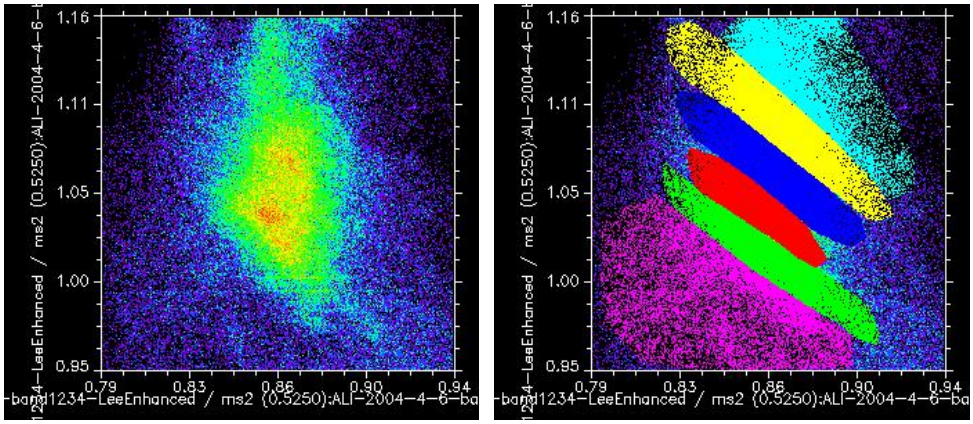

Figure 16: Clustering of ratio data and separation of regions of interest for mapping patchiness of parameters.

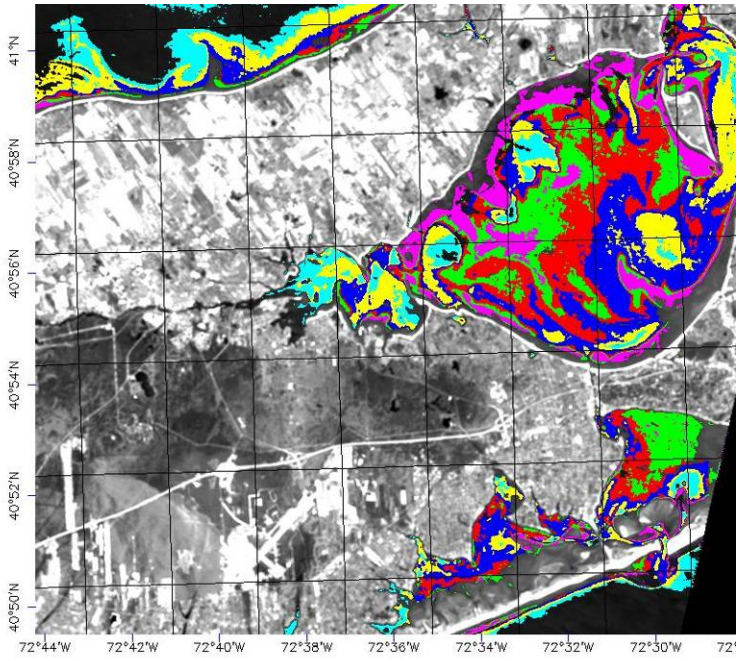

Figure 17: ROI distribution and cluster identification based on ratio imaging.

Although the annotation of provinces to identified patterns is a rather qualitative method and can be subjective, it allows recognizing more details in the distribution and patchiness of plankton although limited by the broad spectral bands of ALI.

Fine scale distribution in patchiness can be obtained with panchromatic data that have a 10 meter resolution together with a horizontal radiance profile as shown in Figure 18. It demonstrates the heterogeneity that one might encounter during bloom conditions. Furthermore, it indicates the problem of sampling from ship operations in determining the distribution of plankton or parameters that are related to blooming. Comparing observations from ships with remote sensing data is very limited especially if the ground sampling is not in full sync during the acquisition of both data sets.

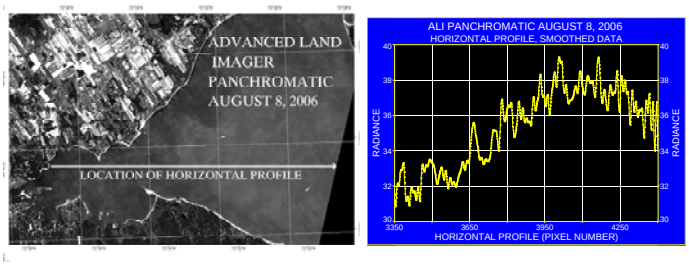

Figure 18: Location of horizontal profile of the panchromatic image of ALI (left) and the corresponding radiance levels (right).

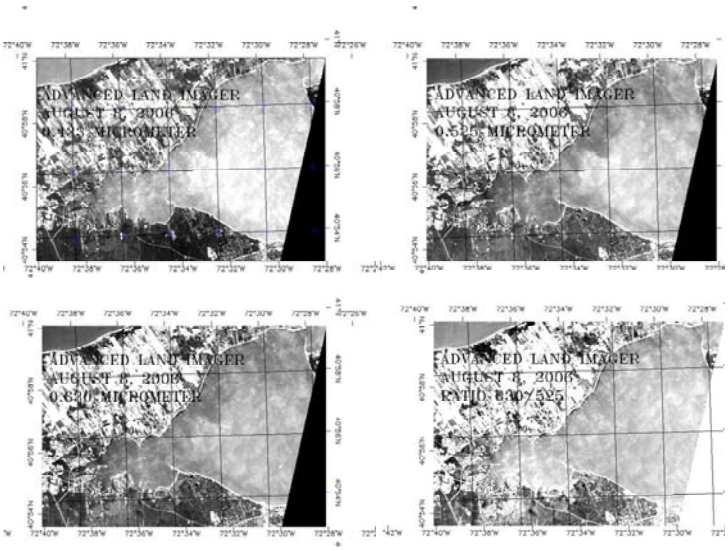

Figure 19: ALI 0.433 µm, 0.525 µm and 0.630 µm images for August 8, 2006. The lower right shows the ratio image 0.630/0.525.

Figure 19 shows ALI data for the spectral bands 433 nm, 525 nm, 630 nm and a ratio image 0.630/0.525 on April 6, 2004 and August 8, 2006. Images recorded on August 8, 2006 show elongated patchiness in a NW-SE direction. In order to obtain more details on the patchiness, the images with 30 meter ground resolution were merged with the 10 meter resolution panchromatic band and the resulting images are given in Figure 20. A comparison of the images from two different dates point to the presence of Langmuir circulation (Lc) in the August 8, 2006 ALI image that is responsible for streak-like alignment of plankton material through the convergence and divergence zones.

Langmuir circulation is often made visible by accumulation of buoyant material and natural films in the regions of surface convergence. These are interpreted as 'windrow' patterns induced by Langmuir circulation, which form in wind speeds of ~3 m sec-1 and above. Wind speed and gust at Mattituck (Figure 21) was recorded to exceed 3 cm s^{-1} and therefore, the linear arrangement of plankton is interpreted as the effect of accumulations of algal material in the surface convergence zones of Lc.

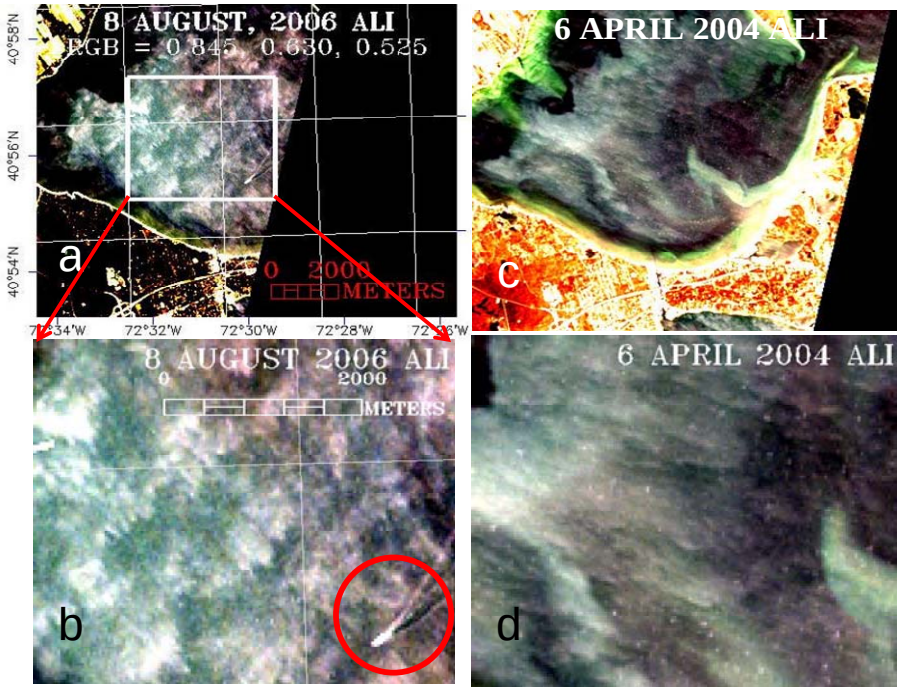

Figure 20: ALI 30 meter resolution images merged with the 10 meter panchromatic band and presented as RGB images for August 8, 2006 (a) and April 6, 2004 (c). The lower images b and d are the corresponding zoom images indicated as white square in Figure a.

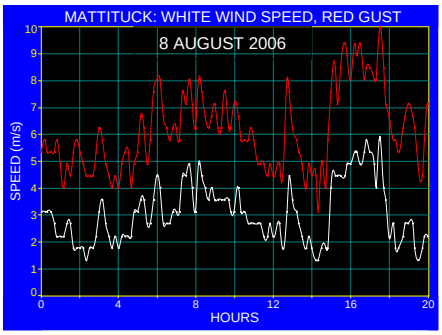

Figure 21: Wind speed and gusts in Mattituck during August 8, 2006.

The presence of high plankton concentrations observed with ALI data (Figures 19, 20a and 20b) is confirmed with observations by Gobler et al. (2008) who detected Coclodinium for the first time in July, and reported for August through September, cell densities commonly at $>10^4$ ml^{-1}. It can be argued that, probably due to the broad time spacing of sampling, some short-lived blooms may not have been observed with the ship data as shown in Figure 22. Under bloom conditions, Lc is able to change the distribution of organisms close to the surface within a time frame of 30 minutes which has been observed with repeat aircraft flights over cynanobacteria blooms (Szekielda et al., 2006). Furthermore, the ship wake shown in Figure 20b, in the red circle, indicates that the observed blooming is close to the surface because low radiance is observed behind the ship where water mixes from below to the surface through propeller action.

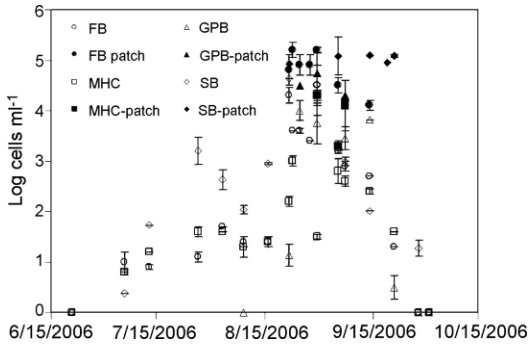

Figure 22: Log of Cochlodinium cell densities recorded during the summer of 2006 in Flanders Bay (FB: circles), Meetinghouse Creek (MHC: squares), Great Peconic Bay (GPB: triangles), and eastern Shinnecock Bay (SB: diamonds). Open symbols represent fixed stations, whereas closed symbols represent dense bloom patches present at each location. Error bars are standard error of triplicate field samples. (after Gobler et al., 2008).

It can be concluded that ALI provides sufficient ground resolution and appropriate spectral bands, although broad, in recognizing blooming in the Peconic Bay. Although not directly proven, it might be useful to derive, together with simultaneous ship observations, local algorithms for a quantitative analysis either for chlorophyll or for spectral recognition of plankton species during blooming events. The selection of regions of interest (see Figure 17), for instance, demonstrate that from the images, interpretation of clusters can be derived from different spectral bands.

4. d. LANDSAT

Several Landsat scenes were available and were acquired at various tidal stages for which tidal stations at Montauk and Jamesport were used as references for comparison with Landsat scenes.

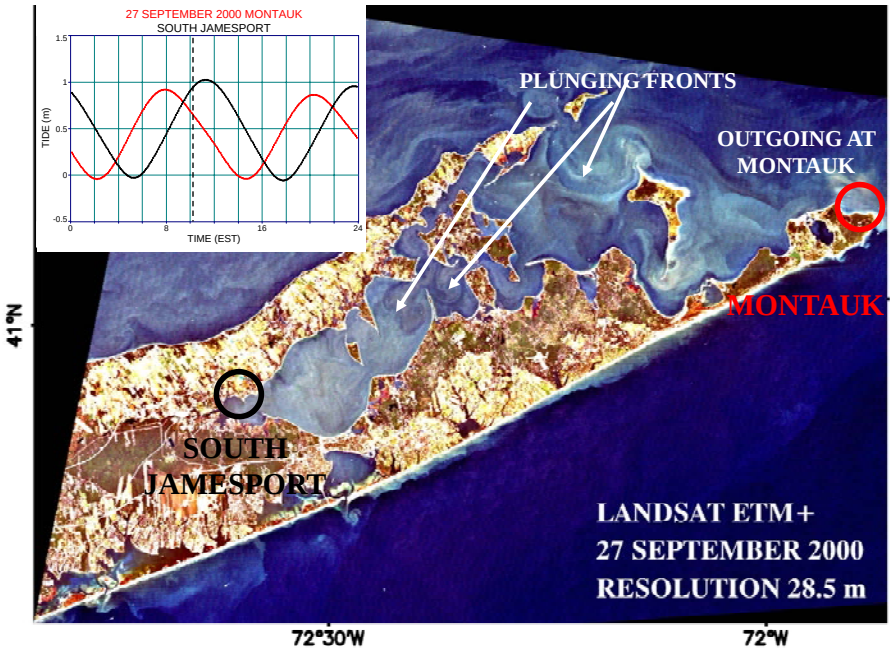

Figure 23: Landsat image obtained on September 27, 2000 with the Thematic Mapper (ETM+). The tidal range for Montauk and South Jamesport are included in the insert as reference for Landsat image interpretation. The dashed line indicates the time of overpass.

Figure 23 presents the Landsat overpass on September 27, 2000 and the corresponding tidal range for Montauk and South Jamesport. During data acquisition of Landsat, tides at South Jamesport were incoming whereas the station at Montauk registered outflowing tide. Figure 24 shows a sub-scene of

this image that emphasizes the surface manifestation between Orient Point and Gardiner Island. This structure has not been reported elsewhere and seems to be a result of frontogenesis. Stegmann and Ullman (2004) investigated the variability in chlorophyll and sea surface temperature fronts in the Long Island Sound outflow based on one kilometer spatial resolution but suggested that strong frontogenic tendencies exist very close to Block Island although unresolved by their analysis.

An interpretation of the image shown in Figure 24 takes into consideration observations by Marmorino and Smith (2007) who observed an inflow jet and plunge front in Sequim Bay, Washington that have similar structures as those observed at the region between Orient Point and Gardiners Island. Strong flow over the bottom makes the flow turbulent and a front line is formed through tidal intrusion of water from Long Island and Block Island Sound. Without any further hydrographical data, it can only be assumed that dense fluid entering the sound leads to a plunging front and formation of a leading internal wave.

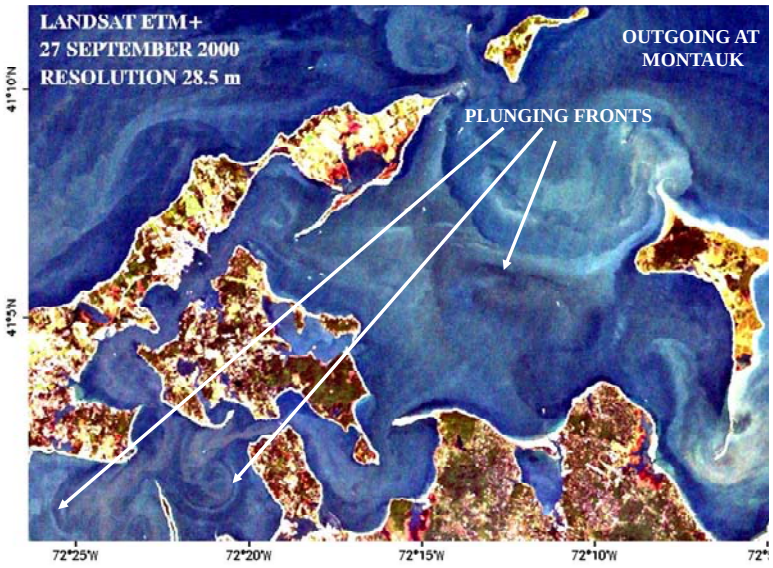

Figure 24: Detailed map of plunging fronts. For overall image, see Figure 23.

The incoming tide through the two channels around Shelter Island generates two jets of which one is seen in directing its water into Noyack Bay, forming a plunging front with what seems to be a leading internal wave. The northern flow around Shelter Island seems to separate from the southern flow and is directed into Little Peconic Bay. As shown in Figure 25, Great Peconic Bay shows no strong gradients at this tidal stage, but elevated radiance levels indicate higher concentrations of particulate matter.

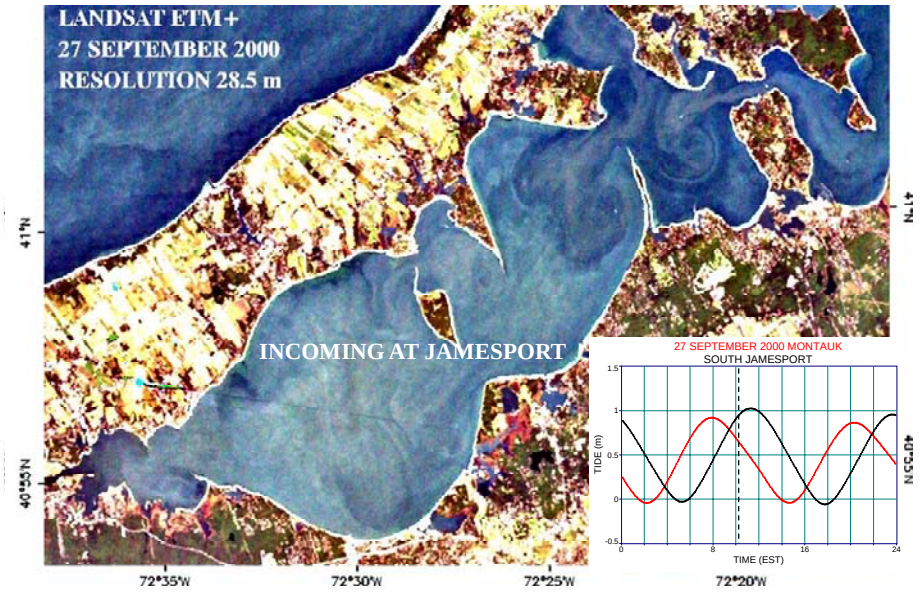

Figure 25: Flanders Bay, Great Peconic Bay, Little Peconic Bay, Shelter Island Sound (Noyack Bay and Southold Bay) as observed on September 27, 2000. For overall view, see Figure 23.

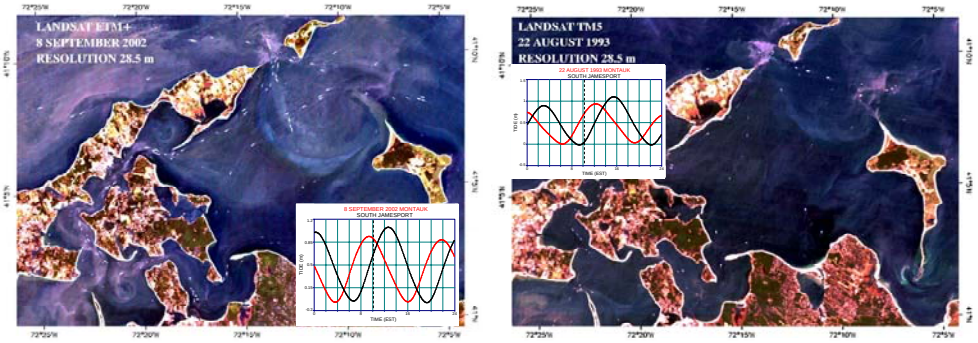

Figure 26: Plunging front observed on September 8, 2002 with Landsat ETM+ (left) and on August 22, 1993 with Landsat TM5 (compare also with Figure 24).

The plunging front (shown in Figure 24) was again observed on September 8, 2002 and on August 22, 1993 with imagery as shown in Figure 26. That the observed front is not a permanent feature is demonstrated with coverage on October 20, 2000 during which both tidal stations at South Jamesport and Montauk, respectively, recorded the tidal range close to low tide (Figure 27).

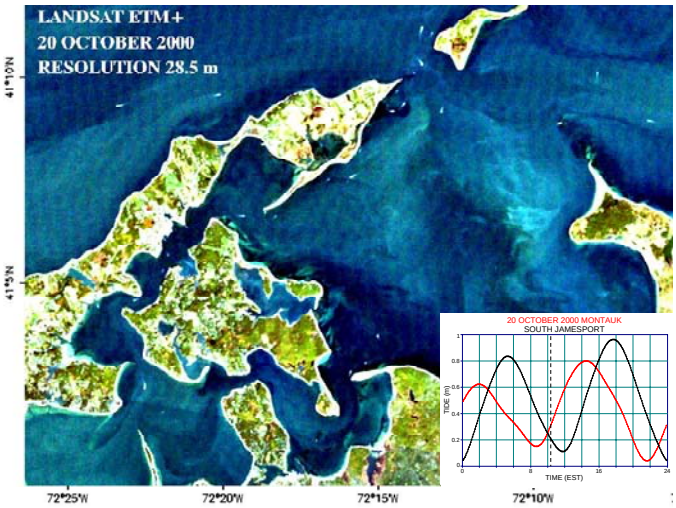

Figure 27: Landsat ETM+ coverage on October 20, 2000 of Gardiners Bay.

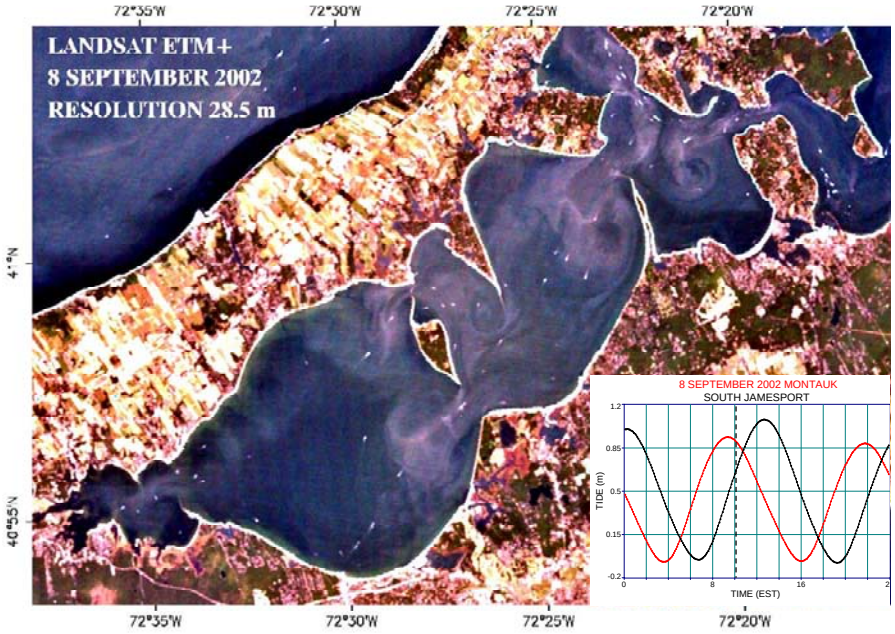

Figure 28: Landsat ETM+ coverage on September 8, 2002

The complicated distribution pattern of particulate matter during incoming tide can be demonstrated with the Landsat ETM+ image that indicates jets and swirls (Figure 28). In particular, the jet passing through the channel between Robins Island and Cow Neck with a mushroom-shaped head and a pronounced semi-circular front may have importance to understanding the hydrography of the Great Peconic Bay. Inflow of water from the Great

Peconic Bay can be recognized with elevated radiance levels that are diagnostic for particulates.

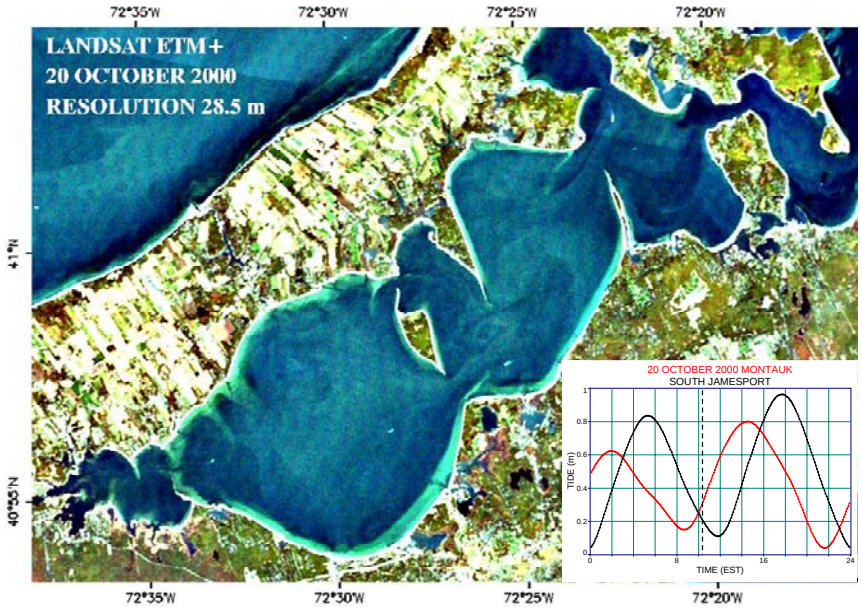

Figure 29: Landsat ETM+ coverage on October 20, 2000.

Observation with Landsat ETM+, shown in Figure 29 at close to low tide, shows none of the above jets and swirls and a rather homogeneous distribution is observed.

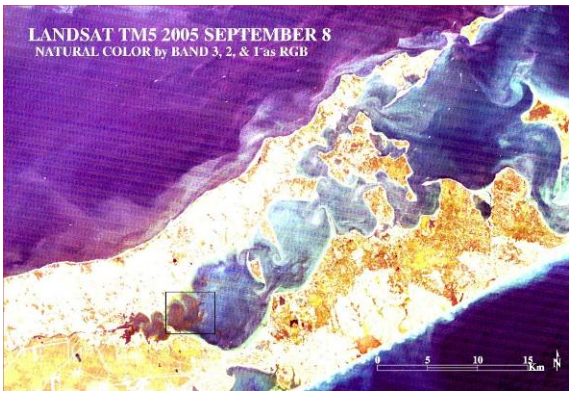

Figure 30: Landsat TM5 on September 8, 2005 at a time when flood starts at Jamesport. The image was displayed originally in natural color but was contrast-stretched for each channel. The rectangle indicates the image shown in Figure 33.

On September 8, 2005 Landsat TM5 data (Figure 30) show in Flanders Bay and in the eastern part of Great Peconic Bay patchiness that indicates bloom conditions. This image coincided with a survey made by Gobler et al. (2008) who observed dinoflagellates *(Coclodinium polykrikoides)* at high concentrations. Whereas the outer part of the Bay does not indicate blooming, Flanders Bay and part of the Great Peconic Bay show blooming conditions. This is in agreement with the spatial distribution of *Cochlodinium* cells as shown in Figure 31.

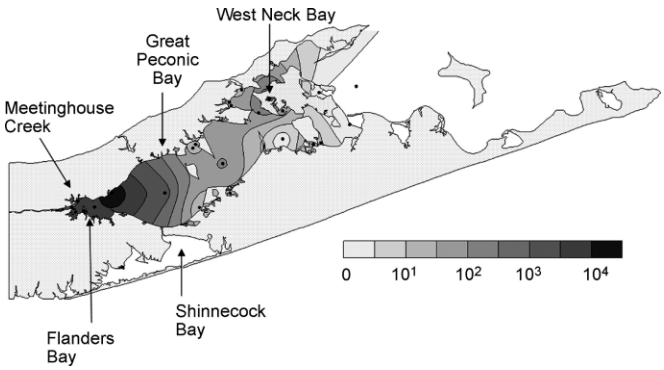

Figure 31: Spatial distribution of Cochlodinium cells in the Peconic Estuary, early September 2005. After Gobler et al. (2008).

Recognition of details on the distribution pattern of the bloom is achieved through enhancement of the image shown in Figure 30 that took into account the spectral response of the bloom in different channels (Figure 33).

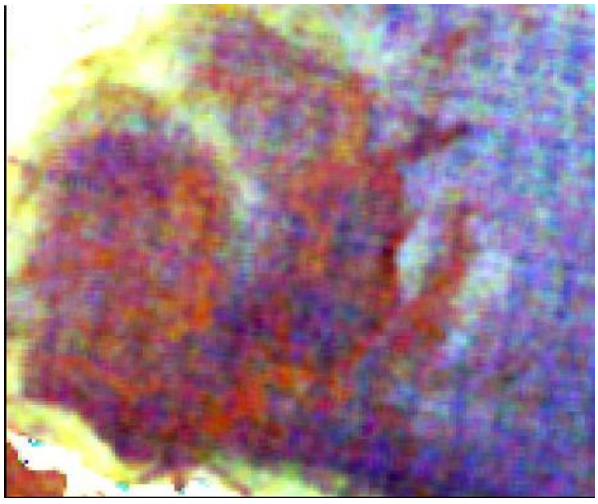

Figure 33: Landsat TM5 September 8, 2005 using a different stretch for the bloom. For location of the bloom, see insert in Figure 30.

A Landsat image from August 22, 1993 recorded outrunning water that started at South Jamesport (Figure 34) and indicated bloom conditions for the Great and Little Peconic Bays. River outflow into Flanders Bay is recognized through a strong color front and transport of particulate matter is observed through the channel between Robins Island and Cow Neck.

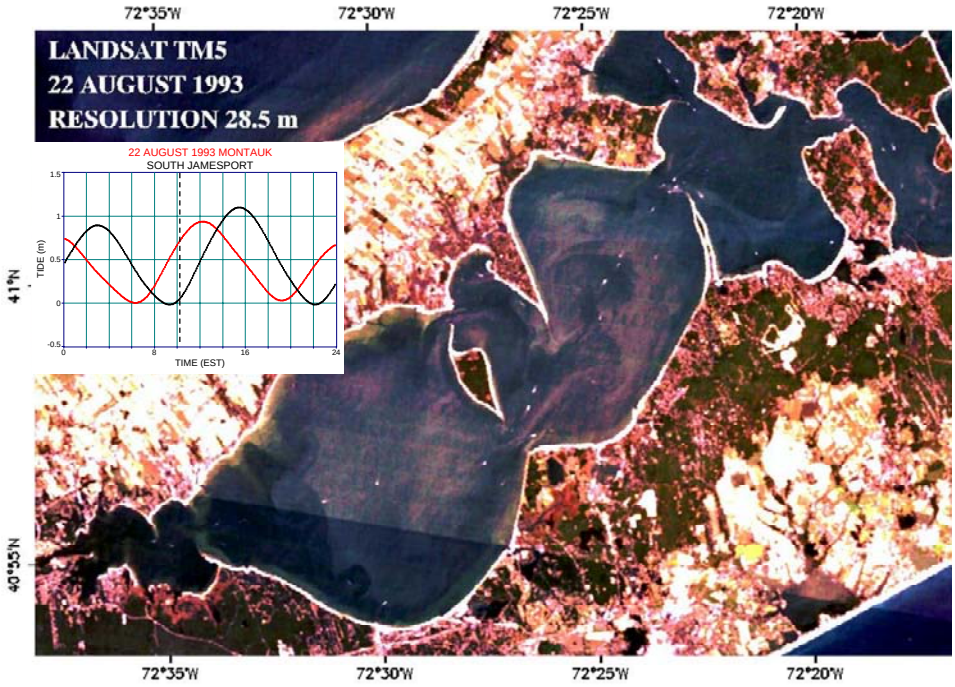

Figure 34: Landsat TM5 coverage for August 22, 1993.

In conclusion, from the analysis of Landsat data, it was demonstrated that the tidal stage has a strong impact on the distribution of particulate matter. In particular, jets, eddies and frontal systems that cannot be determined through sampling procedures from ships, are shown to dominate patterns of distribution of blooms.

5 EVALUATION OF DATA

A major problem in evaluating the satellite data is the scarcity of available ground truthing although many surveys have been undertaken in the Peconic Bays. Furthermore, the qualitative comparison between chlorophyll data obtained by SeaWiFS and ship measurements during 2001 indicated that the ship data may be too low (C. Gobler personal communication) which can be explained by errors in the analytical procedure or by the varying storage of samples. On the other hand, SeaWiFS algorithms are built for ocean water (Case 2 water) and may overestimate chlorophyll in eutrophicated waters. It

has been noted that the distinction between Case 1 and Case 2 waters does not hold and is meaningless in algal blooms where more spectral bands would be required (see also Dekker et al., 2001). Conventional water sampling during algal blooms, particularly when algal blooms are dense and close to the surface, may further complicate interpretation when analyzed with ship measurements alone.

Another source of error in chlorophyll estimates is within conservative methods. Figure 35 gives a comparison of chlorophyll concentrations in Peconic Bay for the standard chlorophyll methods and chlorophyll determined by High Performance Liquid Chromatography (HPLC) and shows that even immediate analysis of samples may have an error of about 30%.

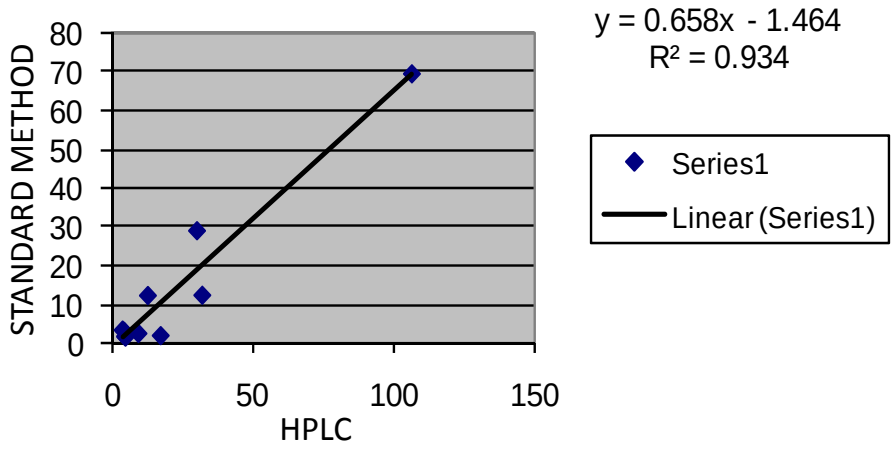

Figure 35: Comparison of chlorophyll concentrations measured with the standard method by C. Gobler (Stonybrook University) and High Performance Liquid Chromatography (K.H. Szekielda, CUNY).

As shown in this study, plankton blooms are very patchy and the spatial-temporal sampling with conservative methods are not adequate whereas a continuous flow-through system may provide more reliable results about the extent of bloom conditions (see also Kutser et al., 2006). In addition, some algae have the capability to regulate their buoyancy and add to the problem of interpreting data from conventional sampling.

As no ship data coincided precisely with the date of overflight, a rather qualitative approach to evaluate the satellite data was undertaken. At first, a comparison was made of data from SeaWiFS and MODIS for September 8, 2005 that were taken approximately one hour apart. Although both sensors showed blooming on September 8, discrepancies were found in the absolute

values and also in the geo-referencing of the data as shown in Figure 36. Similar discrepancies were observed for data taken on September 22, 2005 as shown in Figure 37.

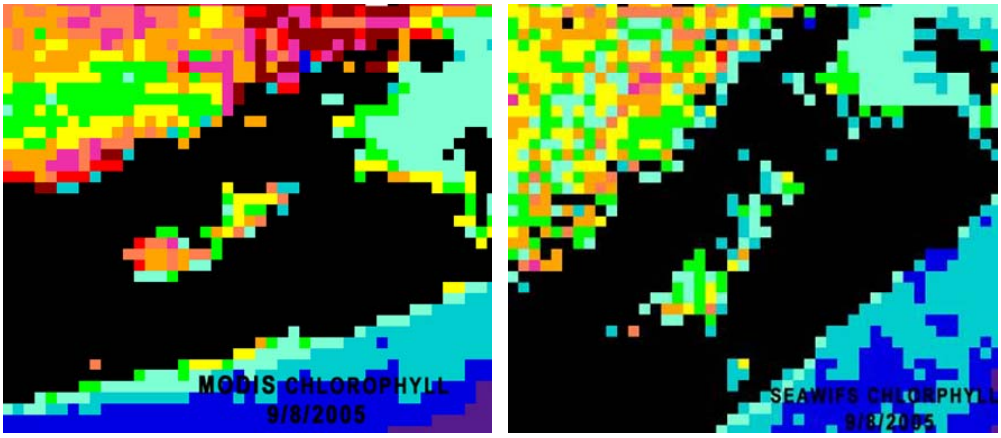

Figure 36: Comparison between MODIS and SeaWiFS derived chlorophyll distribution on September 8, 2005

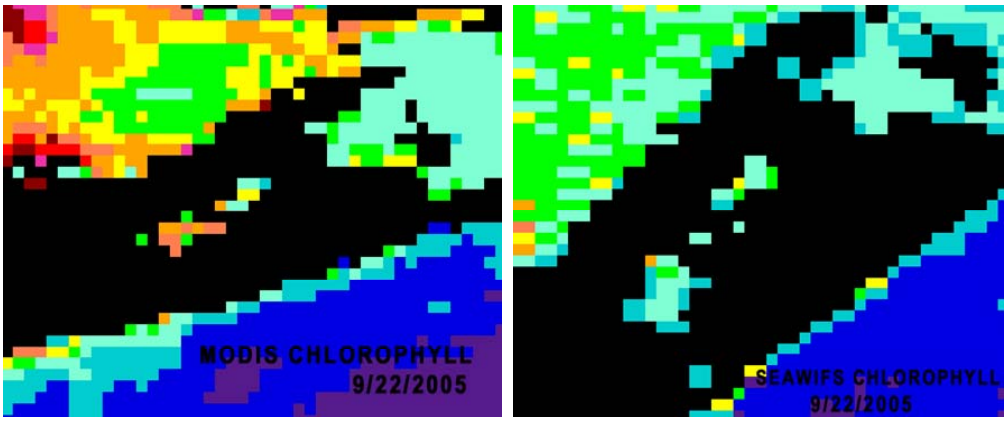

Figure 37: Comparison between MODIS and SeaWiFS derived chlorophyll distribution on September 22, 2005

As mentioned, the algorithms for both satellite-derived pigment concentrations are valid for open ocean water but may not necessarily represent the true concentrations in coastal and inland waters (Case 2 water). Comparison of data from SeaWiFS and MODIS that relate to the position of stations 130 and 170 indicated that bloom conditions were encountered but MODIS concentrations were higher by a factor of almost two. The results of this comparison are shown in Table 4.

Table 4: Peconic Bay chlorophyll concentrations for September 8, 2005 and September 22, 2005 from SeaWiFS and MODIS data.

STATION	DATE	SeaWIFS_Chlor	MODIS Chlor
130	9/8/05	16.222	27.773
170	9/8/05	37.7189	NO DATA
130	9/22/05	6.1552	13.7482
170	9/22/05	NO DATA	10.8508

Based on these findings, a more detailed comparison between the two data sets was established. As the deviation in the geographic location is in the neighborhood of one pixel (about 1000 m), it is not possible to compare the data on a pixel-by-pixel location. Therefore, larger test sites were selected in the form of polygons that are shown in Figure 38. SeaWiFS and MODIS data were selected for the same regions that were hydrographically distinct, and their values extracted for statistical processing.

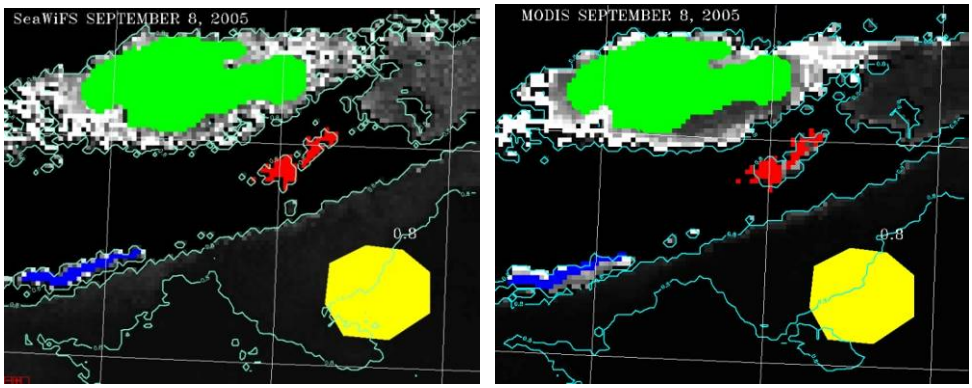

Figure 38: Selected polygons for data extraction in the offshore region (yellow) of Long Island Sound (green), and the Peconic Bays (red) on September 8, 2005 from SeaWiFS and MODIS. Included in the images are the chlorophyll isolines for 0.8 mg l^{-1} in the offshore region.

The data show that MODIS, compared to SeaWiFS, overestimates the chlorophyll concentration by a factor of 2.5. The offshore region in Figure 39 shows a reasonable relationship between the two data sets although the error of the two data sets is about 20%.

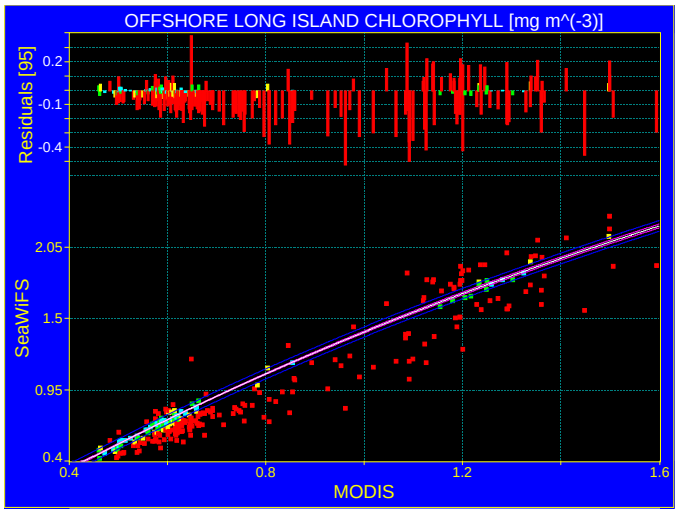

Figure 39: Comparison between SeaWiFS and MODIS of chlorophyll concentrations in the offshore region (yellow polygon in Figure 38).

The comparison of SeaWiFS with MODIS chlorophyll for Long Island Sound is shown in Figure 40 with the corresponding linear regression and frequency distribution.

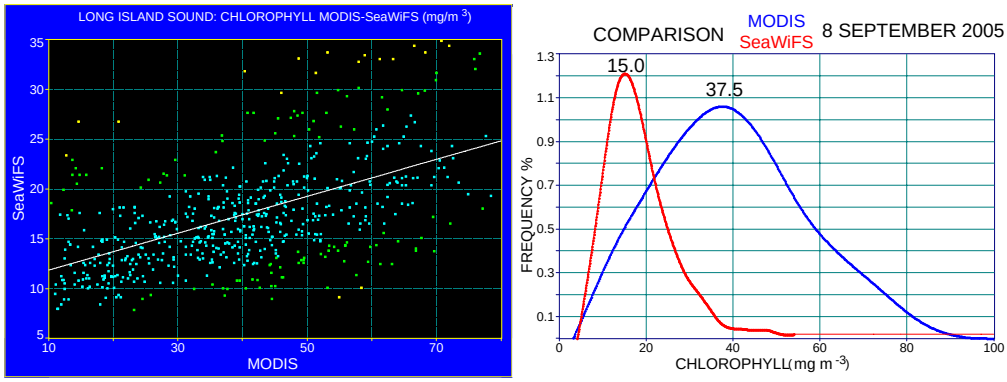

Figure 40: Comparison of MODIS and SeaWiFS in Long Island Sound as indicated by the green polygon in Figure 38. Left figure shows linear regression and the right figure shows frequency distribution of chlorophyll.

For the Peconic Bay, only a few measurements were available but, as shown in Figure 41, no correlation exists.

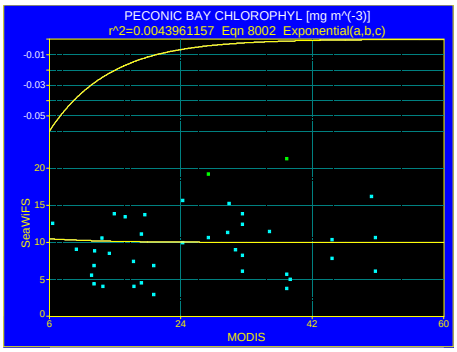

Figure 41: Comparison for MODIS and SeaWiFS in Peconic Bay as indicated by the red polygon in Figure 38.

The discrepancies between MODIS and SeaWiFS are based on the different spectral responses of Case 1 and Case 2 waters and the slight difference in the spectral channel locations on which the algorithms are based. For instance, the only similar wavebands are 412 and 443 nm (SeaWiFS bands 1 and 2, MODIS/Aqua bands 8 and 9) but differences in these bands can be caused by their different spectral response functions (MODIS Ocean Science Team, 2003). Time difference (change of sun angle) is almost eliminated because MODIS data are normalized as water leaving that allows a comparison of radiances that were collected at different times of day (see Gordon and Clark 1981).

Another factor that has to be considered is that in Case 2 water the spectral response of water with high turbidity shifts from shorter to longer wavelength (from blue to green) which results, when applying the same algorithms, in different estimates for chlorophyll concentrations. In order to apply the radiance data from MODIS and SeaWiFS, local empirical algorithms have to be established in connection with ground observations rather than using the chlorophyll data by NASA-GSFC.

6 CONCLUSIONS

Analysis of data from different satellite systems (SeaWiFS, MODIS, ALI and Landsat) demonstrate opportunities to monitor plankton bloom events, the recognition of frontal systems and the impact of tidal flow on the distribution patterns of suspended matter (plankton). SeaWiFS and MODIS proved to be essential tools for monitoring, but the disadvantage is the coarse resolution of about one kilometer. Comparison of SeaWiFS and MODIS chlorophyll data showed that MODIS generates values that are too high by a factor 2.5. Nevertheless, a yearlong observation over the Peconic Bay with SeaWiFS revealed that bloom conditions can be observed although only minimal data

can be obtained with one image for the area. Comparison with available ship observations of chlorophyll indicated however that bloom conditions may be missed with conservative surveys, therefore supporting the advantage of SeaWiFS data.

The study with MODIS data showed the potential of using multichannel remote sensing for clustering and for identification of biogeochemical provinces on a larger scale. The same approach of using clustering techniques was applied to ALI data with a more appropriate ground resolution of 30 meters that allowed for separation of water masses with varying optical properties. Bloom conditions were resolved with ALI and the merging of multispectral data with panchromatic images, resulting in a ground resolution of 10 meters, indicating an advantage of recognizing fine scale structures under bloom conditions.

Landsat data with a ground resolution of 30 meters showed similar results as ALI. As more Landsat images were available than ALI images, it was possible to observe the distribution pattern of particulate matter at various tidal ranges. It is concluded that Landsat data are a meaningful tool for pattern recognition and for recording blooms, as in the case of detection of *Cochlodinium* blooming in 2005.

Taking all the findings derived under this project into account, the following recommendations have been derived.

7 RECOMMENDATIONS

RECOMMENDATION 1

The analysis of MODIS, SeaWiFS and ALI data showed that major changes were observed in Flanders Bay and in the Great Peconic Bay. MODIS however provides values that, compared to SeaWiFS, are unreliable and it was concluded that SeaWiFS is more appropriate for covering the bays. Although analysis of chlorophyll with SeaWiFS for Case 2 water does not give accurate concentrations, SeaWiFS can be used to detect bloom conditions. The disadvantage is the coarse resolution of about one kilometer, but it is sufficient to recognize trends in the changing concentrations based on about 50 data points for the Bay. Full coverage of the whole Bay, the south shore water and part of the adjacent Long Island Sound can be covered during one overpass. Therefore, arrangements with NASA should be initiated to have a continuous transfer of data in almost real-time to the end user.

RECOMMENDATION 2

The Advanced Land Imager (ALI) has a ground resolution of 10 meters in the panchromatic mode and 30 m for other channels that can be merged with the panchromatic channel to generate a ground resolution of 10 meters. ALI has spectral bands in which blooming can be recognized and it is recommended to acquire and analyze ALI data every two weeks.

RECOMMENDATION 3

Hyperion is spectrally well suited to extract spectral properties of water and has the potential to reconstruct spectra that are related to species. Since the maximum width of one Hyperion scene covers 7.7 km, it is recommended to limit the use of Hyperion to the center coordinates of Flanders Bay that would also cover part of the Great Peconic Bay. Full coverage for the two bays with a total width of about 16 km would require two scenes and should be acquired monthly in conjunction with ALI data. The corresponding area to be covered by Hyperion is shown in the following map.

Map of recommended coverage with ALI and Hyperion.

RECOMMENDATION 4

The project experienced some difficulties with the Customer Service Representative of USGS to have satellite coverage arranged when ship support was scheduled. Direct contact should be established with the service in order to obtain priority for satellite coverage and to receive advanced notice

of overflights. This would guarantee simultaneous coordination of ship operation for ground-truth with simultaneous sampling at selected stations.

RECCOMMENDATION 5

The satellite observations detected strong heterogeneity of plankton blooms over small distances making it problematic to cover identified features with single ship measurements. In particular, Langmuir circulation contributes to reorientation of plankton distribution when wind speed is above $3 m \cdot s^{-1}$. Therefore, ground truthing for chlorophyll should be based on continuous measurements and should be executed during the exact time of satellite coverage. Occasional overflights by helicopter with handheld cameras and visual observations to detect early blooming conditions should be undertaken.

RECOMMENDATION 6

It is recommended that a website of the monitored area be established to post observations for access by the fishing industry, scientific community and other agencies. This should include also the integration of data sets collected by agencies operating ship surveys in the Peconic Bay and the south shore region.

PRICE ESTIMATES FOR AN OPERATIONAL MONITORING ROGRAM

Taking into consideration the above recommendations, a price estimate is given below for a potential monitoring program.

The programming of the satellite for accessing images requires a Data Acquisition Request (DAR) from the US Geological Survey. For all new DARs a $750 service fee is charged for scheduling the satellite. The fee is for tasking of the sensor to collect a requested image and covers the labor required to support the scheduling, tracking, and quality assessment of a DAR. The cost per scene for the required data products is given in the following Table:

Data Product	**Cost**
Hyperion – Radiometrically corrected (Level 1R)	$250
Hyperion – Terrain corrected (Level 1Gst)	$500

ALI – Radiometrically corrected (Level 1R)	$250
ALI – Geometrically corrected (Level 1Gs)	$500
ALI – Terrain corrected (Level 1Gst)	$500

The satellite monitoring program and the use of required data, as outlined above, would cost $24,750 per year. Processing and labor vary according to the contractor. Such a project could be implemented with a principal investigator and two graduate students at a cost of about $84,750 per year excluding miscellaneous and overhead.

8. ACKNOWLEDGMENTS

We acknowledge the support of NASA Goddard Space Flight Center for approving SeaWiFS and MODIS data at no cost and the United States Geological Survey for the access to their data base.

9 REFERENCES

Bhargava, D.S., and D.W. Mariam, 1990. Spectral reflectance relationships to turbidity generated by different clay materials. Photogr.Eng. Remote Sensing, 225-229.

Bidigare, R.R., D.N. Karl and L. Van Heukelem, 2000. Fluorometric chlorophyll a: sampling, laboratory methods, and data analysis protocols. In: Ocean Optics Protocols for Satellite Ocean Color Sensor Validation, Revision 2, ed. by G.S. Fargion and J.L. Mueller, NASA TM 2000-209966, Goddard Space Flight Center, Greenbelt, MD., Chapter 14, 162-169.

Bidigare, R.R. and C.C. Trees, 2000. HPLC phytoplankton pigments: sampling, laboratory methods, and quality assurance procedures. In: Ocean Optics Protocols for Satellite Ocean Color Sensor Validation, Revision 2, ed. by G.S. Fargion and J.L. Mueller, NASA TM 2000-209966, Goddard Space Flight Center, Greenbelt, MD., Chapter 14, 154-161.

Bricaud, A., C. Roesler, and J.R. V. Zaneveld, 1995. In situ methods for measuring the inherent optical properties of ocean waters. Limnol. Oceanogr., 40 (2), 393-410.

Charnell, R.L. and G.A. Maul, 1973. An oceanographic observation of the New York Bight from ERTS-1. NOAA TR ERL 2629, 8 pp.

Clark, D.K., 1997. MODIS. Algorithm Theoretical Basis Document,Bio-Optical Algorithms Case 1 Waters, 35 pp.NOAA National Environmental Satellite Service,Washington, D.C. 20233

Dekker, A.G., V.E. Brando, J.M. Anstee, N. Pinnel, T. Kutser, E.J. Hoogenboom, S. Peters, R. Pasterkamp, R. Vos, C. Olbert and T.J.M. Malthus, 2001. Imaging spectrometry of water, 307-359. In: Imaging spectrometry, edit. F.D. van der Meer and S.M. de Jong, 403 pp,Kluwer Academic Publisher, Dordrecht.

Field, C. B., M. J. Behrenfeld, J. T. Randerson, and P. Falkowski, 1998. Primary production of the biosphere: Integrating terrestrial and oceanic components. Science, 281, 237-240.

Franz, B.A., R.E. Eplee, Jr., S.W. Bailey, and M. Wang, 2002: Changes to the atmospheric correction algorithm and retrieval of oceanic optical properties. In: Patt, F.S. and 17 coauthors, 2002: Algorithm updates for the fourth SeaWiFS data reprocessing. NASA Tech. Memo. 2003-206892, Vol. 22, S.B. Hooker and E.R. Firestone, Eds., NASA Goddard Space Flight Center, Greenbelt, Maryland, 29-40.

Garcia-Mendoza, E., and H. Make, 1996. The relationship of solar-induced natural fluorescence and primary productivity in Mexican Pacific waters. Limn. Oceanogr., 41(8), 1697-1710.

Garver, S.A., D. Siegel and B.G. Mitchell, 1994. Variability in near-surface particulate spectra: What can a satellite ocean color imager see? Limnol. Oceanogr., 39 (6), 1349-1367.

Garzoli, S.L., 1993. Geostrophic velocity and transport variability in the Brazi-Malvinas confluence. Deep-Sea Research, 40, 1379-1403.

Gitelson, A., 1992. The peak near 700 nm on radiance spectra of algae and water: relationship of its magnitude and position with chlorophyll concentration. International Journal of Remote Sensing, 13, 3367-3373.

Gitelson, A., S. Laorawat, G.P. Keydan and A. Vonshak (1995). Optical properties of dense algal cultures outdoors and its application to remote estimation of biomass and pigment concentration in *Spirulina platensis*. J. Phycology, 31, 828-834.

Gobler, C.J., D.L. Berry, R. Anderson, A. Burson, F. Koch, B.S. Rodgers, L.K. Moore, J.A. Goleski,B. Allam, P.Bowser, Y.Tang, R. Nuzzi, 2008. Characterization, dynamics, and ecological impacts of harmful Cochlodinium polykrikoides blooms on eastern Long Island, NY, USA. Harmful Algae 7 293–307

Goodin, D.G. L.H. Han, R.N. Frase, D.C. Runquist, and W.A. Stebbins. 1993. Analysis of suspended solids in water using remotely sensed high resolution derivative spectra. Phototogrammetric Engineering & Remote Sensing, 59, 4, 505-510.

Gordon, H. R., and K. J. Voss, 1999, MODIS Normalized water-leaving radiance algorithm theoretical basis document (MOD 18) Version 4, NASA Contract Number NAS503163, 92 pp.

Gordon, H. and D.K. Clark, 1981: Clear water radiances for atmospheric correction of coastal zone color scanner imagery. Appl. Opt., 20(24), 4175-4180.
Gordon, H.R., and W.R. McCluney, 1975. Estimation of the depth of sunlight penetration in the sea for remote sensing. Applied Optics, 14, 2, 413-416.

Gower, J.F., and G. Borstad, 1981. Use of the in vivo fluorescence line at 685 nm for remote sensing surveys of surface chlorophyll a p. 329-338. In: J.F. Gower [ed.], Oceanography from the space. Plenum.

Gower, J.F.R., R. Doerfer, and G.A. Borstad, 1999. Interpretation of the 685 nm peak in water-leaving radiance spectra in terms of fluorescence, absorption and scattering, and its observation by MERIS. Int. J. Remote Sensing, 20, 9, 1771-1786.

Gregg, W.W., M. E. Conkright, J. E. O'Reilly, F. S. Patt, M. H. Wang, J. A. Joder, and N. W. Casey, 2002, NOAA-NASA Coastal Zone Color Scanner reanalysis effort. Applied Optics, 41, 1615-1628.

Han, L., D.C. Runquist, L.L. Liu, and R.N. Fraser, 1994. The spectral response of algal chlorophyll in water with varying levels of suspended sediment. Int. J. Remote Sensing, 15, 3707-3718.

Hatten, G., C. Salo, C. Merrow, and K.Parker, 1999. Moderate Resolution Spectroradiometer (MODIS), MCST/MODIS IOT, Research & Data Systems, Corp. Operations Concept Document, Version 2.1 MCST Document # July 1999. Prepared by: Greg Hatten, Chad Salo, Cindy Merrow, and Kirsten

Parker MCST/MODIS IOT Research & Data Systems, Corp. Greenbelt, MD 20770

Greenbelt, MD 20770. Operations concept document, Version 2.1, NASA-MCST Document # July 1999.

Hoge, F., and R. Swift, 1987. Ocean color spectral variability studies using solar induced chlorophyll fluorescence. Applied Optics, 26, 18-21.

Holm-Hansen, O., C.J. Lorenzen, R.W. Holmes and J.D.H. Strickland, 1965. Fluorometric determination of chlorophyll. J. Cons. Cons. Int. Explor. Mer., 30: 3-15.

Hooker, S.B., and C.R. McClain, 2000. The calibration and validation of SeaWiFS data. Progress in Oceanography, 45, 427-465.

Kirk, J.T.O., 2000. Light and photosynthesis in aquatic ecosystems. Cambridge University Press, 509 pp.

Kutser,T., 2004. Quantitative detection of chlorophyll in cyanobacterial blooms by satellite remote sensing. Limnology and Oceanography, 49, 2179-2189.

Kutser, T., L. Metsamaa, N. Strömbeck an E. Vahtmäe, 2006. Monitoring cyanobacterial blooms by satellite remote sensing. Estuarine, Coastal and Shelf Science, 67, 303-312.

Latasa, M., R.R. Bidigare, M.E. Ondrusek and M.C. Kennicutt II, 1996. HPLC analysis of algal pigments: a comparison exercise among laboratories and recommendations for improved analytical performance. Mar Chem., 51: 315-324.

Legeckis, R. and A.Gordon, 1982. Satellite observations of the Brazil and Falkland Currents-19751976 and 1978. Deep-Sea Research, 29, 375-401.

Longhurst, A., S. Sathyendranath, T. Platt and C. Caverhill, 1995. An estimate of global primary production in the ocean from satellite radiometer data. J. Plankton Res., 17, 1245-1271.

Morel, A. and S. Maritorena, 2001: Bio-optical properties of oceanic waters: A reappraisal. J. Geophys. Res., 106(C4), 7163-7180.

Morel, A., D. Antoine, and B. Gentili, 2002: Bidirectional reflectance of oceanic waters: accounting for Raman emission and varying particle scattering phase function. Appl. Opt., 41(30), 6289-6306.

McClain, C.R., G. Feldman, and W. Esaias, 1993. Oceanic biological productivity. In: Atlas of satellite observations related to global change, Ed.: R.J. Gurney. J.L. Foster and C.L. Parkinson, Cambridge University, University Press, 470 pp.

McKee, D., A. Cunningham, and K. Jones, 1999. Simultaneous measurements of fluorescence and beam attenuation: instrument characterization and interpretation of signals from stratified coastal waters. Estuarine, Coastal and Shelf Science, 48, 51-58.

MODIS Ocean Science Team. Algorithm Theoretical Basis Document ATBD 19 Case 2 Chlorophyll a, Version 7, 30 January 2003, 67 pp.

Morel, A., and S. Maritorena, 2001. Bio-optical properties of oceanic waters: A reappraisal. J. Geophysdical Res., 106, 7163-7180.

Mueller, J.L. 2000: SeaWiFS algorithm for the diffuse attenuation coefficient, K(490), using water-leaving radiances at 490 and 555 nm. In O'Reilly, J.E. and co-authors: SeaWiFS Postlaunch Calibration and Validation Analyses, Part 3. S.B. Hooker and E.R. Firestone, Eds., NASA/TM-2000-206892, Vol. 11, NASA Goddard Space Flight Center, Greenbelt, Maryland, 24-27.

O'Reilly, J.E. and 21 co-authors, 2000: Ocean color chlorophyll a algorithms for SeaWiFS, OC2, and OC4: Version 4. In: O'Reilly, J.E. and 24 co-authors, 2000: SeaWiFS postlaunch calibration and validation analyses, part 3. NASA Tech. Memo. 2000-206892, Vol. 11, S.B.

Platt, T., and S. Sathyendranath, 1988. Oceanic primary production: Estimation by remote sensing at local and regional scales. Science,241, 1613-1620.

Quibell, G., 1992. Estimating chlorophyll concentrations using upwelling radiance for freshwater algal genera. International Journal of Remote sensing, 13, 2611-2621.

Richardson, L.L., 1996. Remote sensing of algal bloom dynamics, BioScience, 46: 492-501.

Richardson, L.L., D. Buisson, C.J. Liu and V. Ambrosia, 1994. The detection of algal photosynthetic accessory pigments using airborne visible-infrared imaging spectrometer (AVIRIS) spectral data. MTS Journal, 28, 10-21.

Roesler, C.S., and M.J. Perry, 1995. In situ phytoplankton absorption, fluorescence emission, and particulate backscattering spectra determined from reflectance. J. Geophys. Res., 100, 13,279-13,294.

Rundquist, D.C., L. Han,J.F. Schalles, and J.S. Peake, 1996. Remote measurement of algal chlorophyll in surface waters: The case for the first derivative of reflectance near 690 nm. Photogr.Eng. Remote Sensing, 62, 195-200.

Sathyendranath, S., T. Platt, E.P.W. Horne, W.G. Harrison, O. Ulloa, R. Outerbridge and N. Hoepffner, 1991. Estimation of new production in the ocean by compound remote sensing. Nature, 353, 129-133.

Signorini, S.R., S.B. Hooker, and C.R. McClain, 2003: Bio-optical and geochemical properties of the south Atlantic subtropical gyre. NASA/TM-2003-212253, NASA Goddard Space Flight Center, Greenbelt, Maryland, 43 pp.

Stegmann, P.M., 2004. Variability in chlorophyll and sea surface temperature fronts in the Long Island Sound outflow region from satellite observations. Journal of Geophysical Research, 109, doi: 10.1029/2003JC001984.
Stramski, D., R. A. Reynolds, M.Kahru, and B. G. Mitchell, 1999, Estimation of particulate organic carbon in ocean from satellite remote sensing. Science, 285, 239-242.

Szekielda, K.-H., C. Gobler, F. Moshary, B. Gross and S. Ahmed, 2003. Spectral reflectance measurements of estuarine waters. Ocean Dynamics, 53, 98-102.

Szekielda, K.H., J. Bowles, D.B. Gillis and W. D. Miller.
Use of airborne hyperspectral radiance data for pigment identification. Submitted to *Sensors*. September 2008.

Szekielda, K.H., G. Marmorino, S. J. Maness, T. Donato, J. H. Bowles, W. D. Miller, W. J. Rhea, 2007. Airborne hyperspectral imaging of cyanobacteria accumulations in the Potomac River. *Journal of Applied Remote Sensing*, *1*.

Szekielda, K.H. 2005. Use of the first and second chlorophyll absorption bands for marine biogeochemical patch recognition. *Indian Journal of Marine*

Sciences, Special Issue: Ocean Color, vol. 34 (4), 387-395.

Szekielda, K.H., 2005. Pattern recognition of marine provinces. *International Journal of Remote Sensing*, Vol. 26, No. 7, London, 1499-1503.

Szekielda, K.H., T.F. Donato, S.J. Maness, J.H. Bowles, G.O. Marmorino, D.B. Gillis, D.R. Korwan, G. Lamela, M.J. Montes, W.J. Rhea and W.A. Snyder, 2006. Hyperspectral imaging spectroscopy for eutrophication monitoring: Spatial and temporal events.
The Seventh Annual Marine and Estuarine Shallow Water Science and Management Conference, September 25-27, 2006.

Tsai, T., and W. Philpot. Derivative analysis of hyperspectral data. Remote Sensing of Environment, 66, 41-51.

Vincent, R.K., Xiaoming Qin, R. M.L. McKay, J. Miner, K. Czajkowski, J. Savino and T. Bridgeman (2004). Phycocyanin detection from LANDSAT TM data for mapping cyanobacterial blooms in Lake Erie. Remote Sensing of Environment 89, 381-392.

Waters, K.J, 1995. Effects of Raman scattering on the water-leaving radiance. J. Geophys. Res., 100, 13,151-13161.

Wood, A.M., D.A. Phinney and C.S. Yentsch, 1998. Water column transparency and the distribution of spectrally distinct forms of phycoerythrin-containing organisms. Marine Ecology Progress Series, 162, 25-31.

Wright, S.W., S.W. Jeffrey, R.F.C. Mantoura, C.A. Llewellyn, T. Bjornland, D. Repeta and N. Welschmeyer. 1991. Improved HPLC method for the analysis of chlorophylls and carotenoids from marine phytoplankton.

10 ANNEXES

ANNEX 1

Listing of satellite coverage for Peconic Bay

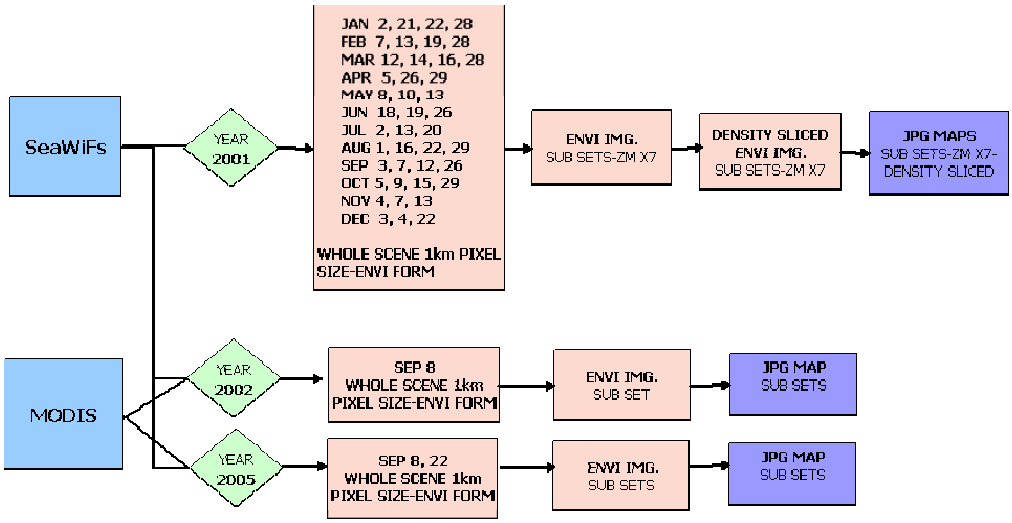

ANNEX 1 (continued)

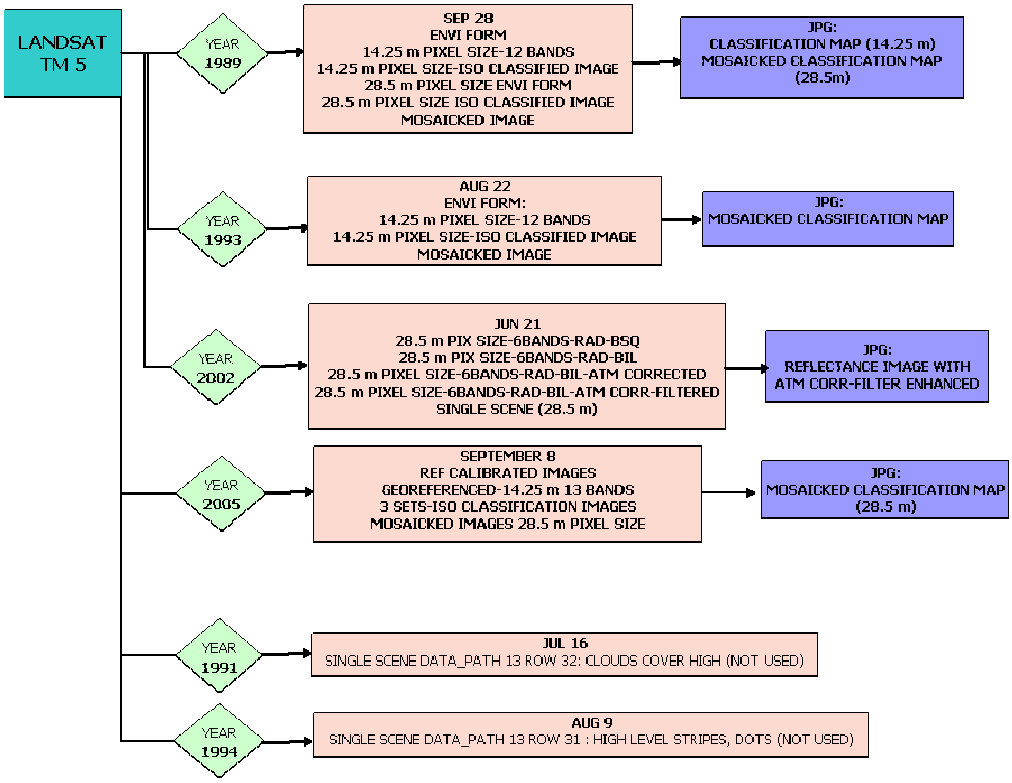

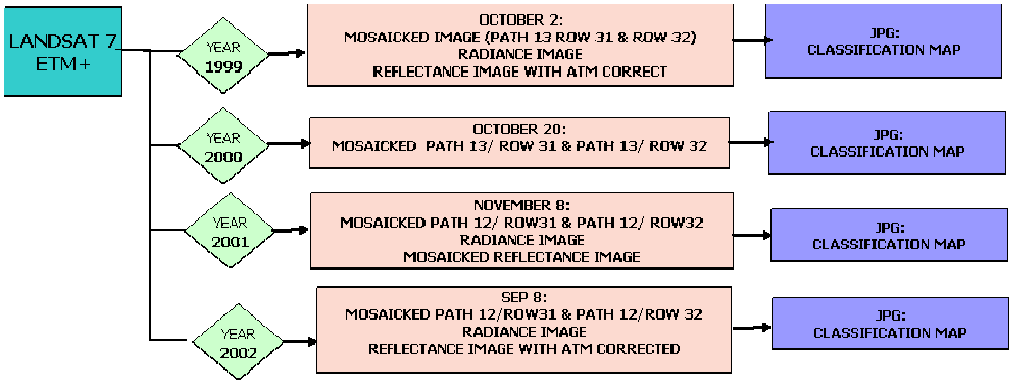

ANNEX 1 (continued)

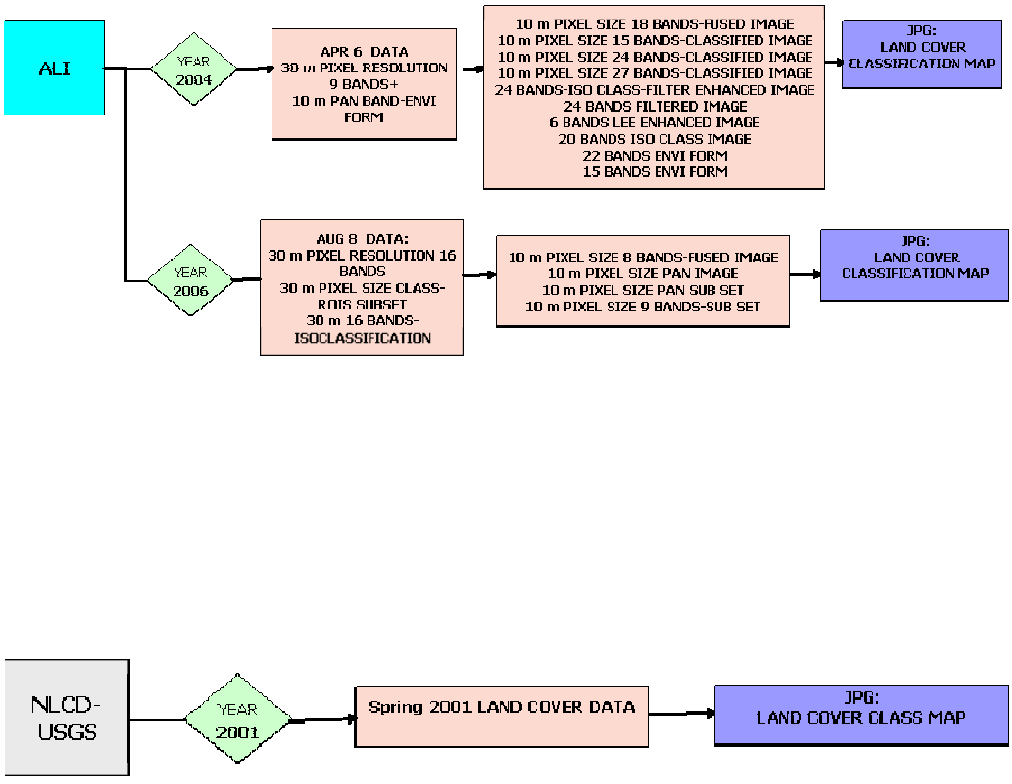

ANNEX 2

SeaWiFS data for the year 2001 that were cloud-free and have been subjected to image preprocessing.

Time in GMT

SeaWifs Data Lists

YEAR 2001

MON	DAY	ID#	time	DN			MONT	DAY	ID	dn		MONT	DAY	ID	dn	georef
1	2	002	171810	Y			5	7	127	Y		9	3	246	Y	
	10	010	180706	Y				8	128	Y	good img		6	249	Y	
	21	021	174806	Y				9	129	Y	cloudy		7	250	Y	
	22	022	165309	Y				10	130	Y	good img		10	253	Y	
	28	028		Y				13	133	Y	cloudy		11	254	Y	
													12	255	Y	
2	1	032		Y			6	7	158	Y			13	256	Y	
	3	034		Y				12	163	Y	bad		15	258	Y	
	7	038		Y				18	169	Y	good img		16	259	Y	
	11	042		Y				19	170	Y			17	260	Y	
	12	043		Y				20	171	Y			18	261	Y	
	13	044		Y				26	177	Y			26	269	Y	
	19	050		Y				27	178	Y						
	28	059		Y								10	5	278	Y	
							7	2	183	Y			8	281	Y	
3	12	071		Y				9	190	Y			9	282	Y	
	16	075		Y				12	193	Y			10	283	Y	
	28	087		Y				13	194	Y			11	284	Y	
								21	202	Y	good img		12	285	Y	
4	5	095		good img				27	208	Y	ok		15	288	Y	
	14	104		Y									16	289	Y	
	19	109		Y			8	1	213	Y			24	297	Y	
	26	116		n				2	214	Y			29	302	Y	
	29	119		good img				8	220	N						
								16	228	Y		11	4	308	Y	
								22	234	Y			7	311	Y	
								25	237	Y			8	312	Y	
								29	241	Y			9	313	Y	
													13	317	Y	
													14	318	Y	
													21	325	Y	
												12	3	337	Y	
													4	338	Y	
													22	356	Y	

ANNEX 3

SeaWiFS data for year 2001 that were processed and geometrically correted.

SeaWiFS
PAGE 1

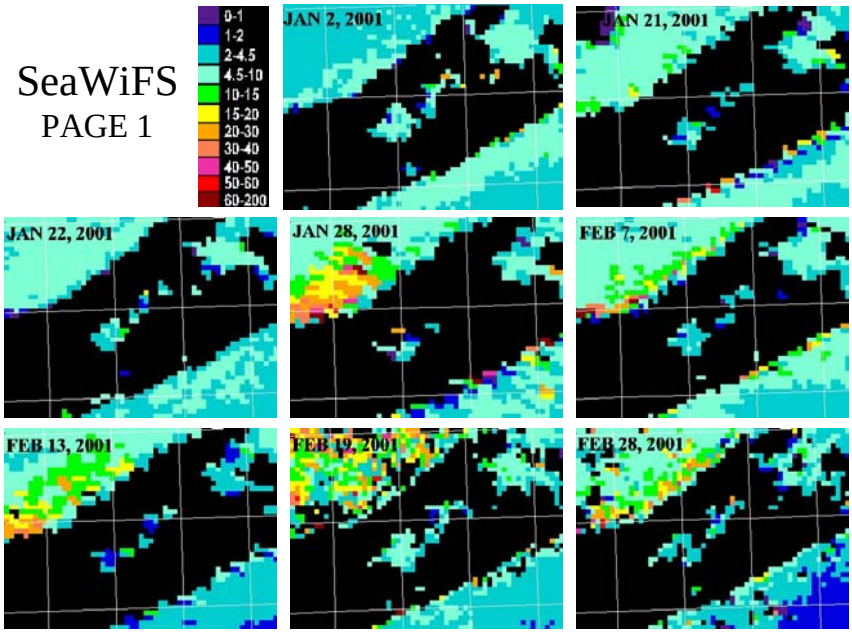

SeaWiFS
PAGE 2

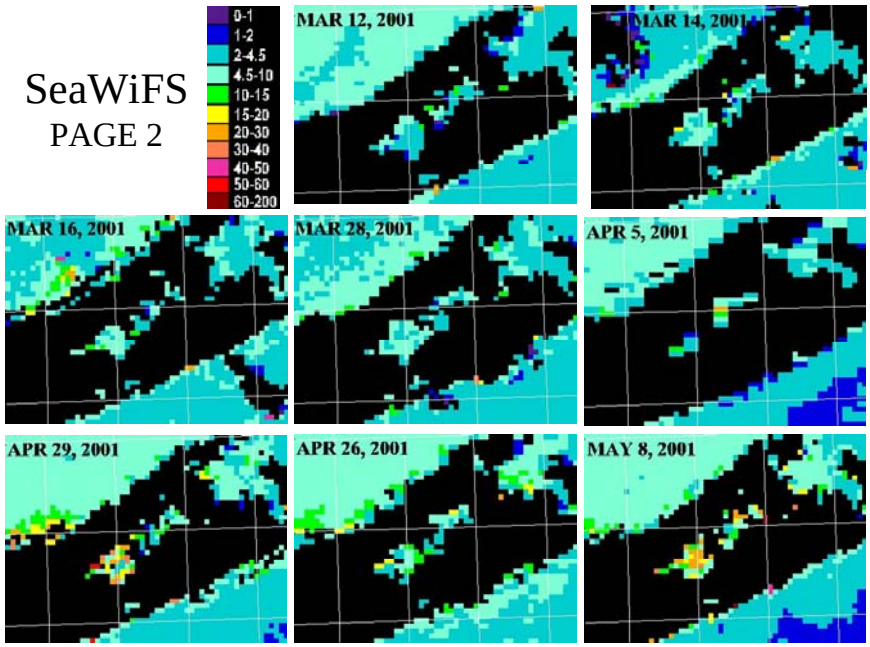

SeaWiFS
PAGE 3

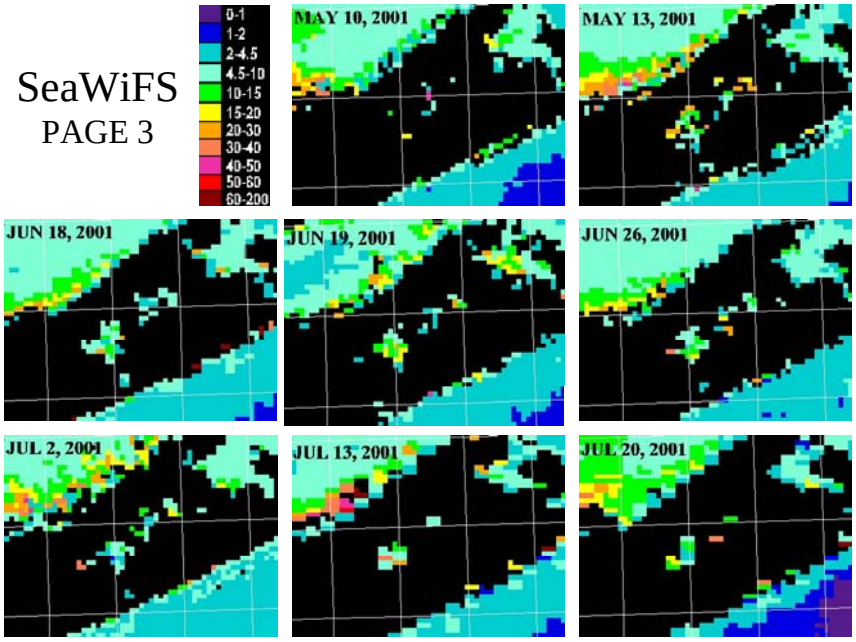

SeaWiFS
PAGE 4

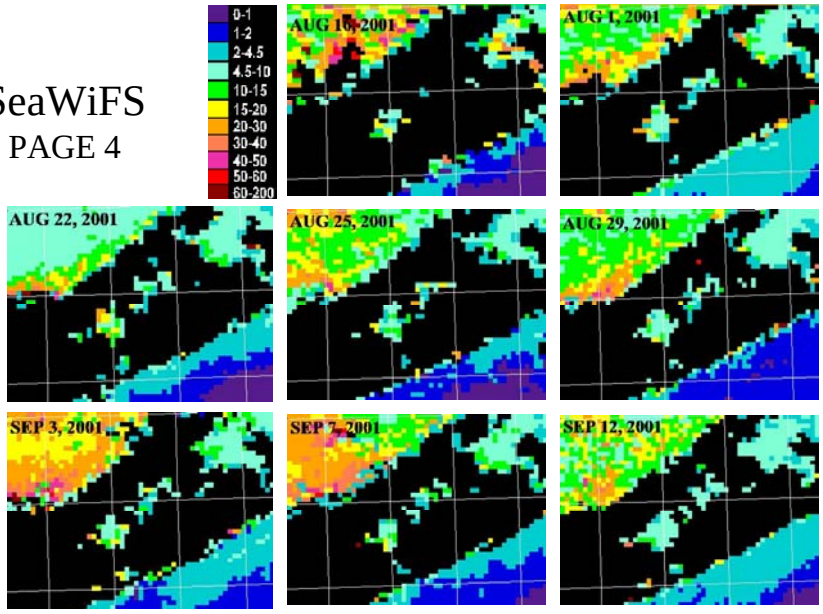

ANNEX 3 (continued)

SeaWiFS
PAGE 5

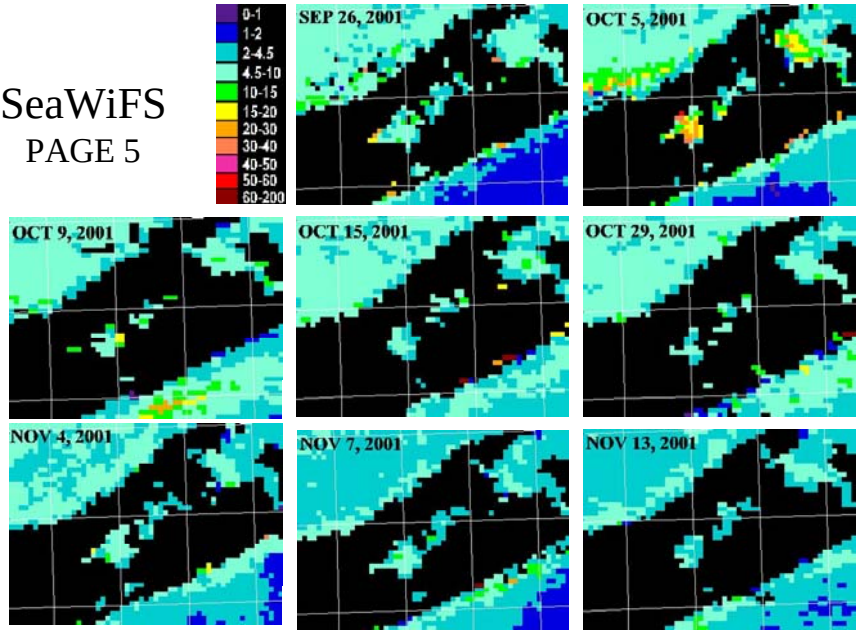

SeaWiFS
PAGE 6

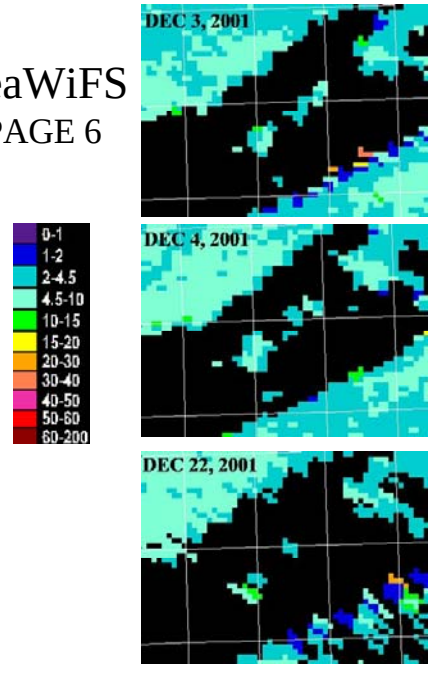

ANNEX 4

HYPERION

Based on findings with MODIS, HYPERION data with a higher ground and spectral resolution were tested. HYPERION has 196 spectral bands covering the range from 400 to 2,500 nm with each band having a width of 10 nm and a spatial resolution of 30 meter. The image used is shown in Figure 1 was acquired and evaluated for the potential application in the Peconic Bay. It was concluded that HYPERION might be the better sensor for use in the Peconic Bay which is also documented with the spectra that can be obtained from the hyperspectral imager as shown in Figure 1.

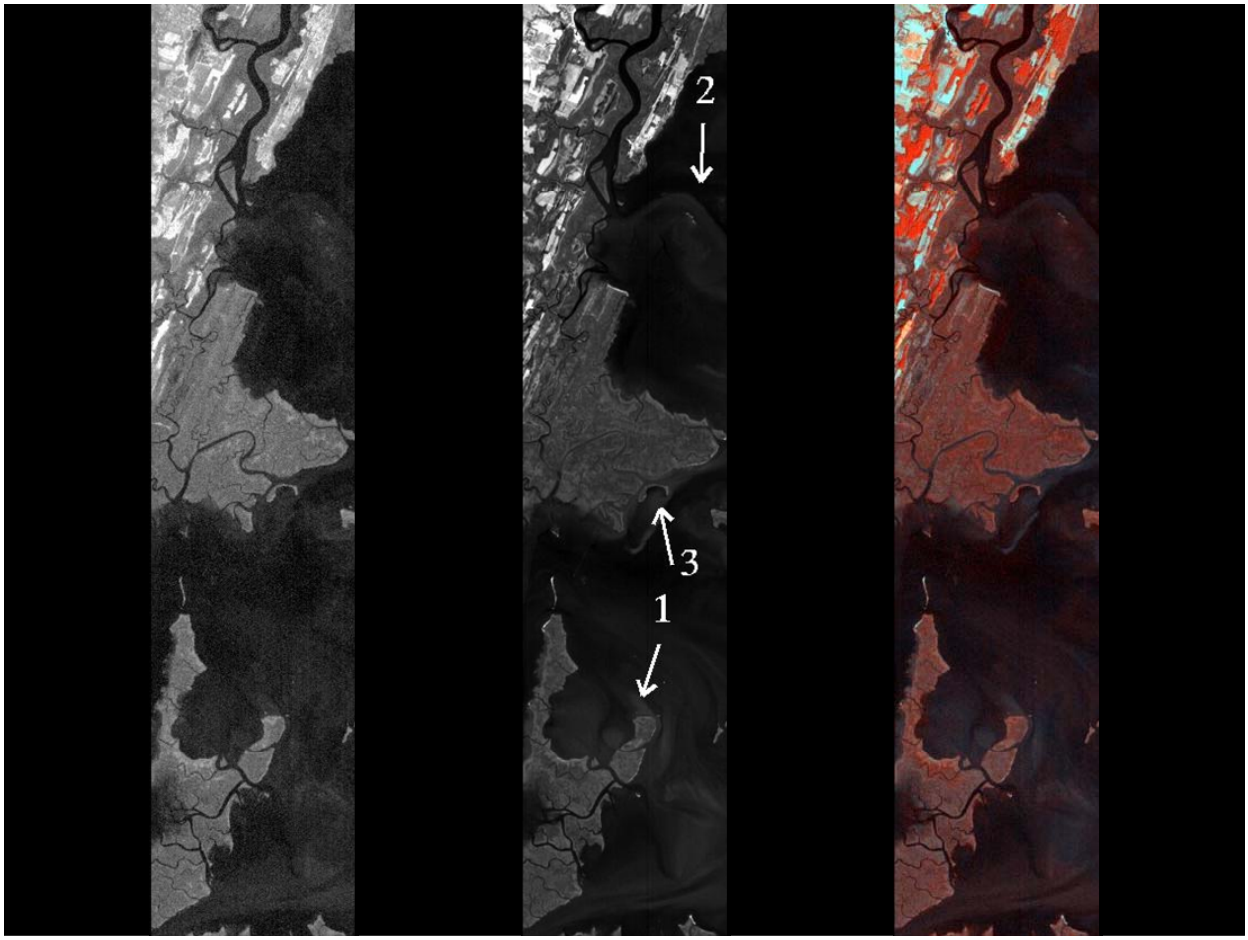

Figure 1: Image obtained with Hyperion. Left ratio image 701nm/671nm; middle image from the 701nm band. Right color composite: R = ratio 701 nm/ 671 nm, G = 701 nm, B 671 nm. The center image shows the location of spectra that were analyzed and shown in Figures 2.

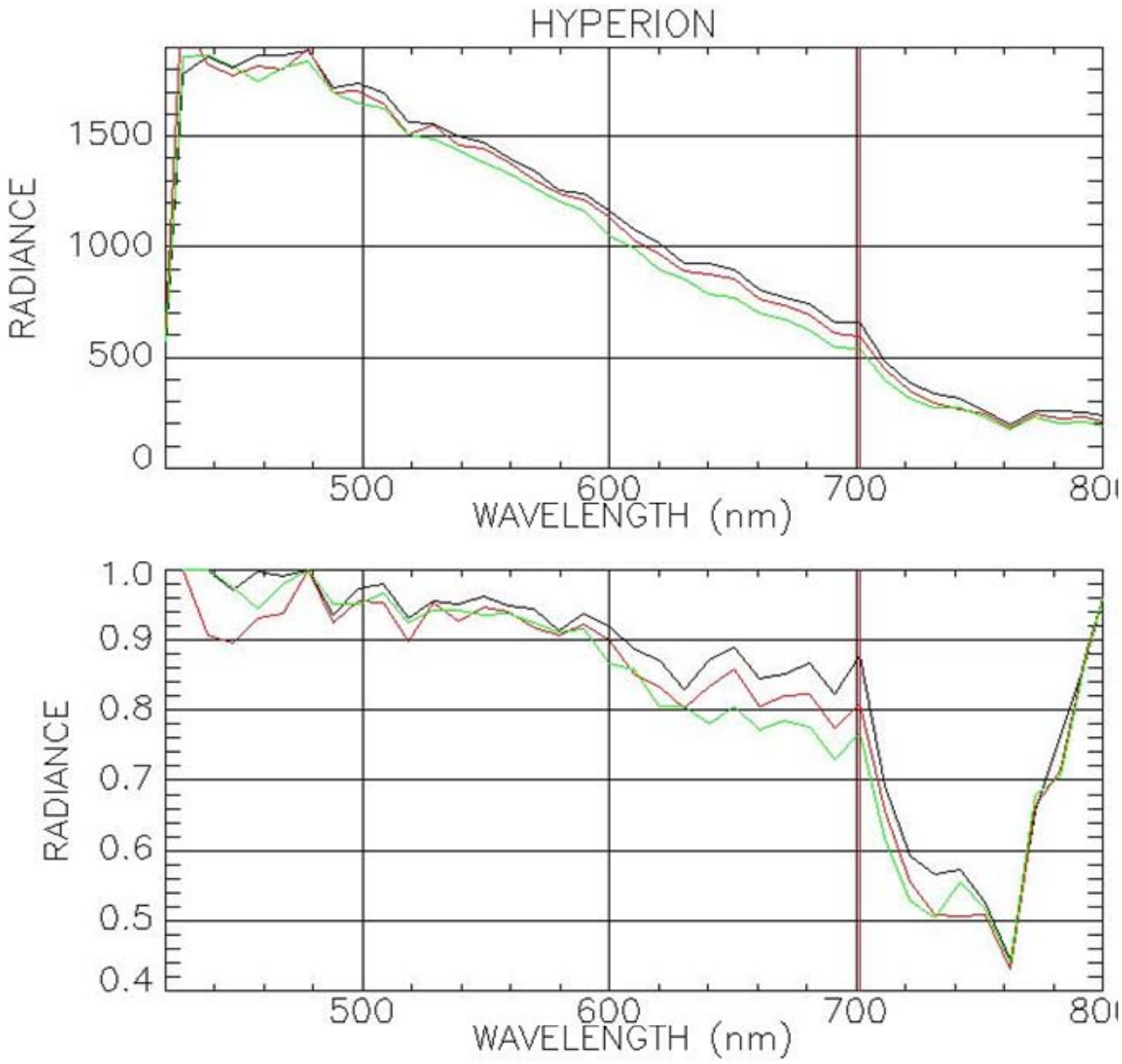

Figure 2: HYPERION spectra collected over coastal water (see Figure 1). Upper graph original spectrum, lower part shows the spectrum with the continuum removed.

PART B: ESTIMATION OF THE LAND COVER CHANGE IN SUFFOLK COUNTY, NEW YORK: USING LANDSAT AND ALI DATA

1 INTRODUCTION

The application of land cover change information in time is a critical factor for quantifying linkages and feedbacks between land use and land cover change and other related social, economic, and environmental components. In addition land cover change information can be used to develop efficient management strategies for the various land cover types. To meet this demand, investigators have become increasingly interested in satellite data, in part because of their historical archives as well as their good spatial coverage. For example, satellite data have been used to map forest extent, determine habitat fragmentation, enforce conservation laws, and minimize greenhouse gas emissions from deforestation (US Global Change Research Program, 2008).

The land cover datasets of the Multi-Resolution Land Characteristics Consortium (MRLC) are available for the 1992 and 2001 National Land Cover Database (NLCD) at the web site http://www.mrlc.gov. The NLCD 2001 land cover database is a product specifically designed for a broad array of users and comparable spatially and temporally in the nationwide scales through standardized remote sensing datasets incorporated with normalization and transformation of Landsat imagery, ancillary data and derivatives for percent imperviousness and percent tree canopy (Hormer et al, 2004). The NLCD land cover dataset can be useful for nationwide assessments or regional scale comparisons. However, this database has limitation for local scale assessments or inter-annual change detections in specific areas due to the standardization and normalization applied during remote sensing image processing and the model algorithms imbedded for the classification process. The land cover categories such as open space to high intensity developed classes are differential expressions of imperviousness regardless of their generic properties such as variation of reflectance levels that can give direct indication of environmental impacts.

The normalization of three data sets collected in spring, peak summer, and fall season further limit the usefulness of the data. By normalizing these data, it is not possible to do change detection at the inter-annual scale. Consequently, it hinders the direct understanding of geophysical impacts and the influence various management practices have on land cover change at local scales.

The following research effort focused on the development of land cover classification directly presenting surface physical properties based on remote sensing data, and how this classification may be applied to analyze land cover changes on both the inter-annual and decadal temporal scales at the local or county spatial scales.

2 DATA SOURCES

The major data sets used for this study include Landsat TM 5 28/9/1989, 9/8/2005, and Landsat 7 Enhanced Thematic Mapper Plus (ETM+) 10/2/1999, 11/08/2001, and

9/8/2002. As ancillary satellite data, the Advanced Land Imager (ALI) 4/6/2004, and 8/8/2006 were also used. NLCD 2001 data were processed as a classification map to compare the result from Landsat 2001 data classification. In addition the corresponding GIS vector data were applied in the quantification analysis.

3 METHODS

3a. Satellite Image Preprocessing

In order to provide complete Landsat coverage for Suffolk County, the analysis required the use of two data sets which were merged using tools provided as part of the Environment for Visualizing Images (ENVI) program. Each individual image, contained within the two data sets, was converted to radiance values separately. This processing step of transforming the data to radiance values in either the Band Interleaved by Line (BIL) or Band Interleaved by Pixel (BIP) format is required in order to make the necessary atmospheric corrections for the generation of surface reflectance values.

3b. Atmospheric Corrections

For quantitative analysis of surface reflectance, removing the influence of the atmosphere is a critical pre-processing step. To compensate for atmospheric effects, ENVI's atmospheric correction module, FLAASH (Fast Line-of-sight Atmospheric Analysis of Spectral Hypercubes) incorporates the MODerate resolution atmospheric TRANsmission 4 (MODTRAN 4) radiation transfer code in order to compute an estimate of the true surface reflectance. The following procedure was used to retrieve atmospherically corrected reflectance images:

1. From the ENVI main menu bar, select one of the following: Basic Tools>Preprocessing>Calibration Utilities>FLAASH or Spectral >FLAASH.
2. To select the input radiance image: Click Input Radiance Image to open the FLAASH Input File dialog > Select the input file, then click OK. In the Radiance Scale Factors dialog, select Use single scale factor for all bands> Enter Scale factor: 0.1 (for a unit micro watts per squared centimeters* nm *str).
3. To set file output parameters: Click Output Reflectance File > navigate to the desired output directory and enter the new file name in the text box.
4. Enter the scene center location in latitude and longitude.
5. From the Sensor Type button menu, select the name of the sensor: Landsat 7 in Multispectral sensor types (The sensor altitude and the pixel size are automatically set when the sensor type is selected).
6. From the Flight Date drop-down list, select the month and day the scene was collected. Use the arrow increment buttons to select a year, or enter the four-digit year in the text box. In the Flight Time text boxes, enter the Greenwich Mean Time at which the scene was collected, in HHMMSS format, or use the arrow increment buttons to set the time.
7. Selecting Atmospheric Model Settings: choose one of the standard, Atmospheric MODTRAN model → e.g. Mid-Latitude Summer (MLS) for Landsat7 data acquired Sept 8, 2002, the scene center about 40 degree N.

8. Water Retrieval setting is No. Leave Water Column Multiplier : 1
9. Selecting an Aerosol Model: choose one: e.g. Maritime, or Rural.
10. Aerosol Retrieval : "No" to use the value in the Initial Visibility text box.
    Enter Initial Visibility (km): either referring to local weather information for visibility (e.g. Visibility 16 km over the Great Peconic Bay scene at Sept 8, 2002 image), or approximated followings : Clear : 40 to 100 km , Moderate Haze : 20 to 30 km, Thick Haze : 15 km or less.
11. Click "Advanced Settings" button>
    Re-define Scale Factors For Radiance Image: 0.1 (in case of Landsat 7).
12. Change Output Reflectance Scale Factor: 1000 (for Landsat 7 reflectance retrieval).→ click OK> Apply" button to run FLAASH Atmospheric Correction model.

3c BAND RATIOS

Band ratios were generated to enhance the spectral differences between bands and increase the number of input source bands in order to generate more detailed class separations. The process of dividing one spectral band by another produces an image that provides relative band intensities. For example, band ratios used to derive the land cover classification from the six channels of Landsat data include: The ratios of (band 4-band 3)/(band 4+band 3) for vegetation intensity, average of band 4 and 5 for discriminating highly reflective land covers, average of band 5 and 7 for separating bright sandy materials from impervious painted objects, subtracting band 2 from band 5 for wetness separation, and the average of band 1, 3, and 4 for discerning dark soil from dark asphalt pavement.

4 RESULTS

4a LAND COVER CLASSIFICATION MAPPING

As a reference, a land cover classification map was generated using the NLCD 2001 data by overlaying raster layers. Figure 1 shows a full coverage for Suffolk County with 15 land cover classes and their coverage as acres. Figure 2 presents the classified map, with each class-percent-coverage, for the area of Suffolk County that matched the mosaicked Landsat coverage. As previously mentioned the NLCD data, a combination of multiple surveys taken 3 times during the year and supplemented with aerial imagery, has limited utility for local scale investigations or inter-annual change detections in specific areas. However, the data collection and verification procedure was extremely rigorous and should be used to qualitatively to assess the present classification and land cover change detection study. In order to estimate county-wide changes of land cover during the last 15 years image classifications using Landsat data from 1989 to 2005 were carried out. The analysis produced images with more than the baseline/standard 15 classes generated from the NLCD data. Since the classification applied in this study was based on physical properties of objects, it was possible to construct a more detailed classification. The following Figures 3 through 7 are the products of land cover classification mapping between 1989 and 2005 with the corresponding statistics shown in Table 1.

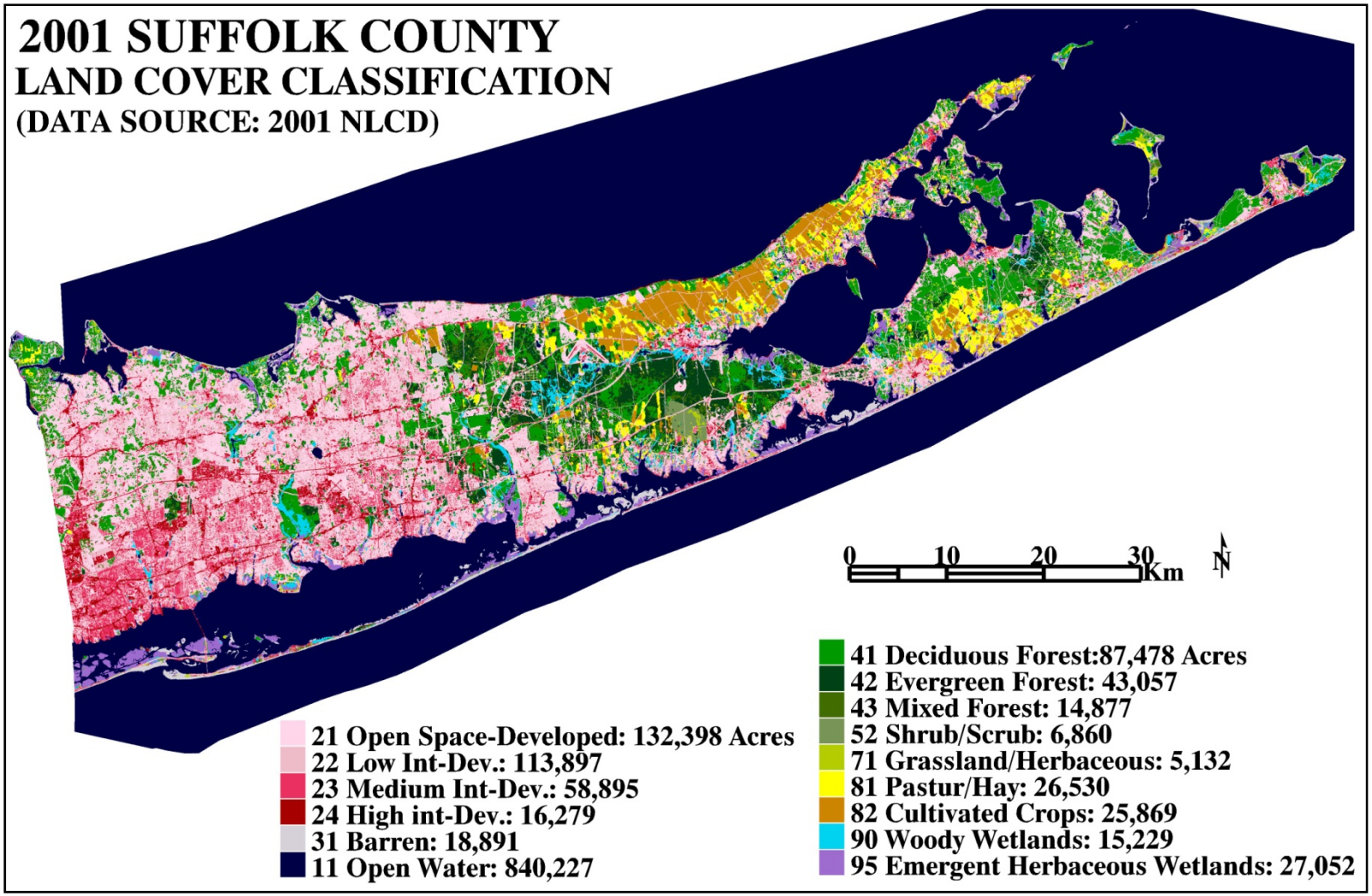

Figure 1: NLCD 2001 Land Cover Classification. The procedure generated 15 classes that were used for comparison with Landsat images.

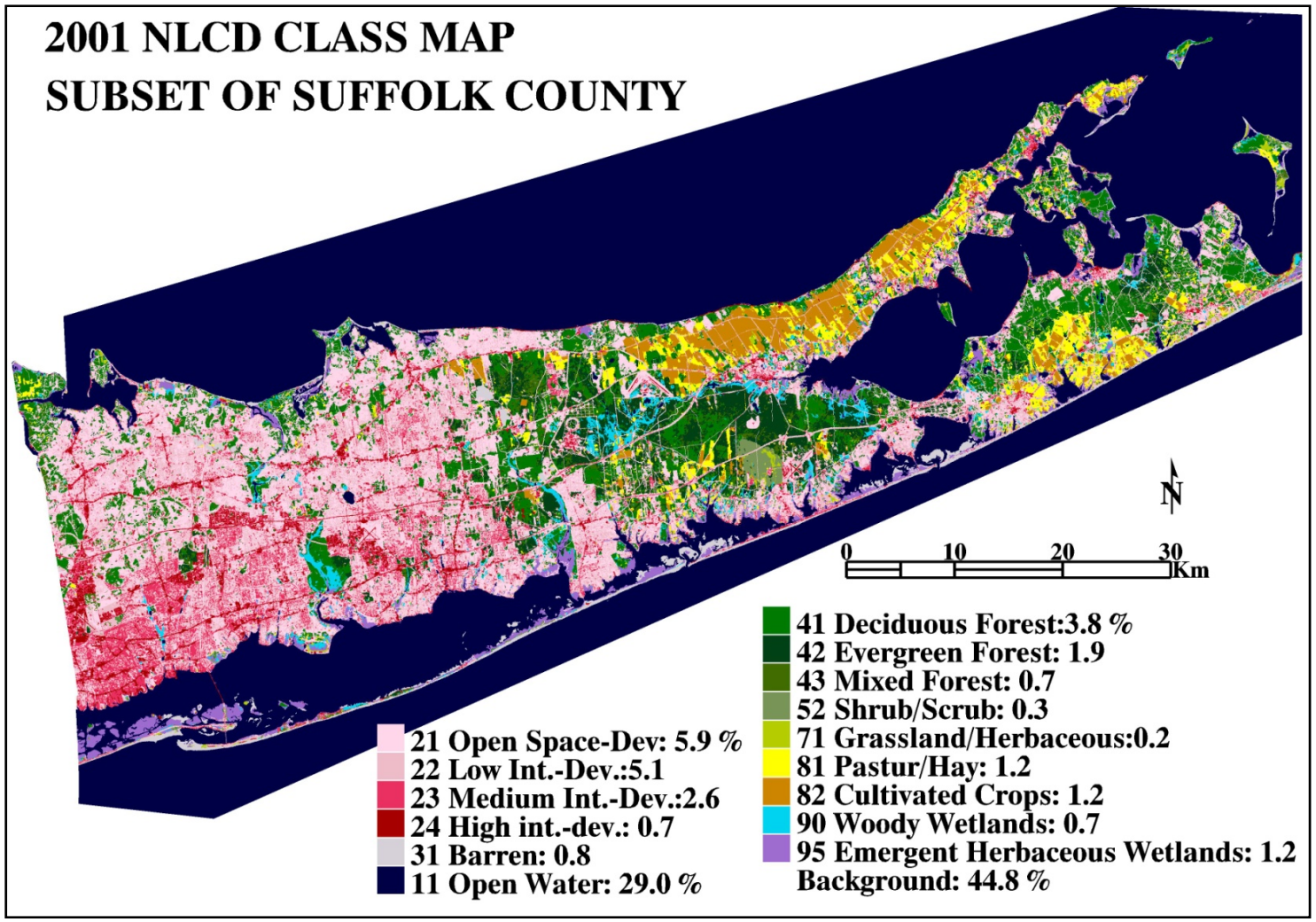

Figure 2: Subset of the NLCD 2001 land cover classification map matching to the same area of the mosaicked Landsat image. The percent coverage for each class is presented next to the class name.

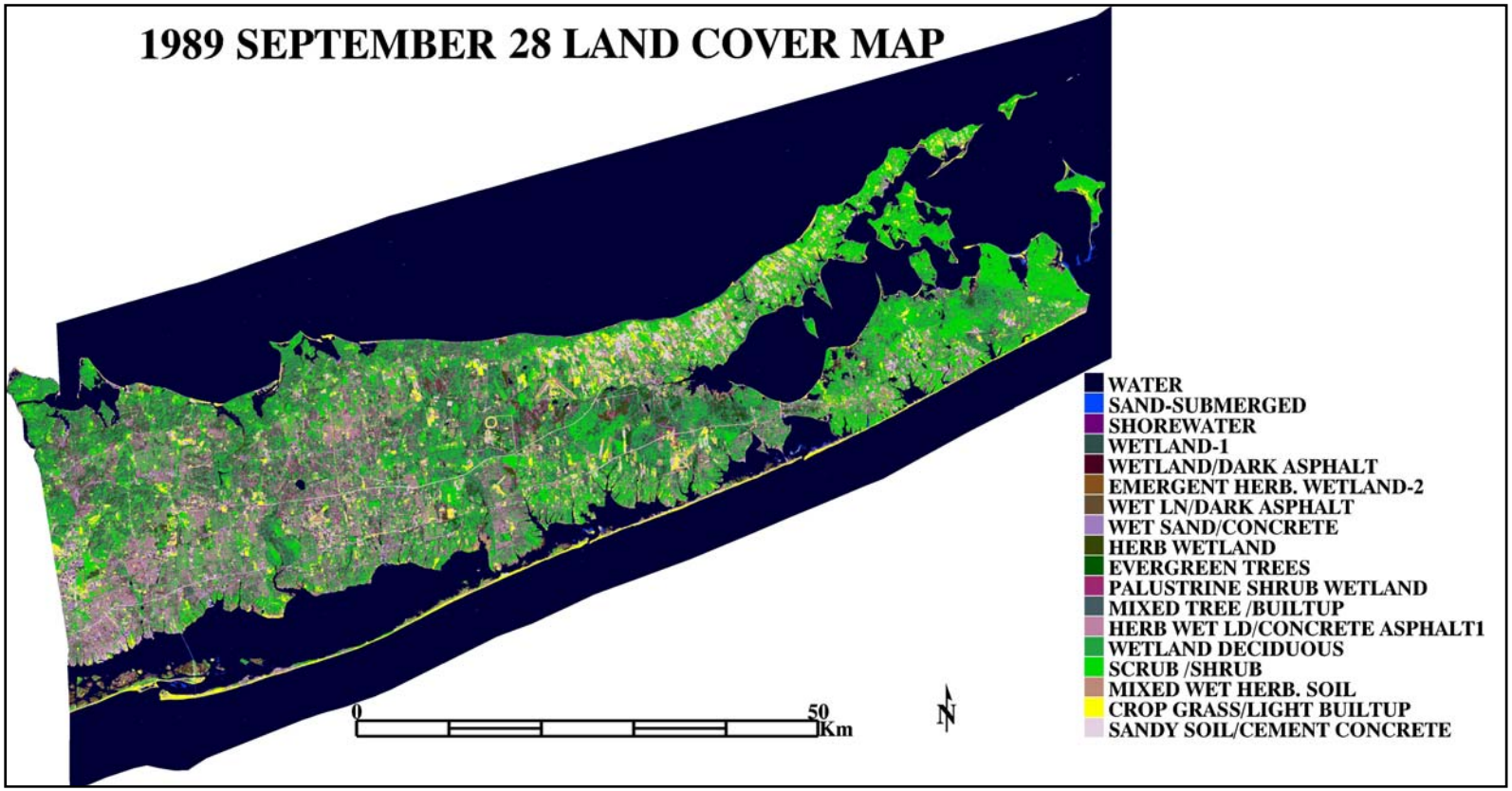

Figure 3: Land cover classification map generated from the Landsat TM 5 image of September 28, 1989.

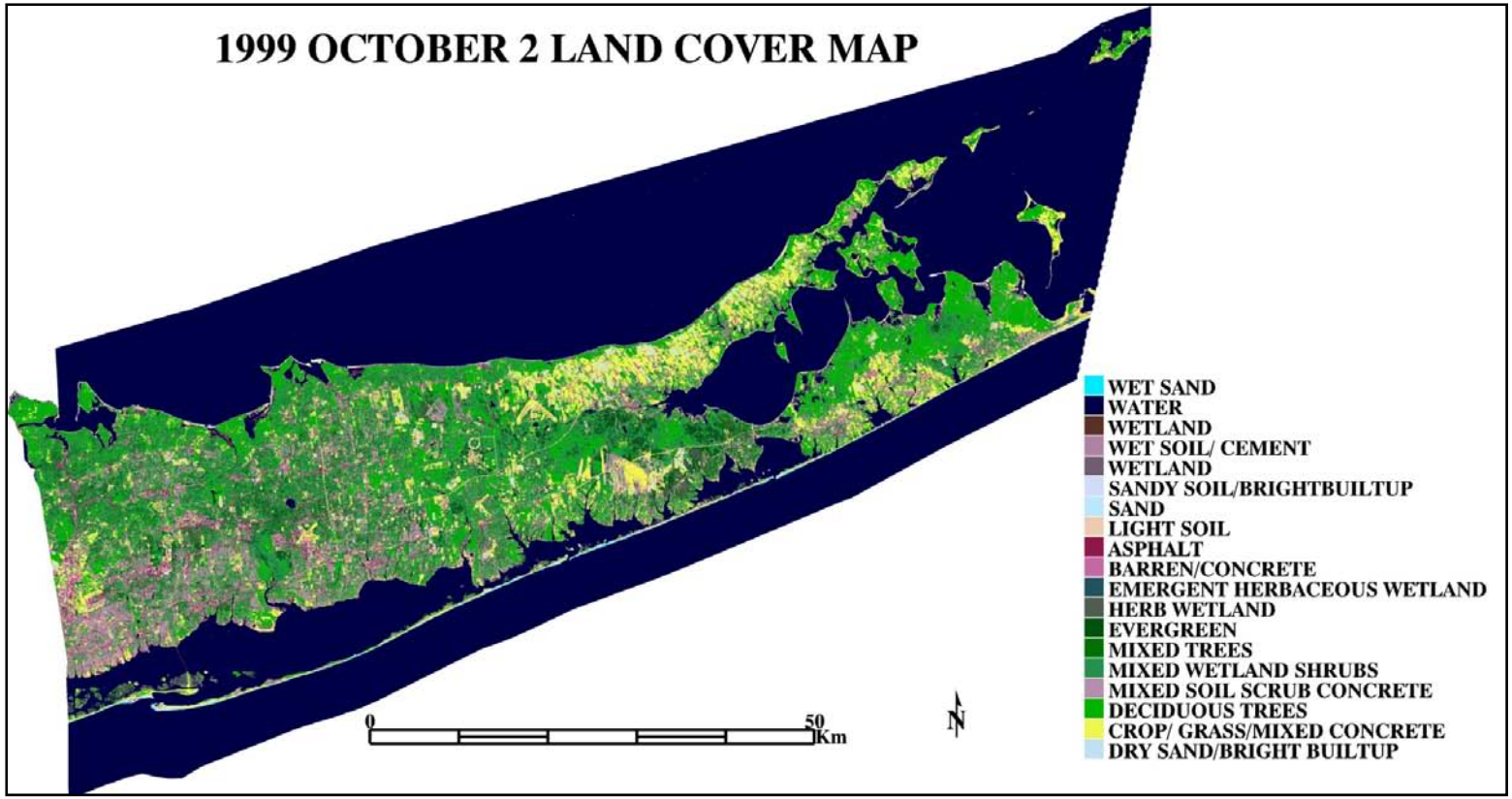

Figure 4: Land cover classification map generated from the Landsat 7 ETM+ image of October 2, 1999.

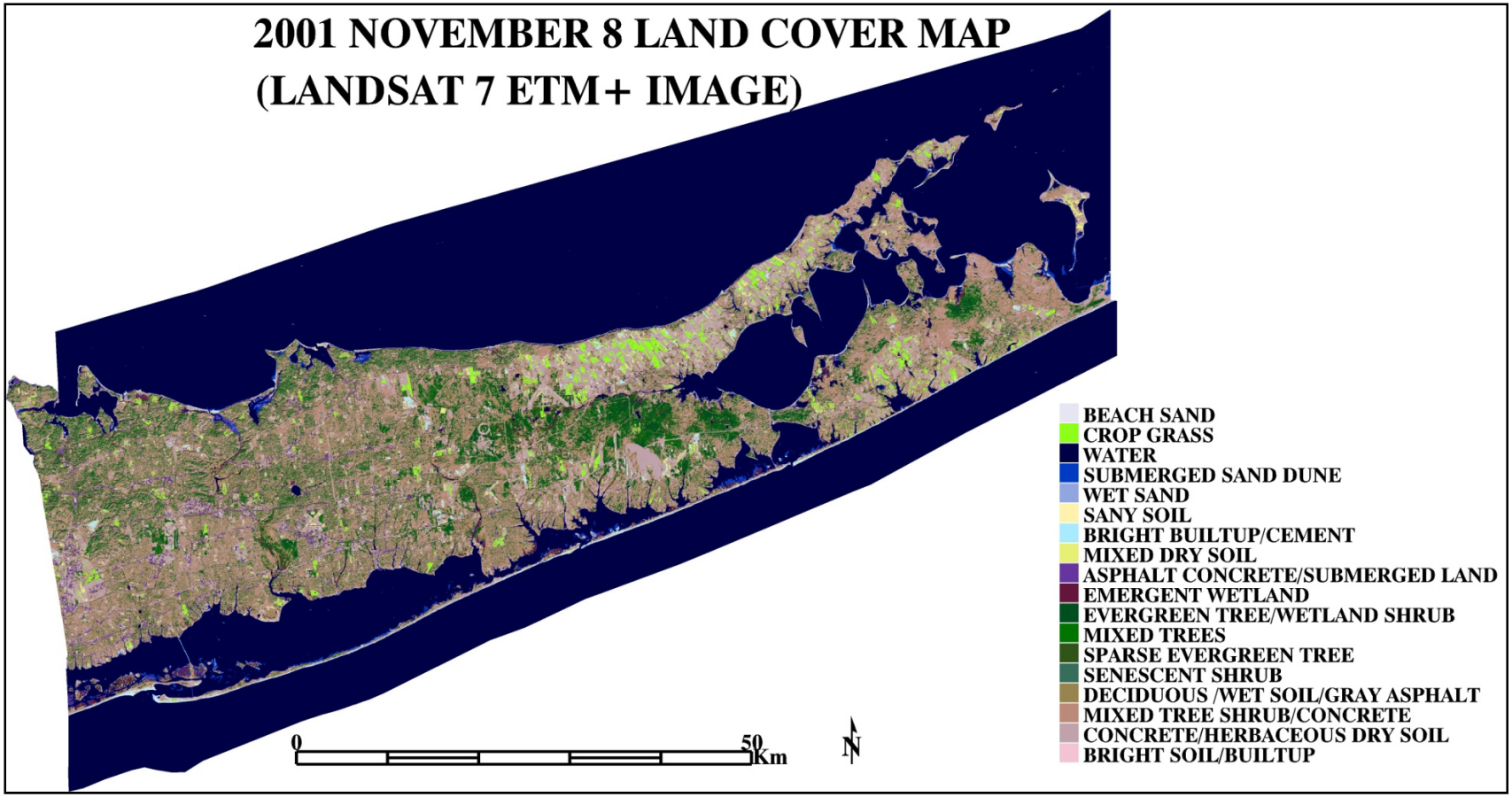

Figure 5: Land cover classification map generated from the Landsat 7 ETM+ image of November 8, 2001.

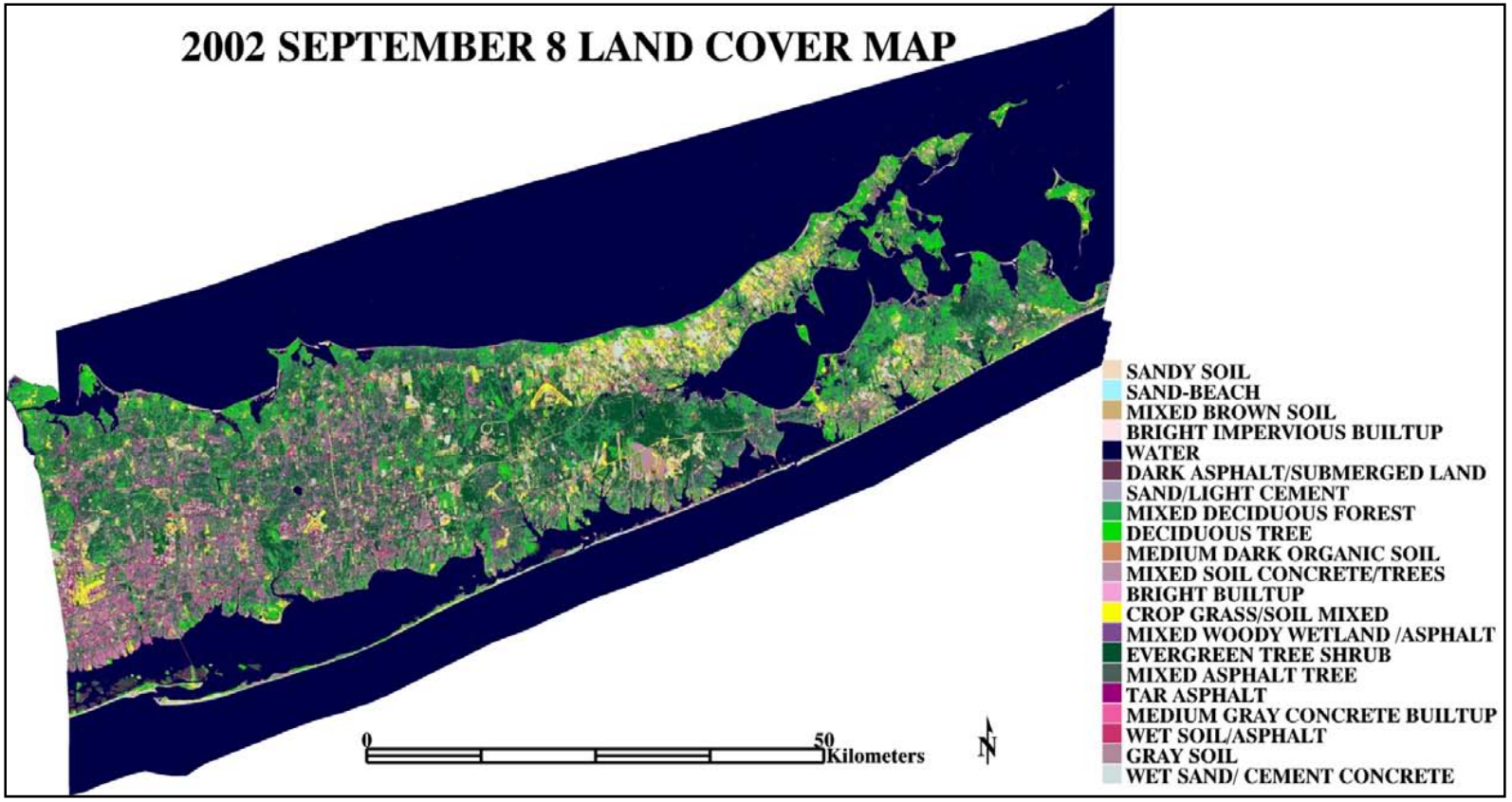

Figure 6: Land cover classification map generated from the Landsat 7 ETM+ image of September 8, 2002.

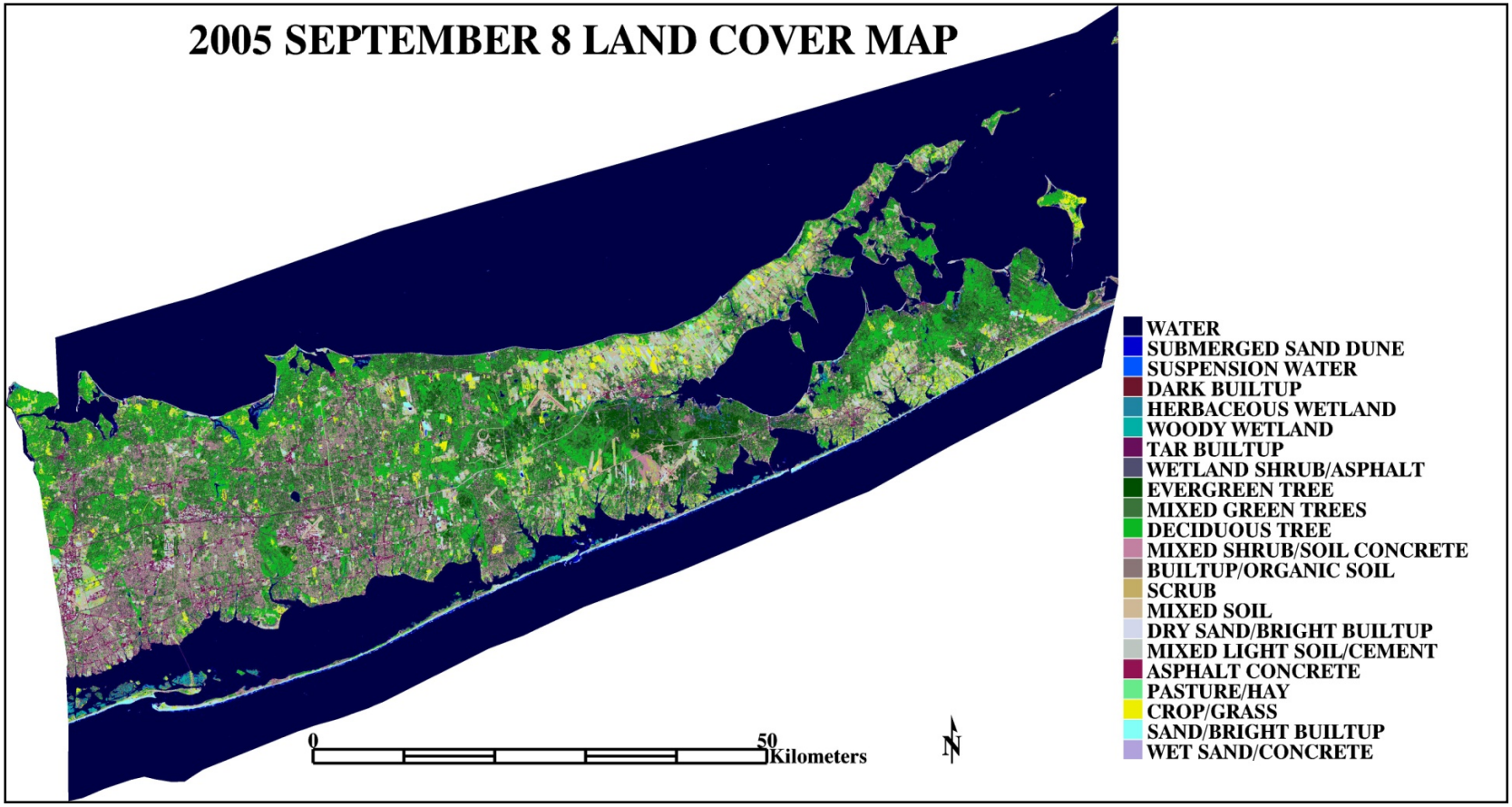

Figure 7: Land cover classification map generated from the Landsat TM 5 image of September 8, 2005.

Table 1: Summary statistics for the land cover classifications of September 28, 1989, October 2, 1999, November 8, 2001, September 8, 2002 and September 8, 2005.

CLASS	DISTRIBUTION PERCENT (%)				
	1989/9/28	1999/10/2	2001/11/8	2002/9/8	2005/9/8
WETLAND/TAR ASPHALT	0.12	0.12		0.31	
EMERGENT HERBACEOUS	O.17	0.22	0.59	0.83	0.11
WET SAND/CONCRETE	0.72	1.02	0.08	1.04	0.04
WOODY WETLAND	0.56	0.59	1.82	1.77	0.27
EVERGREEN FOREST	1.74	0.97	2.16	4.80	2.29
MIXED GREEN TREES		1.71	1.22		3.82
DECIDUOUS FOREST	4.92	4.96		2.06	4.04
MIXED DECIDUOUS SHRUB			6.74	3.44	3.20
DECIDUOUS			3.01		
SHRUB/SCRUB	4.85	3.71			0.56
MIXED WETLAND SHRUB		3.43			1.14
MIXED TREE BUILTUP	2.20			1.46	
MIXED HERBACEOUS WET	2.99	3.71			
MIXED SOIL TREE	1.72	3.43			
CROP GRASS SOIL/BRIGHT	1.12	2.79	4.61		
CROP/GRASS			0.61	1.21	0.90
PASTURE/HAY					1.01
SANDY SOIL/CEMENT	1.59				0.76
SANDY SOIL		0.04	0.03	0.08	
DRY SAND		0.07	0.05	0.04	
ASPHALT (TAR/DARK)		0.22	0.55	1.04	1.13
DRY SAND/BRIGHT BUILTUP		0.49	0.02	0.09	0.19
BRIGHT BUILTUP			0.24	0.02	
DRY SOIL			0.31		0.83
MIXED SOIL-GRAY, BROWN			0.31	0.10	0.57
UNCLASSIFIED	46.74	50.97	48.24	47.70	48.32

4b SUBSET COMPARISON OF CLASSIFIED IMAGES FROM ALI

Since there were no ground observations available to compare the results from the previous Landsat imagery classifications, the higher spatial and spectral data from ALI 2004, and 2006 image classification results were used for an alternative approach. Unlike Landsat data, ALI provides nine channels within the visible and shortwave infrared portion of the spectrum and includes one panchromatic band. These additional bands enhanced land cover classifications. Figures 8 and 9 are the classification results from ALI images taken on April 6, 2004 with 23 classes and August 8, 2006 with 22 classes at a 10 m pixel resolution. The summary of each classification is presented in Table 2.

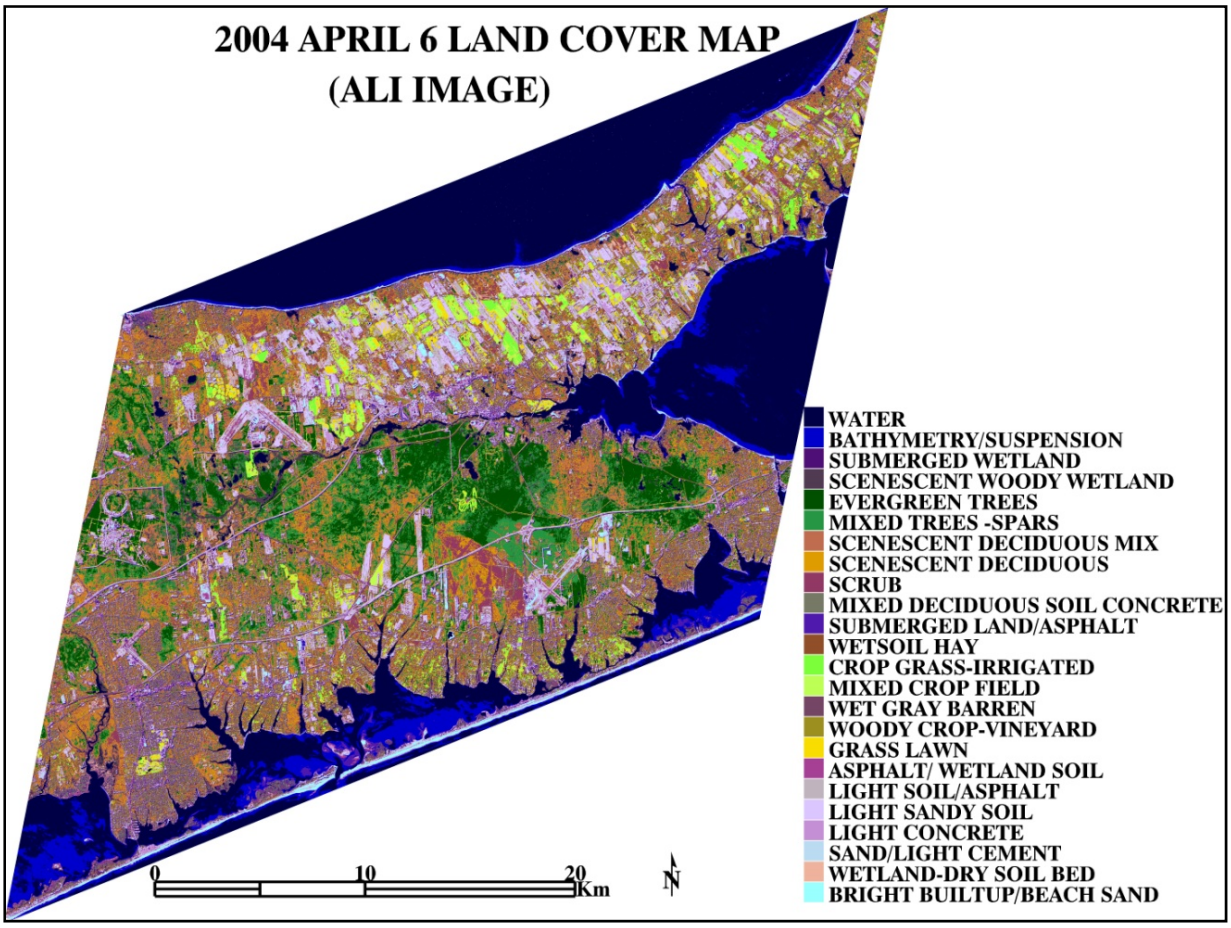

Figure 8: Land cover classification map generated from ALI April 6, 2004 image. The area covers about 38 km x 47 km over the central part of Suffolk County.

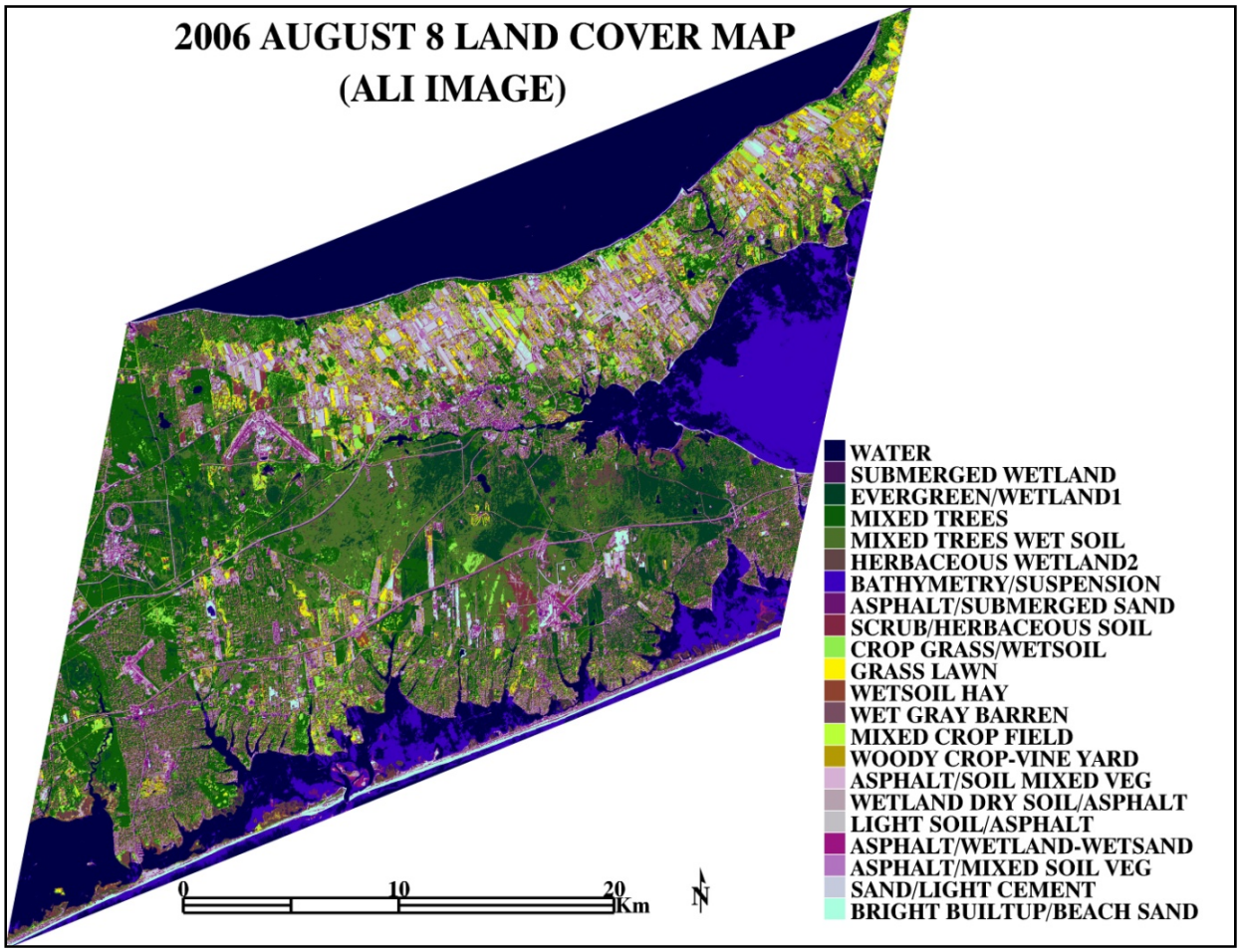

Figure 9: Land cover classification map generated from ALI August 8, 2006 image. The area covers about 38 km x 47 km over the central part of Suffolk County.

Table 2: Summary of land cover classification results from ALI recorded on April 6, 2004 and August 8, 2006.

CLASS	4-6-2004 (%)	8-8-2006 (%)
EMERGENT WETLAND	2.11	1.17
HERBACEOUS WETLAND	NONE *	1.94
WOODY WETLAND	1.62	2.33
SCENESCENT WETLAND SHRUBS	3.33	NONE
EVERGREEN FOREST	3.56	5.87
SPARSE CONIFERS	4.10	NONE
MIXED TREES-FOLIATED GREEN	3.64	6.25
DECIDUOUS-DEFOLIATED /SCRUB	2.66	7.46
CROP-IRRIGATION FIELD	0.60	2.33
GRASS LAWN	NONE	1.16
PASTURE/HAY (DRY LAND)	0.84	1.03
HAY (WET SOIL)	NONE	1.43
WOODY CROP-VINE YARD	1.79	0.98
MIXED CROP SOIL (BROWN/GRAY)	NONE	1.03
DRY LIGHT GRAY SOIL	3.07	0.83
MIXED SPARSE GRASS LAWN & SOIL/LIGHT	1.16	NONE
MIXED GRAY ASPHALT HERBACEOUS DRY	1.71	NONE
MIXED CONCRETE & HERB DRY SOIL	3.01	NONE
WET SOIL /ASPHALT	NONE	1.08
WETLAND SCRUB	2.72	NONE
LIGHT SOIL/ASPHALT	NONE	1.07
ASPHALT/MIXED SOIL TREES	NONE	1.71
SAND/LIGHT CEMENT	0.70	2.04
BRIGHT BUILTUP/BEACH SAND	0.37	0.72
CONCRETE ASPHALT	0.72	NONE
DARK GRAY ASPHALT/SUBMERGED LAND	1.22	0.96
DARK GRAY WETLAND/CONCRETE	2.28	NONE
TAR PAVE/BATHYMETRY	NONE	0.17
UNCLASSIFIED (BACKGROUND)	43.23	43.23

*NONE indicates no distribution appeared in this class.

Results from the analysis indicated that significant differences in land cover classes were observed between ALI images. The land classifications were greatly influenced by season or the time of the image was taken with respect to the annual cycle, as well as weather conditions preceding collection of the data. Precipitation, even several days in advance of the image, can blur delineation of vegetation types, whereas images collected during dry periods produce sharper distinctions between regions. For example the image collected on April 6, 2004 (Figure 11) during the dry and defoliated season indicates better discrimination among vegetation classes. For the same region, the sensitivity of the classification procedure to the annual growing cycle can be seen in the August 8, 2006 image (Figure 10). In this image a more diversified classification over agricultural cultivation fields appear by the fully growing summer season. As expected the classifications will also be limited by the image resolution. For these particular images, with a 10-m pixel resolution, the classification procedure generated a great deal of mixed classes especially over narrow concrete or asphalt tar paved roads, highways and small buildings with various neighboring surfaces. The ALI classification was also sensitive to moisture content, illustrated by the even differentiation within the same crop field. The additional bands ms1' at 0.433 µm, ms4' at 0.845 µm, and ms5' at 1.200 µm included in ALI data, can be beneficial for detecting crop growth condition, inland water quality and more detailed soil differentiation in crop fields.

Figure 10: ALI August 8, 2006

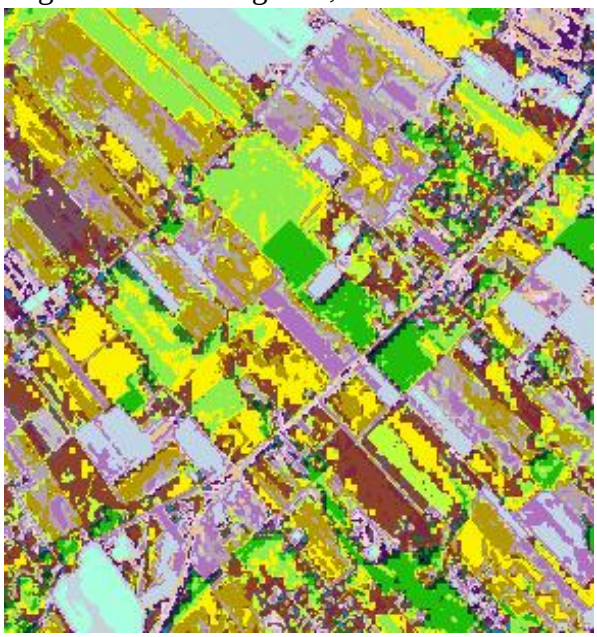

Figure 11: ALI April 6, 2004

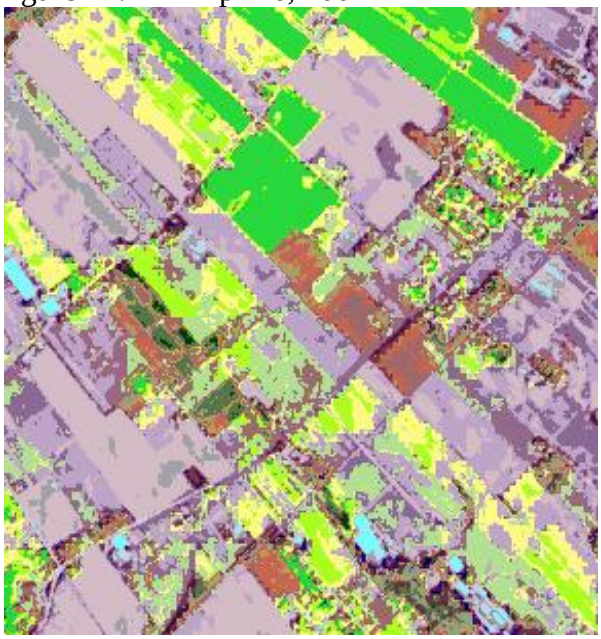

Figure 10 and 11: Subsets of agricultural fields near the northern part of Mattituck, Suffolk County. Figure 10 ALI August 8, and Figure 11 ALI April 6, 2004.

Both Landsat and ALI data can be used effectively for land cover classification, however the higher resolution of ALI data does provide better separation for many of the classes. Figure 12 shows a subset of the ALI April 6 2004 classification image and the Landsat 7 ETM+ image acquired on November 8 2001 (Figure 13). This area is composed of residential housings, airport runways, crop fields, forests and wetlands. Both scenes were collected during dry and defoliated

seasons, ALI in early spring and Landsat in late fall. Within the residential area, the ALI classification map was able to separate each housing unit from neighboring surfaces, as well as, delineate the main roadways in the region. In addition the ALI classification map differentiated the various compositions of soil fields which were not well discernable using the ETM+ data. The price, availability and coverage of Landsat ETM+ data make it attractive for use in classification studies. Researchers and managers should consider using ETM+ data for identification of regions experiencing substantial changes in land cover only. For more detailed changes in land cover or for studies in sensitive regions such as wetlands, higher resolution ALI data should be applied.

Figure 12. ALI 2004-4-6

Figure 13. ETM+ 2001-11-8

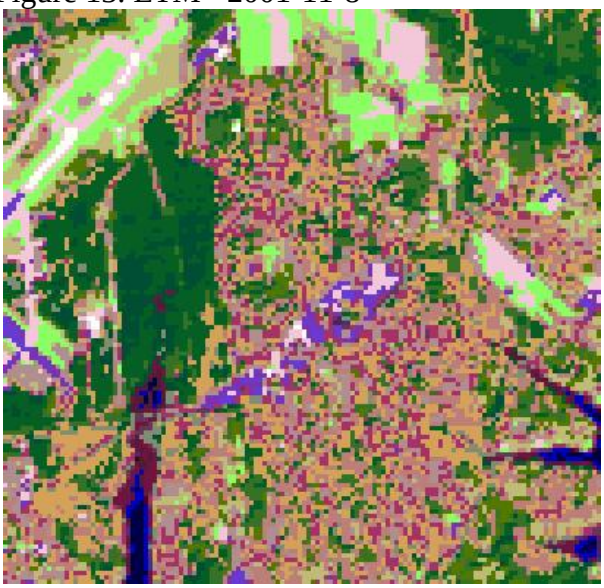

Figure 12 and 13: Comparison between the ALI classification map at 10 m resolution and the ETM+ classification map at 28.5 m resolution. Figure 12: 10 m resolution of ALI data on April 6, 2004. Figure 13: 28.5 m resolution of ETM+ on August 8, 2001. Both images are in the southern part of Oakdale, Suffolk County.

In addition, acquisition of ALI data should be given careful consideration as it is only available upon special request. For specific site or class analysis such as wetland inventory, additional images may be needed to provide the correct temporal resolution to discern vegetation types. Wetlands in particular have different grasses that bloom in spring, summer and fall and a single image scene may have difficulty delineating the boundaries. The sensitivity of the classification procedure to the seasonal growing cycle was exemplified in the classification of the ALI August 8 2006 image where delineation of vegetation types over forest areas was difficult due to mixing of green leaf trees with coniferous trees. Analysis of this data set also resulted in more mixing classes between asphalt or concrete roads and wet soil or tree standing areas. However, the classification map did shows a good indication of the wetland extent associated with clearing up of the spring season species as shown in Figure 12. In addition this type of map may provide valuable information about senescent time changes associated with changes in local and global climate. Considering the different blooming-senescent times for wetland grasses, accurate

detection of the type and stage of wetland grass can be determined through greater temporal resolution throughout the growing cycle.

Figure 14: ALI August 8, 2006 (BAND 5, 4, 2) Figure 15: ALI August 8, 2006 classified map

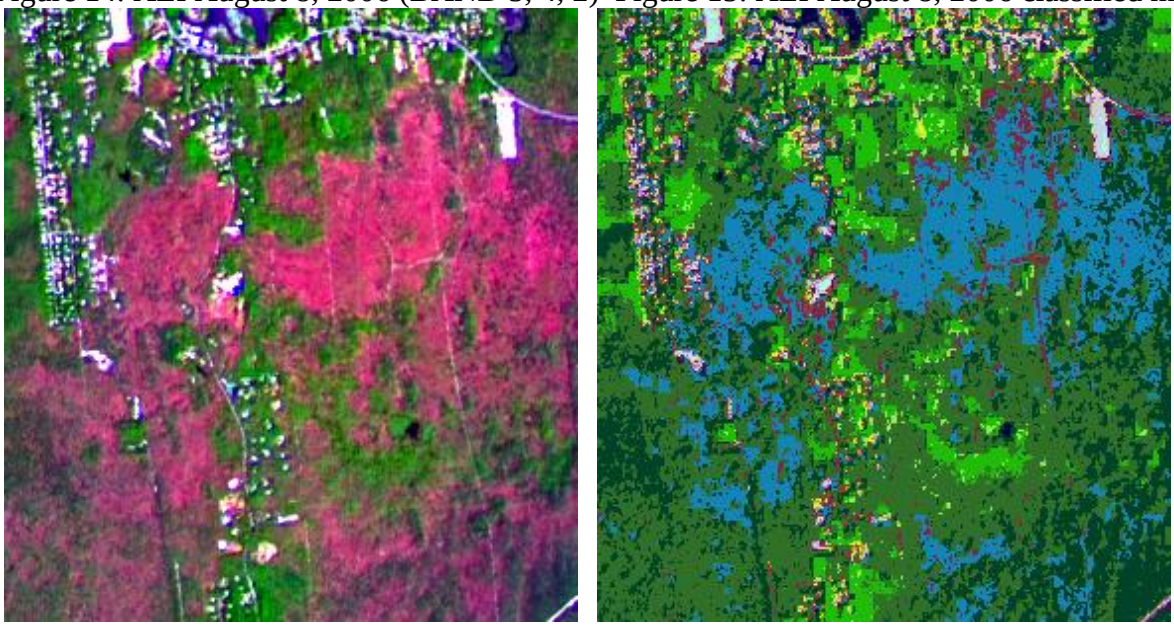

Figures 14 and 15 documenting of wetland extent during the summer season over Flanders, Suffolk County. Figure 14: ALI August 8, 2006 image (color composite of bands 5, 4, and 2 as RGB); Figure 15: Classified image.

4c CHANGE DETECTION FOR SUFFOLK COUNTY

Based on the classification maps, an analysis of overall land cover change in Suffolk County between the year 1989 and 2005 was attempted. Results from the analysis indicate that changes in land cover classes were large and unpredictable. Considering some of the limitations or concerns associated with the collection of the data sets, mentioned above, a specific analysis was focused on the land cover class “Evergreen Forest”, which is expected to exhibit much less variation. For this assessment, all Landsat classification maps and two ALI classification maps were subset to the same area. The summary is shown in Table 3. Referring to the summary table, the amount of only the evergreen forest class, excluding the class for mixed green trees, declined its coverage from 1989 until 2001. The analysis indicates that the evergreen forests then regain their coverage in the year 2002. Based on the previous assessment of instrument resolution and classification results the ALI 2004 data, which indicated 3.56% evergreen forest, was considered reliable.

In order to illustrate the influence of atmospheric conditions on the land cover change analysis, weather conditions leading up to the ALI and Landsat classifications were analyzed. The influence of precipitation is most noticeable in the 2001 map and 2002 map. As the last column in Table 3 shows, significant variations were associated with previous day/days precipitation amount which resulted in misclassification or confusion between wetland and submerged land/dark asphalt. Results from the 2005 classification map indicate an overestimation is

associated with misclassification of dark asphalt and tree standing asphalt. This result illustrates the importance of using satellite data acquired on the day following at least 4 or 5 days dry weather conditions.

Table 3: Distribution statistics of land cover class “Evergreen Forest” between 1989 and 2006.

CLASSES	PERCENT	SENSOR	DATE	WEATHER CONDITIONS
EVERGREEN FOREST (overestimated by inclusion of wetland green trees)	3.29%	TM5	9/28/1989	Rain 2 days early (Sept 26)
MIXED GREEN TREE	4.93%			
SUM	8.22%			
EVERGREEN FOREST	2.91%	ETM7	10/2/1999	Heavy rain 2 days early (Sept 30) heavy
SHRUB (WETLANDS)	1.58%			
MIXED GREEN TREE SHRUB	2.81%			
SUM	7.31%			
EVERGREEN FOREST (WETLAND SHADOW)	2.36%	ETM7	11/8/2001	Light rains 4-5 days early
MIXED CONIFER SHRUB	3.17%			
SPARSE GREEN TREES	2.83%			
SUM	8.36%			
EVERGREEN FOREST	2.70%	ETM7	9/8/2002	Heavy rains 4 & 6 days early
YOUNG GREEN SHRUB	0.91%			
MIXED TREES	4.73%			
SUM	8.34%			
EVERGREEN FOREST	3.56%	ALI	4/6/2004	Short time light rains 2 to 5 days early
SPARSE CONIFERS	4.10%			
SUM	7.65%			
EVERGREEN FOREST (*overestimation by containing some asphalt tree mixing area)	6.04%	TM5	9/8/2005	No precipitation in previous 7 days
MIXED TREES (WET	2.19%			
SUM	8.23%			
EVERGREEN FOREST	5.87%	ALI	8/8/2006	1 day early

4d CHANGE DETECTIONS WITHIN WETLAND AREAS

As an example of a specific site change detection study, Peconic Bay watershed area was subset from all the Landsat classified maps. The land cover composition and their distributions vary between seasons as well as between years. Figure 16 and 17 represent the distribution statistics of land cover classes based on 2001 NLCD (Figure 16) and 2005 TM5 classification (Figure 17) over Peconic Bay watershed area. The summary Table 4 shows detail distribution percentage within the area.

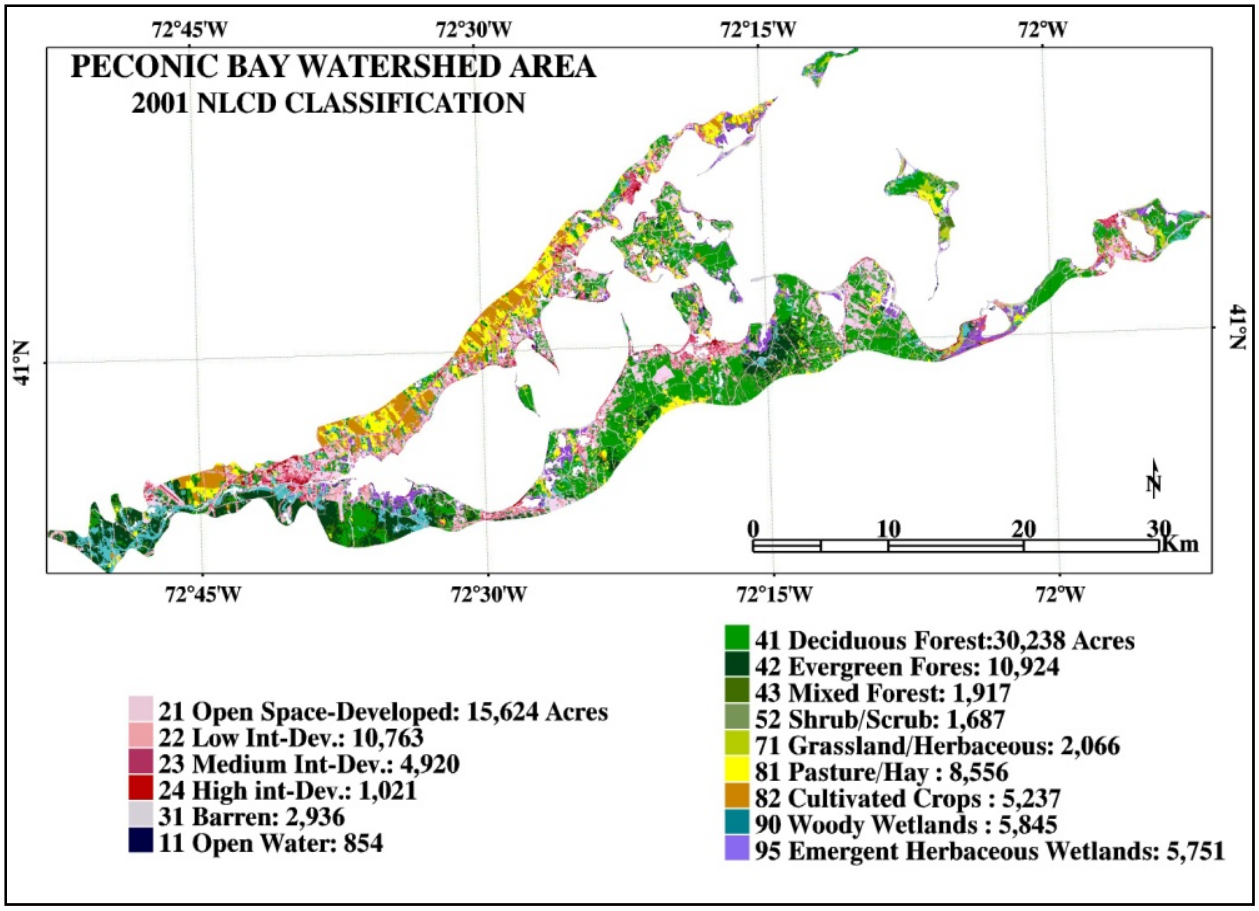

Figure 16: Land cover classification on 2001 NLCD over Peconic Bay watershed area.

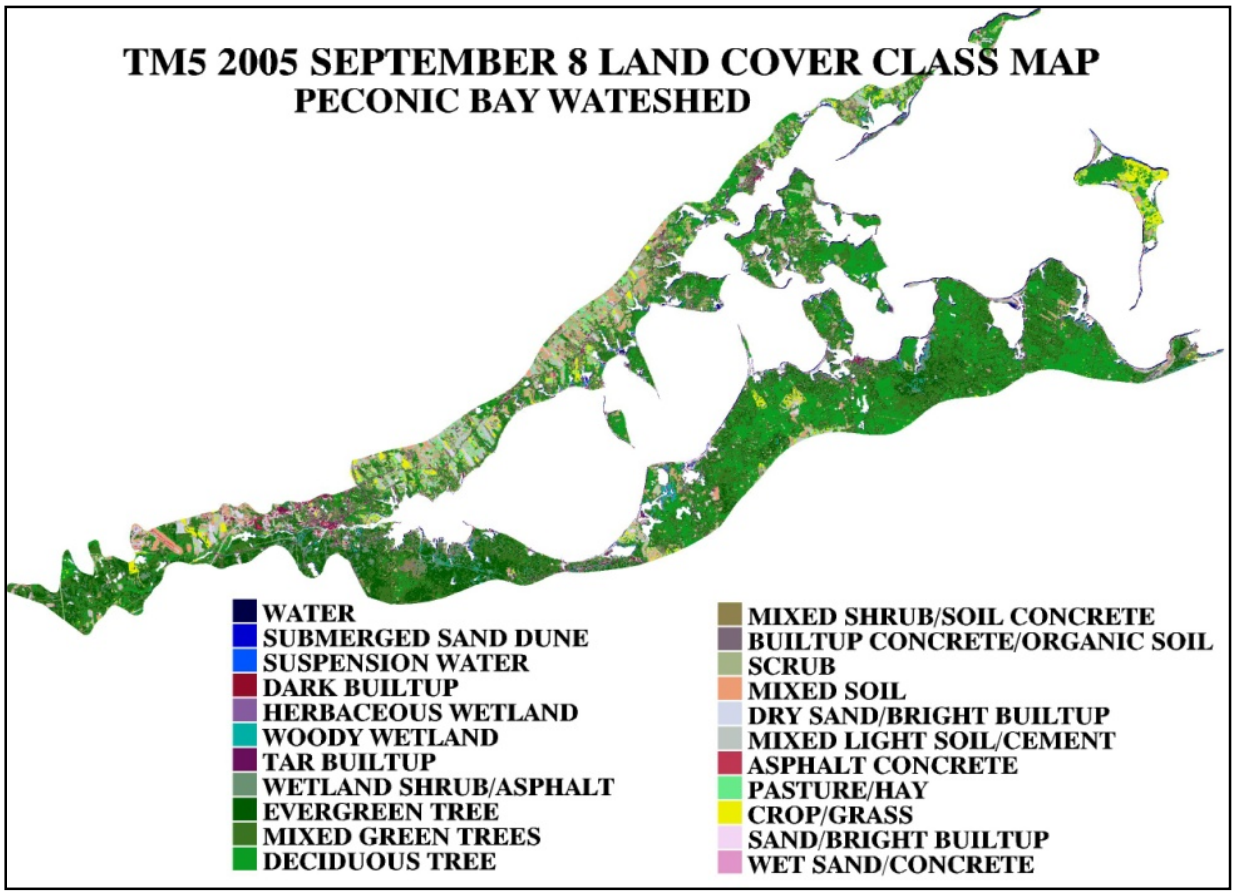

Figure 17: Land cover classifications on 2005 TM5 over Peconic Bay watershed area.

Subset comparison of the wetland areas between the classified maps of Landsat and ALI was also conducted. Related to different spatial resolution as well as spectral compositions, the results of ALI maps show more details of wetland composition. This implies that assessing wetland extent and wetland inventory using about 30 m pixel resolution Landsat data is not adequate. The following images in Figure 18, 19 and 20 are examples taken over the tidal wetland area in Flanders Bay. In the figures, the yellow lines enclose the area for the tidal wetland area as published in 2001 by the USGS. The comparison between the two different seasonal maps of ALI 2004 (Figure 18) and 2006 (Figure 19) show that it is necessary to acquire dry season ALI images especially for the assessment of wetland area. The composition of wetlands in the summer season ALI 2006 map is more simplified in overall classes.

Table 4: Summary statistics of class distribution in 2001 based on NLCD and 2005 based on Landsat TM 5 over Peconic Bay watershed area.

CLASS-2001 NLCD	%	CLASS-2005/9/8	%
OPEN SPACE-DEVELOPED	2.20	SUBMERGED SAND DUNE	0.08
LOW INTENSITY-DEVELOPED	1.51	SUSPENSION WATER	0.02
MEDIUM INT-DEV	0.65	DARK BUILTUP	0.09
HIGH INT.-DEV.	0.15	HERBACEOUS WETLANDS	0.08
BARREN	0.36	WOODY WETLANDS	0.25
DECIDUOUS FOREST	4.11	TAR BUILTUP	0.21
EVERGREEN FOREST	1.62	WETLAND	0.87
MIXED FOREST	0.25	EVERGREEN TREES	2.05
SHRUB/SCRUB	0.24	MIXED GREEN TREES	3.14
GRASSLAND/HERBACEOUS	0.24	DECIDUOUS	3.33
PASTURE/HAY	1.25	MIXED SHRUBS/SOILS	1.20
CULTIVATED CROPS	0.78	CONCRETE	0.46
WOODY WETLANDS	0.81	SCRUB	0.45
EMERGENT HERB.	0.75	MIXED SOILS	0.48
		DRY SAND/ BRIGHT	0.35
		MIXEDLIGHT SOILS	0.53
		ASPHALT CONCRETE	0.13
		PASTURE/HAY	0.58
		CROP/GRASS	0.47
		SAND/BRIGHT BUILTUP	0.07
		WET SAND/CONCRETE	0.00
BACKGROUND	85.0	BACKGROUND	85.0

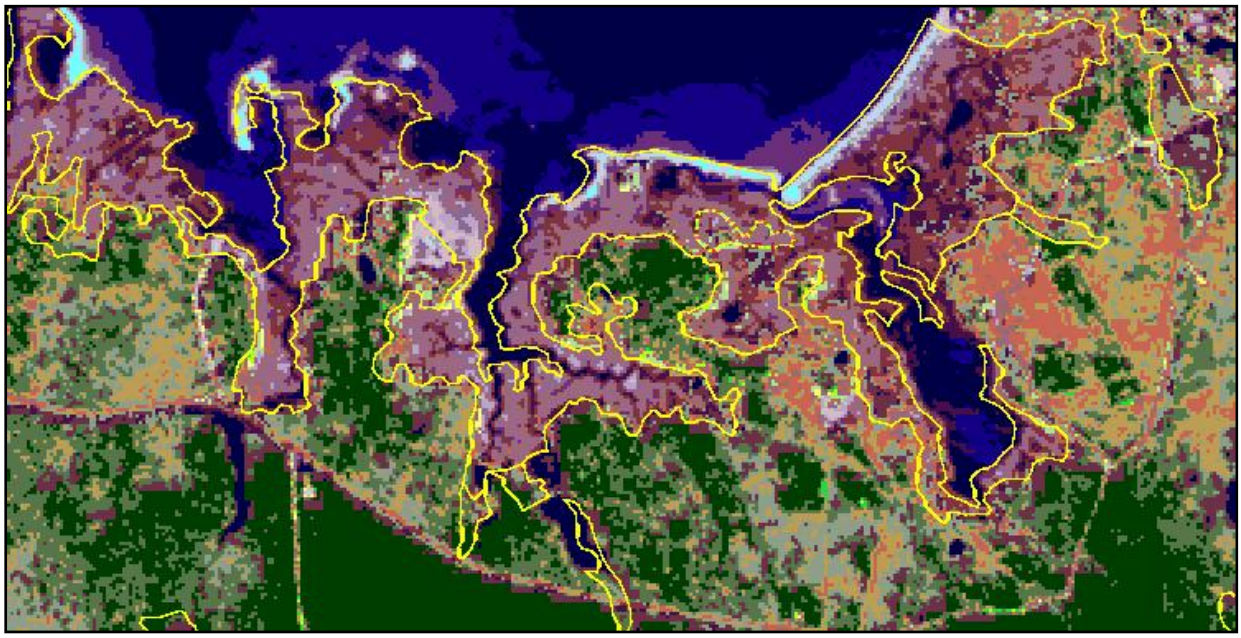

Figure 18: Wetland area in Flanders Bay shown with ALI on April 6, 2004 at 10 m pixel resolution.

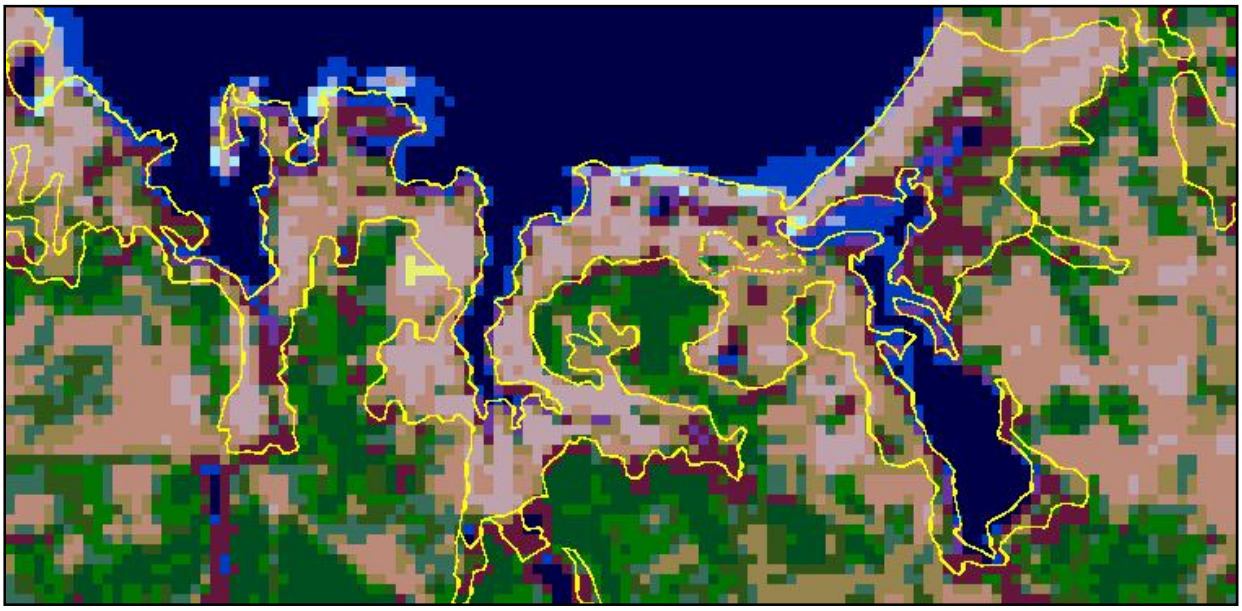

Figure 19: Wetland area in Flanders Bay shown with ETM on November 8, 2001 at 28.5 m resolution.

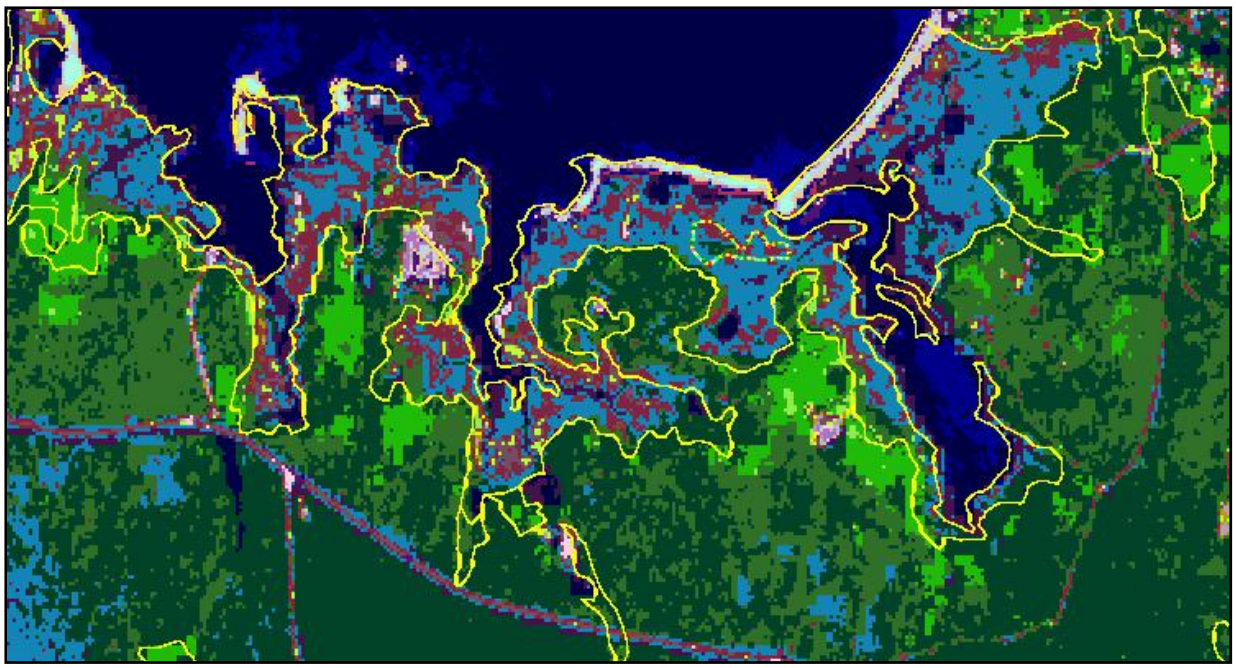

Figure 20: Wetland area in Flanders Bay shown with ALI on August 8, 2006 at 10 m resolution.

Table 5 summarizes only those classes above 3%. Although ALI data are better than Landsat data for wetland inventories, they are too coarse to delineate diverse wetland grasses or specific shrub types.

Table 5: Composition within wetland for classes above 3 %.

CLASS	TM5 11/8 2001	ALI 4/6 2004	ALI 8/8 2006
HERBACEOUS	22		
MIXED TREE SHRUBS	17.6	7.1	8.7
DECIDUOUS/WET SOIL	17.6	4.2	
HERBACEOUS WETLAND	14.2	22.1	30.5
EVERGREEN	8.1		10.5
ASPHALT	5.9	5.7	
SENESCENT SHRUB	5.7	4.8	4.7
SUBMERGED LAND	4.2	10.2	10.3
WATER		3.8	5.1
WOODY WETLAND		4.5	
WET LAND (BARREN)		20	4.1
CONCRETE (DRY SOIL)		3.3	
WETLAND SCRUB			14.7

5 CONCLUSIONS

The analysis of land cover classifications based on Landsat data shows significant variation from season to season as well as different months. However, these data reveal more detail surface properties than NLCD data. Based on the specific purpose, the Landsat data can be a very important source of information and an efficient approach to updating land cover information in timely manner. When using Landsat data for land cover classification, special techniques such as band ratios and proper atmospheric corrections are critical. However, considering the moderately coarse resolution of this data, there are still many surfaces that appear mixed. From a technical processing aspect, users should proceed cautiously when mosaicking is used because a great deal of spectral confusion occurs. This results in overall increased mixing of classes. Therefore, the best way to process the data is to use single image scenes for detailed land cover classification.

Change detection studies using unsupervised classification products from the Landsat data are difficult to compare and not possible to evaluate the accuracy. When considering wetlands analysis, for more detailed information sub-pixel classification or spectral mixture analysis based on separated subset classification may be necessary (Ozesmi and Bauer, 2002).

As references, two images from ALI were used in this study. Compared to Landsat data, it provides nine observation bands between visible and short wave infrared. Since it includes one additional blue range wavelength, one more in the near infrared, and the other in the short wave infrared, it shows great sensitivity over water bodies and vegetated regions. It also gives a better spatial resolution. ALI data can be easily generated to 10 meters resolution using its panchromatic band. It can be more appropriate for specific site analysis such as a single site of wetland region, lake(s), or forest.

6 RECOMMENDATIONS FOR LAND COVER INVENTORY AND CHANGE DETECTION

RECOMMENDATION 1
The analysis of Landsat and ALI data demonstrated that inventories derived by satellites are strongly influenced by season. For instance, species detection/delineation during the growing season is different and it is recommended that images would be collected in early spring, late fall or early winter, and in the middle of summer. Images collected during the summer season would provide valuable information for the area of early senescent shrub species including wetland grasses, and other plant growth conditions.

RECOMMEDDATION 2
The sensitivity of image classification in relation to the annual cycle was illustrated through comparison of the 2002 Landsat 7 ETM+ and 2005 Landsat TM5 images. Analysis of these images suggests significant changes in land classification even though they were taken during the same season. One of possible influential factors would be the weather condition of previous days before those images were collected. Images should be collected with no precipitation at least 2 to 5 days before acquisition. This implies that land classification comparisons made from simple snapshots in time without knowledge of their position relative to the annual cycle will be difficult to interpret. Therefore, it is recommended that baseline climatology of the annual

vegetation cycle be established for use in future assessment studies. This might be important with respect to climate change and the future associated impact on vegetation scenarios. Monthly collection of data is recommended. As pointed out above, Landsat ETM+ not only is easily accessible but also not expensive. County wide coverage with 7 bands, fusion of the data with the panchromatic band could produce about 20 different classes.

RECOMMENDATION 3

ALI data are reasonably priced and it is recommended to use ALI for land cover classification in sensitive areas, using an approximate resolution of 10 m. Use of ALI data for land classification could be linked with the images that are required as part of the water monitoring program. However, for a specific analysis such as detailed inventory for the wetland species, the consideration of cooperating ALI data with a high resolution satellite data such as QuickBird images would be recommended. The QuickBird image can be a good alternative source replacing ground survey work since it has one meter resolution with four spectral bands collected from the wavelength range from visible to near infrared.

6 REFERENCES

HOMER C., C. HUANG, L. YANG, B. WYLIE, AND M. COAN, 2004, Development of a 2001 National Land-Cover Database for the United States, Photogrammetric Engineering & Remote Sensing Vol. 70, No. 7, July 2004, pp. 829–840.

OZESMI, S.L., AND M. E. BAUER, 2002, Satellite remote sensing of wetlands, Wetlands Ecology and Management 10:381-402.

U.S. Global Change Research program, 2008, Land use and land cover change, USGCRP Program Element, http://www.usgcrp.gov/usgcrp/ProgramElements/land.htm.